EFFECTS OF MYRISTOYLATION ON THE STRUCTURE AND STABILITY HISACTOPHILIN

By

Joseph Meissner

A thesis
presented to the University of Waterloo
in fulfillment of the
thesis requirement for the degree of
Master of Science
in
Chemistry

Waterloo, Ontario, Canada, 2007

I hereby declare that I am the sole author of this thesis. This is a true copy of the thesis, including any required final revisions, as accepted by my examiners.

I understand that my thesis may be made electronically available to the public.

ABSTRACT

Hisactophilin is a histidine rich, actin binding protein from *Dictyostelium discoideum*. The structure of Hisactophilin, an all-beta protein, is typical of the beta-trefoil superfamily of proteins. In addition, hisactophilin is myristoylated, which is a relatively common co-translational modification involving the covalent attachment of a myristic acid group to the N-terminal glycine of a protein. For most modified proteins, a myristoyl group is involved in reversible protein-protein and protein-membrane interactions via a myristoyl switch. The majority of studies on the molecular basis of myristoyl switches have focused on characterizing calcium-myristoyl switches, whereas research has suggested that hisactophilin binds reversibly to membranes by means of a pH dependent myristoyl switch. A number of *in vivo* studies of the modified protein have been completed to study the function of hisactophilin; however, the structure and stability of the protein have only been characterized using the recombinant non-myristoylated protein. In contrast, this study focuses on the effects of myristoylation on hisactophilin structure and stability. Myristoylated hisactophilin has been prepared by a dual plasmid expression system in *E. coli*. Optimization of the efficiency of myristoylaion was completed for the preparation and purification of myristoylated hisactophilin. Characterization of the structural changes caused by myristoylation were undertaken using multidimensional homo- and heteronuclear NMR experiments. Circular dichroism (CD) was used to obtain low resolution structural data and characterize protein stability as a function of pH using chemical denaturation. The molecular consequences of myristoylation on protein stability and structure, as well as the molecular basis for pH dependent myristoyl switch will be discussed.

ACKNOWLEDGMENTS

It is a pleasure to acknowledge the many people who have been so helpful in the preparation of this thesis

First of all, I must thank my supervisor, Dr. Elizabeth Meiering. Her enthusiasm for this project and her knowledge were extremely motivating. Her guidance, advice and, most important, her devotion to the education of her students was greatly appreciated.

Thank you all the members of my lab for providing a stimulating and fun environment to work in. I am especially grateful to Joe Gaspar for helping and guiding me with every aspect of this project. I would like to thank Young-Mi (Gracie) Hwang for her help with Mass Spectrometry and for sharing our small lab across the hall.

I would also like to thank Christine Hand and Valerie Goodfellow for not only sharing their expertise in HPLC, but also their always-entertaining stories.

Thank you to the Guillemette Lab for use of their CD instrument, as well as the Honek Lab and Dmitrienko Lab for use of their HPLC instruments.

To my family – thank you for all your love and for pretending to understand all that this project is about. I greatly appreciate your involvement and support. Most importantly, I would like to thank my wife Karen. Without all of your love, understanding and encouragement none of this would be possible.

TABLE OF CONTENTS

LIST OF TABLES

LIST OF FIGURES

LIST OF ABBREVIATIONS

3D	Three Dimensional
1D	One Dimensional
τ_m	Mixing time
ΔG	Free energy
Å	Angstrom
ADP	adenosine diphosphate
AMP	ademosine monophosphate
Arf	ADP ribosylation factor
^oC	degrees Celsius
CaN	calcineurin
cAPK	cyclic AMP dependent protein kinase
CD	circular dischroism
CoA	Coenzyme A
COSY	correlation spectroscopy
Da	Dalton
kDa	kiloDalton
D. discoideum	*Dictyostelium discoideum*
D.d.	*Dictyostelium discoideum*
ddH_2O	distilled deionized water
DEAE	diehtylaminoethyl
DMSO	dimethylsulfoxide
DSC	differential scanning calorimetry

DTT	dithiothreitol
E. coli	*Escherichia coli*
E.c.	*Escherichia coli*
EDTA	ethelenediamine tetraacetic acid
FGF	fibroblast growth factor
FID	free induction decay
G	gram
GdnHCl	guanidine hydrochloride
GTP	guanidine triphosphate
TOCSY	total correlation spectroscopy
hArf	human ADP ribosylation factor
hNMT	human n-myristoyltransferase
HPLC	high pressure liquid chromatography
RP	reverse phase
HisI	hisactophilin I
HisII	hisactophilin II
HSQC	heteronuclear single quantum correlation
IL-1β	interleukin 1β
IPTG	isopropyl-thio-β-D-galactoside
L	litre
LB	Luria-Broth
M	molar
mA	milli amp

MAP	methionine aminopeptidase
MHz	mega hertz
Min	minute
Myr	myristoyl
MW	molecular weight
native-PAGE	native poly acrylamide gel electrophoresis
NMR	nuclear magnetic resonance
NMT	N-myristoyltransferase
NOE	nuclear Overhauser effect
NOESY	nuclear Overhauser effect spectroscopy
Non-Myr	non-myristoylated
pdb	protein data bank
ppm	parts per million
PPO	2,5-diphenyloxazole
psi	pounds per square inch
rpm	rotations per minute
s	seconds
S. cerevisiae	*Saccharomyces cerevisiae*
SDS-PAGE	sodium dodecyl sulphate polyacrylamide gel electrophoresis
T	temperature
T_m	melting temperature
TFA	trifluoroacetic acid
μCi	micro curies

UV	ultraviolet
ΔA	change in absorbance
ΔC_p	change in heat capacity
ΔH	change in enthalpy
ΔH_m	change in enthalpy at T_m
ΔS	change in entropy
ΔS_m	change in entropy at T_m
yNMT	yeast N-myristoylatransferase
Q-TOF	quadropole time of flight

Note: the standard three letter and one letter amino acids codes have been used throughout.

CHAPTER 1 – INTRODUCTION

Co- and post-translational modifications of proteins occur relatively frequently and are often necessary for proper protein function. These protein modifications may also play a role in the structure, stability and folding of a given protein. For simplicity, most studies of protein stability and folding use recombinant proteins that are expressed in *Escherichia coli*. *E. coli* is an excellent system for the production of highly pure protein; however, *E. coli* cells typically lack many enzymes responsible for protein modifications. Thus some non-modified recombinant proteins may possess significantly different properties from those of the natural protein. Little is known about the effects that protein modification has on the structure, stability and folding; a deeper understanding of this would be interesting for comparing the properties of recombinant proteins and the naturally modified proteins.

An example of a modified protein that has been extensively studied in its unmodified recombinant form is hisactophilin. Hisactophilin is a histidine-rich, actin-binding protein found in the model organism *Dictyostelium discoideum*. Hisactophilin is modified by myristoylation, which is the attachment of a myristic acid group to the N-terminus. A number of *in vivo* studies of the modified protein have been completed to characterize its function (Schleicher *et al*., 1995; Scheel *et al.*, 1989; Hanakam *et al*., 1995; Hanakam *et al*., 1996); however, structure, stability and folding have been characterized using only the recombinant non-myristoylated protein (Habazettle *et al*., 1992; Hammond *et al*., 1998; Liu *et al*., 2001; Liu *et al*., 2001). The function of the myristoyl group of hisactophilin is not yet well defined. For many proteins, the myristoyl

group is involved in reversible protein-protein and protein-membrane interactions, referred to as a myristoyl switch.

1.1 – Protein N-myristoylation

Protein N-myristoylation is one of the most common lipid modifications of proteins (Resh, 1999). This modification occurs for eukaryotic (Resh, 1999) and viral proteins (Maurer-Stroh and Eisenhaber, 2004), but not for bacterial proteins. N-myristoylation consists of the co-translational attachment of a 14-carbon saturated fatty acid to the N-terminal glycine of a protein via an amide bond (Gordon *et al.*, 1991) (Figure 1.1). Although this common protein modification is necessary for many different cellular processes (Resh, 1996; Resh, 1999), myristic acid is considered to be a rare fatty acid (less than 2% of cellular fatty acids) (Gordon *et al.*, 1991). Myristic acid attachment to the protein is catalyzed by a well studied enzyme, N-myristoyl transferase (NMT). The attachment process begins with the activation of myristic acid by FAA1 acyl CoA synthetase to yield myristoyl CoA (Gordon *et al.*, 1991). A second necessary prerequisite step is the removal of the protein's initiating methionine by methionine amino peptidase (MAP), to produce a protein with a free N-terminal glycine (Gordon *et al.*, 1991). The mechanism of myristoylation follows a Bi Bi reaction mechanism (Rudnick *et al.*, 1991). Initially, myristoyl CoA binds to NMT to yield the activated complex myristoyl CoA: protein N-myristoyl transferase. This complex then binds selectively to the target protein (which is attached to the ribosome) and forms an amide bond between the myristic acid and the N-terminal glycine residue. Next the CoA is released followed by the release of the myristoylated protein.

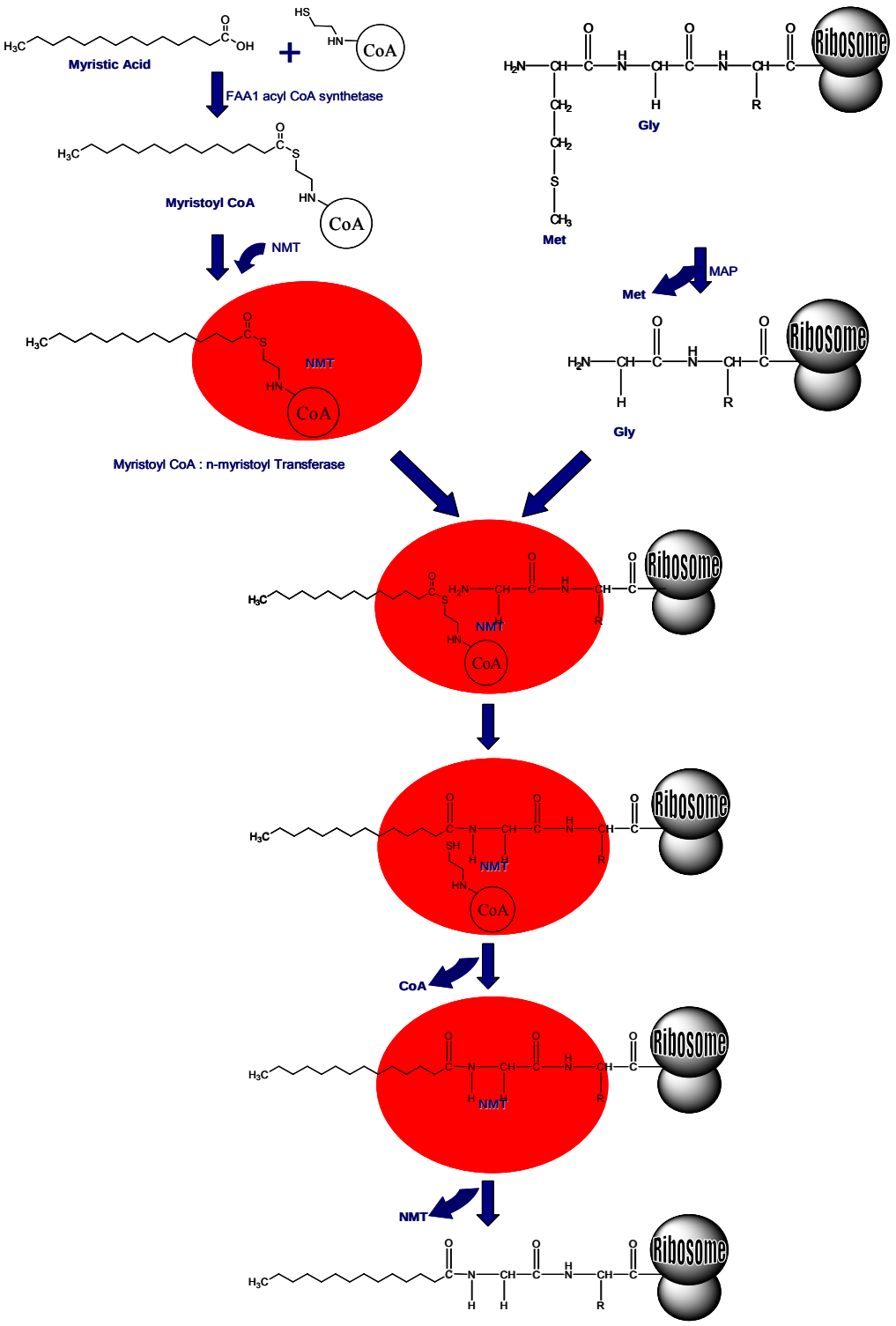

Figure 1.1 – Process of protein N-myristoylation
Process begins with the activation of myristic acid with FAA1 acyl CoA synthetase to yield myristoyl CoA. This activation is followed by binding of myristoyl CoA with NMT (Red circle). Simultaneously, protein, which is in process of being translated, has its initiating Met cleaved by MAP. Protein binds to NMT and the myristoyl group is covalently linked to the N-terminus via an amide bond. This process is followed by release of CoA and finally NMT to yield myristoylated protein.

1.2 – N-myristoyltransferase

Myristoylation occurs for many different eukaryotic and viral proteins and is considered to be vital in many cellular processes. Because of this occurrence, NMT is considered an essential enzyme for many different species. NMT has been found with many variations in amino acid sequence in a large number of organisms (Bhatnagar *et al.*, 1999). Figure 1.2 is a phylogenetic tree outlining NMTs of various species and their relation through conserved residue sequences in their binding pocket. The most widely studied NMTs are those from *Saccharomyces cerevisiae* (yeast NMT) (Bhatnagar *et al.*, 1999) and humans (Farazi *et al.*, 2001).

NMT is able to act upon a wide variety of different proteins within a given species (Maurer-Stroh *et al.*, 2002). Although N-terminal glycine is an absolute necessity for protein myristoylation, not all proteins with N-terminal glycine are myristoylated. These observations suggest the existence of a consensus motif for NMT protein substrates that extends upstream of the N-terminal glycine (Duronio *et al.*, 1991). Initial studies of *S. cerevisiae* demonstrated the importance of the first six residues (after methionine removal), which form an N-terminal consensus sequence of Gly-$X_{uncharged}$-$X_{neutral}$-$X_{neutral}$-Ser/Thr-Lys (Utsumi, 2001). This motif may be applicable for yeast NMT specificity, but with the presence of many differences in isozymes of NMT and species-specific substrate specificity, a more general approach to defining the consensus motif is needed. These differences in specificity are due to evolutionary differences in sequence at the NMT substrate binding pocket (N-terminus of NMT) found in different species and different isozymes (Maurer-Stroh *et al.*, 2002).

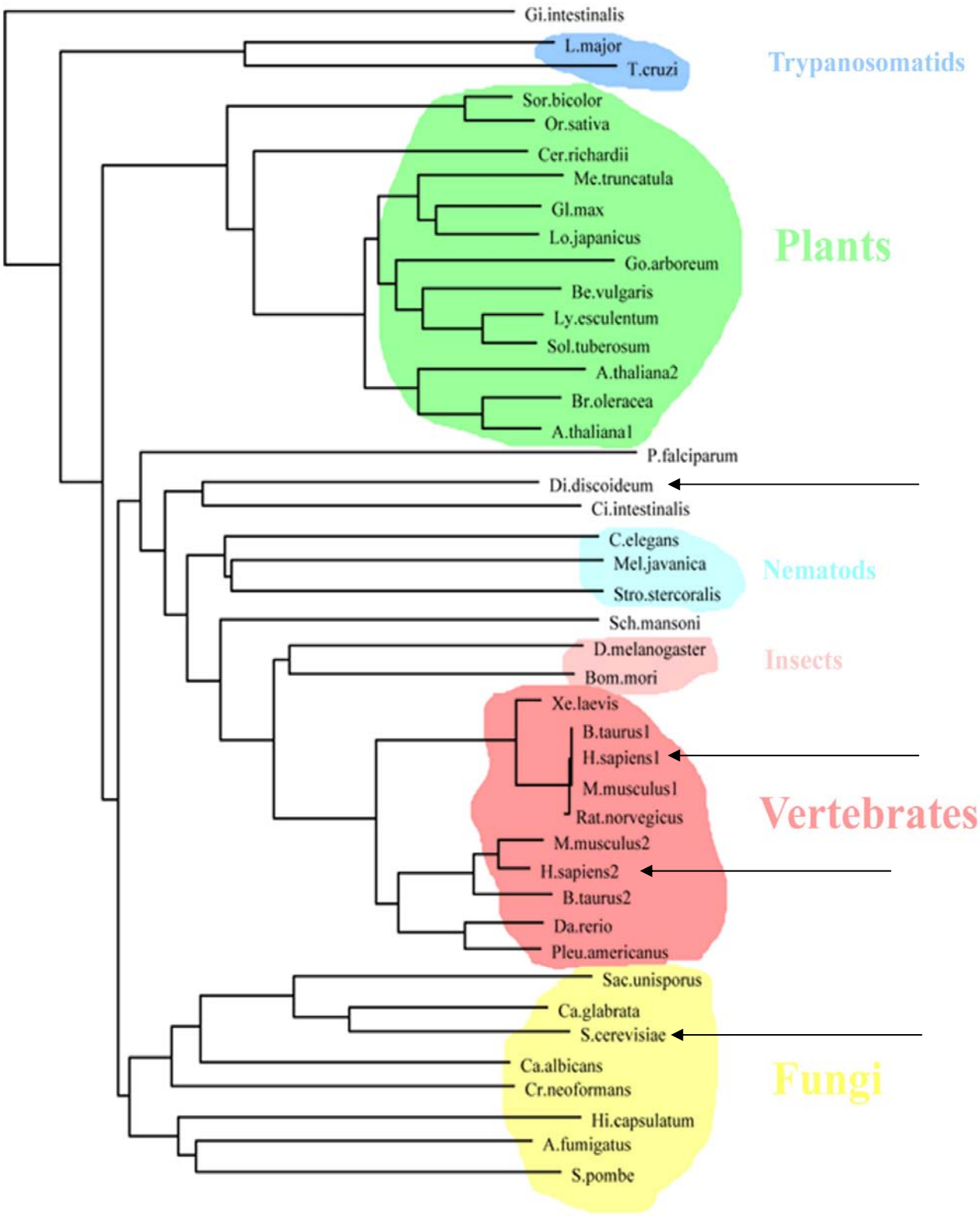

Figure 1.2 – Phylogenetic tree of various NMTs
Note the differences between *D. discoideum*, human (*H. Sapiens*) and yeast (*S. cerevisiae*) NMT phylogeny, indicated by arrows (Maurer-Stroh *et al.*, 2002).

Although NMT exhibits species-specific substrate specificity, extensive sequence comparisons of myristoylated proteins revealed additional conserved features (Maurer-Stroh *et al.*, 2002). These conserved features fall into two regions characterized by specific physical requirements. These regions consist of the binding pocket region (residues 1-6) and the linker region (residues 7-17). The residue requirements for myristoylation are described below and the primary structure of hisactophilin is given in Figure 1.3 for comparison.

M-
1 G-N-R-A-F-K-
7 S-H-H-G-H-F-L-S-A-E-G-
18 EAVKTHHGHHDHHTHFHVENHGGKVALKTHCG
50 KYLSIGDHKQVYLSHHLHGDHSLFHLEHHGGKVS
85 IVSIKGHHHHYISADHHGHVSTKEHHDHDTTFEEIII

Figure 1.3 – Primary sequence of the myristoylated protein hisactophilin
The initial methionine is not included for residue numbering since it is cleaved during translation by MAP. Two regions of conserved features are highlighted. Residues 1 to 6 make up the binding pocket region and 7 to 17 make up the linker region (Maurer-Stroh *et al.*, 2002).

The first NMT substrate recognition region is the binding pocket region which consists of residues 1 to 6 of the substrate protein. These first 6 residues (again after methionine cleavage) need to fit deep within the NMT binding pocket to allow for myristoylation (Maurer-Stroh *et al.*, 2002). At position 1, glycine is required, without exception, for all myristoylated proteins. Positions 2 and 3 require small residues to

allow fitting into the rather narrow binding pocket of NMT. In addition, higher eukaryotic substrates require hydrophilic residues; whereas fungal substrates require hydrophobic residues. Position 4 is preferentially occupied by large hydrophobic side chains (including tryptophan, phenylalanine and proline for higher eukaryotes); however, some species of fungi are unable to fit large residues and smaller residues are preferred in this position. Position 5 is generally occupied by a small polar residue; however, a number of proteins with aspartic acid or phenylalanine (including hisactophilin) at position 5 are still found to be myristoylated. This position is found to be highly conserved among phyla and can vary for different species (this may be an important factor for high efficiency of myristoylation of hisactophilin discussed in Chapter 3). Finally, position 6 shows a preference for lysine or, less often, threonine.

The second region of conserved residues is the linker region. The close interaction of the binding pocket region with NMT was originally thought to be the only constraint in substrate specificity; however, long range electrostatic interactions are, apparently, also important. Residues 7 to 11 interact with the mouth of the binding pocket. Residues 7, 8 and 9 tend to have a flexible backbone and are hydrophilic; whereas, residues 10 and 11 are relatively small and/or polar. Residues 12-17 are the long-range linker region, and residues have a tendency to be polar residues.

1.3 – Myristoylated Proteins

The proteins that undergo myristoylation have a variety of different functions and structural characteristics. The function of myristoylated proteins most often involves signal transduction pathways or intracellular transport (Farazi *et al.*, 2001). The function of the myristoyl group is to aid in protein-membrane and protein-protein interactions (reviewed in Taniguchi, 1999). The myristoyl group contributes in membrane binding by the simple means of the hydrophobic effect; however, the energy of this interaction alone is not sufficient for protein anchoring and other molecular interactions are also significant (McLaughlin and Aderem, 1995; Resh, 1999). In most cases membrane binding is achieved by myristoylation along with electrostatic interactions of positively charged amino acids with negatively charged phospholipid head groups. Neither the hydrophobic nor the electrostatic interactions alone have sufficient energy to anchor the protein to the membrane, and removal of one set of interactions will result in decreased binding. This dual system of interaction for membrane binding is found in many different myristoylated proteins. Figure 1.4 describes a number of different dual systems of interaction.

The structural characteristics of myristoylated proteins have been studied for a variety of different proteins. X-ray crystallography and stability studies have suggested that myristoylation may have significant effects on protein stability (Resh, 1999). In addition, some protein structures possess a hydrophobic groove on the protein for binding the myristoyl group. When bound in this groove the myristoyl group is unable to insert into the plasma membrane, which will result in decreased membrane binding for the protein. In many cases the myristoyl group is able to move out of the hydrophobic groove and into an "on" position. This scenario has been termed a "myristoyl switch"

and is common among myristoylated proteins. Differences in switch triggers can be categorized as myristoyl-ligand, myristoyl-electrostatic or myristoyl-proteolytic switches (Figure 1.4) (Resh, 1999); these switches have been seen in some of the following examples.

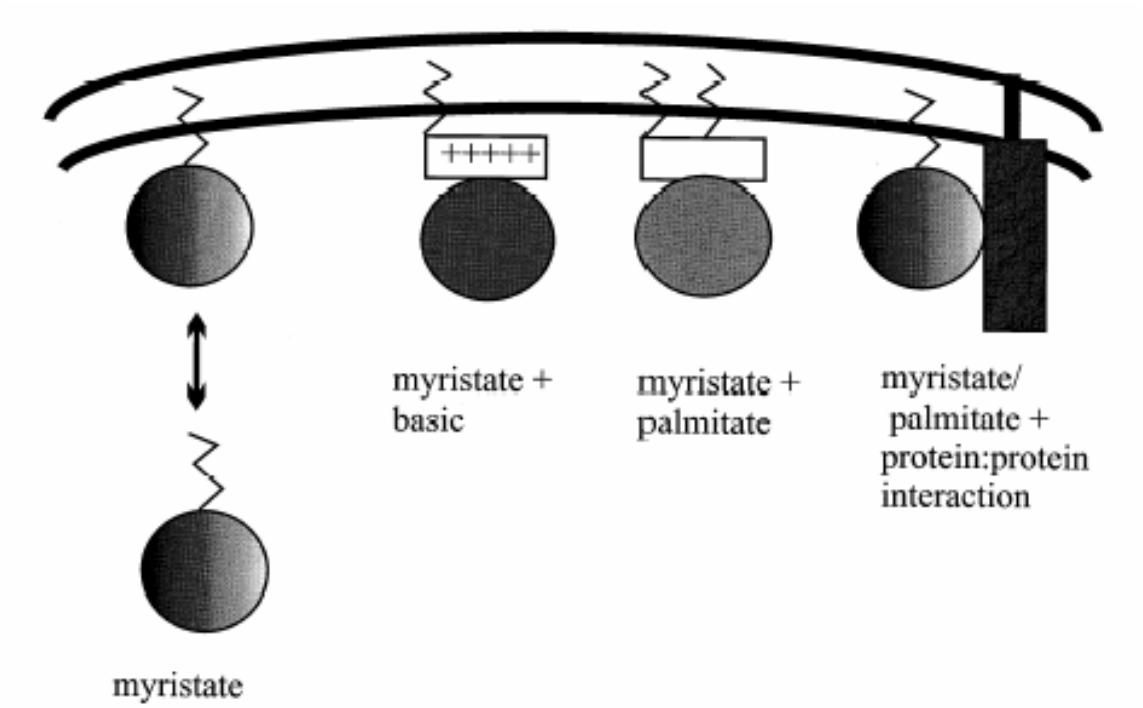

Figure 1.4 - Possible dual system models of membrane interactions.
The myristoyl group alone is not sufficient for membrane anchoring, but, in the presence of electrostatic forces (basic), other acyl chains or other protein interactions membrane anchoring is possible. The spheres represent the myristoylated protein, and the zigzagging lines represent aliphatic chains (Resh, 1999).

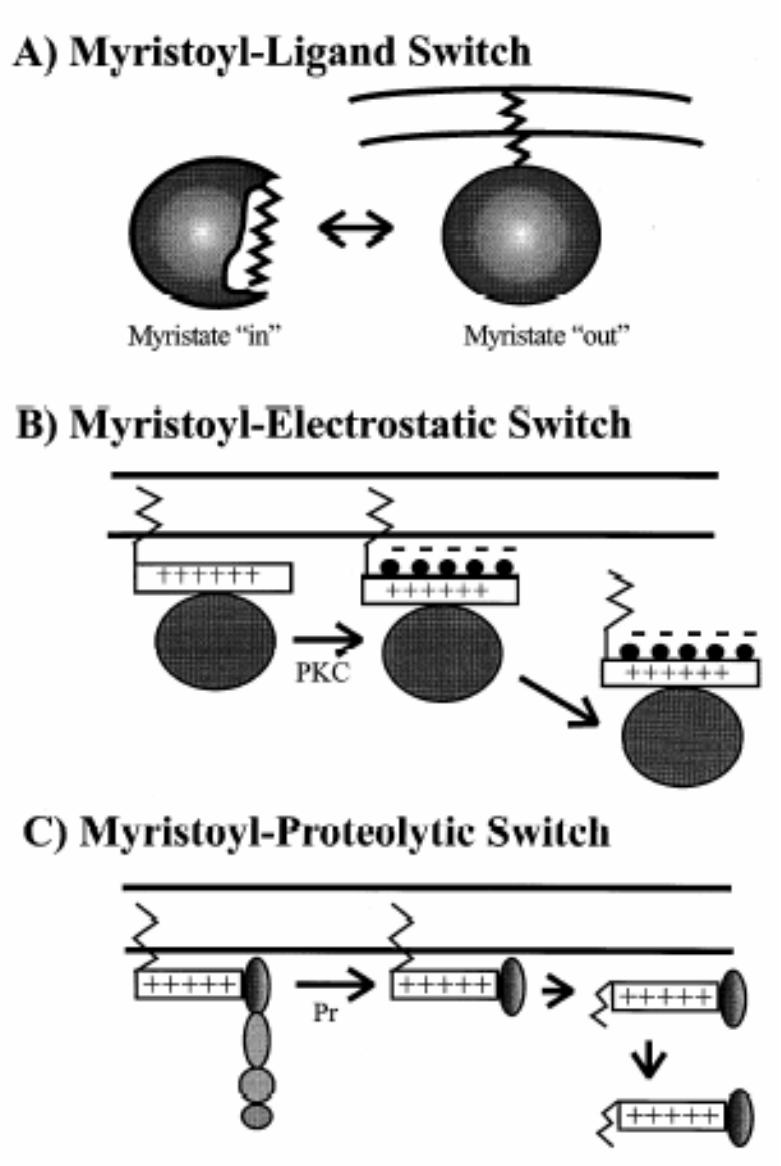

Figure 1.5 – Examples of different myristoyl switches.
Myristoyl switches allow for the reversible binding of proteins to membranes. (A) Demonstrates the ligand-myristoyl switch in which binding of a ligand changes the conformation from "on" to "off" and facilitates membrane binding. (B) Is the myristoyl-electrostatic switch. Here phosphorylation or other means (i.e. pH) changes the charge on the protein to cause dissociation. (C) is the myristoyl-proteolytic switch where protein cleavage causes sequestering of the myristoyl group and dissociation (Resh, 1999).

1.3.1 – Cyclic AMP Dependent Protein Kinase

Cyclic AMP dependent protein kinase (cAPK) plays a crucial role in almost every eukaryotic organism by catalyzing the phosphorylation of regulatory proteins involved in cellular growth, metabolism and homeostasis (Gangal *et al.*, 1999). The myristoyl group of this protein is thought to lie within a large hydrophobic pocket formed by the N-terminus and the catalytic domain (Figure 1.6) (Zheng *et al.*, 1993). It was initially proposed that the myristoyl group was present merely for increased structural stability (Yonemoto *et al.*, 1993). However, more recent information has revealed that the myristoylated catalytic subunit of the protein may be involved in some type of myristoyl-electrostatic switch (Gangal *et al.*, 1999; Tholey *et al.*, 2001). Information regarding the mechanism of the possible myristoyl-electrostatic switch of cAPK is limited, but myristoylation has been shown to have a crucial role in the overall structural stability of the protein.

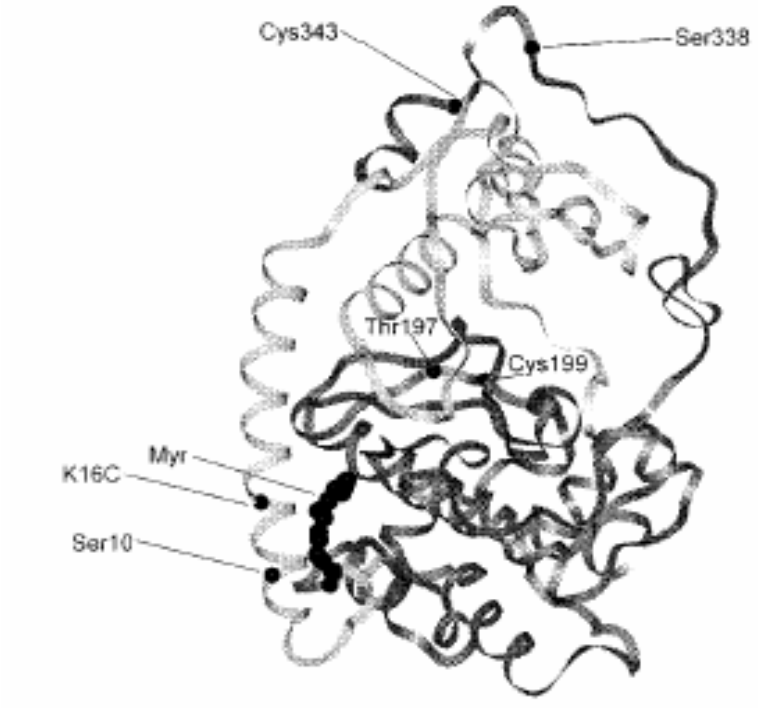

Figure 1.6 - Backbone structure of C subunit of cAPK. Note the location of the myristoyl group in the hydrophobic pocket which increases protein stability (Gangal *et al.*, 1999).

1.3.2 – Calcineurin

Calcineurin (CaN) is a heterodimeric Ser/Thr protein phosphatase involved in many different biological roles such as ion channel regulation, gene transcription and neuronal depression (Kennedy *et al.*, 1996). The myristoyl group of this protein is situated in a hydrophobic groove situated between two alpha helices of the EF-hand structure of the protein (Rusnak and Mertz, 2000). Membrane binding capabilities of the protein that are independent of myristoylation have been determined, and evidence of a myristoyl switch has yet to be found (Rusnak and Mertz, 2000; Kennedy *et al.*, 1997). The physiological role of the myristoyl group may not be known, but the myristoylation is known to significantly increase thermal stability of the protein (Kennedy *et al.*, 1996).

1.3.3 – Recoverin

Recoverin is a calcium binding protein which blocks phosphorylation of rhodopsin to prolong the photoresponse (reviewed in Ames *et al.*, 1996). Recoverin is a member of the EF-hand superfamily of proteins and is myristoylated (Ames *et al.*, 1996; Dizhoor *et al.*, 1992). This protein has been characterized in detail with respect to its membrane binding ability via a calcium-myristoyl switch (Zozulya and Stryer, 1992; Ames *et al.*, 1997) (Figure 1.7). For recoverin, in the calcium-free state the myristoyl group is sequestered within a relatively deep hydrophobic pocket between helices (Tanaka *et al.*, 1995) (Figure 1.8). The myristoyl group is "clamped" in this pocket by an N-terminal helix; this helix is unstructured in the non-myristoylated form of the protein and some studies suggest that the myristoyl group stabilizes the formation of this helix (Ames *et al.*, 1994b). Through NMR experiments the structure and the location of the myristoyl group change markedly upon cooperative calcium binding (Ames *et al.*, 1994b;

Senin *et al.*, 2003). The myristoyl group extrudes from the protein, becoming solvent accessible and is then able to interact and bind to membranes (Figure 1.7) (Ames *et al.*, 1995). The structures of both the calcium-free and calcium-bound states have been determined by NMR and are shown in Figure 1.8 (Ames *et al.*, 1997). The binding of recoverin to the membrane occurs through insertion of the myristoyl group into the membrane along with other electrostatic forces; this process has little effect on the protein structure (Valentine *et al.*, 2003).

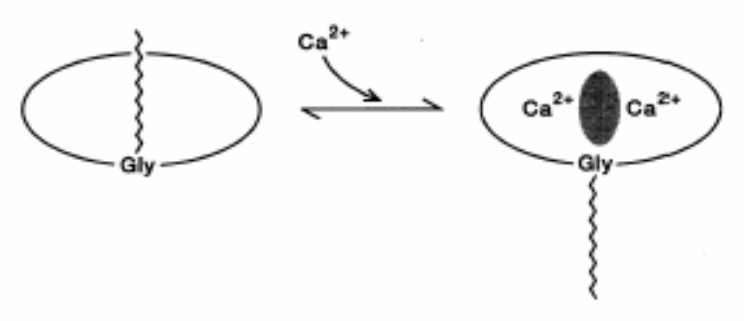

Figure 1.7 – Schematic diagram of the Ca^{2+}-myristoyl switch
The binding of two or Ca^{2+} ions induces a conformational change exposing the myristoyl group which promotes membrane interaction (Ames *et al.*, 1995)

Figure 1.8 – Ribbon diagram of Ca^{2+}-free and Ca^{2+}-bound myristoylated recoverin Ca^{2+}-free is found on the right and Ca^{2+}-bound is on the left. The myristoyl group is coloured pink and Ca^{2+} is gold (Ames *et al.*, 1997)

1.3.4 – Frequenin and Other Neuronal Calcium Sensors

Frequenin and other neuronal calcium sensors are calcium-binding proteins which regulate many different cellular functions such as neurotransmitter release, potassium channels and voltage-gated calcium channels of both excitable and non-excitable cells (O'Callaghan *et al.*, 2002). These proteins are closely related to recoverin in that they both are calcium binding proteins of the EF-hand superfamily and are myristoylated (Burgoyne, 2004). Denaturation experiments using guanidine HCl (GdnHCl) have shown that myristoylation of neuronal calcium sensors increase the structural stability of the protein (Muralidhar, 2005). This protein has been found to bind to membranes in a myristoyl and calcium dependent manner similar to that of recoverin (O'Callaghan *et al.*, 2002; Ladant, 1995; Ames *et al.*, 2000). However, research has determined that the NMR and fluorescence spectrum are nearly identical upon calcium binding (Ames *et al.*, 2000). These findings suggest that the myristoyl group is not confined to a hydrophobic pocket of the protein in the absence of calcium as in recoverin.

1.3.5 – ADP-ribosylation Factors

ADP-ribosylation factors (Arfs) are the protein cofactor for cholera toxin-catalyzed ADP ribosylation and also serve a regulatory role in protein secretion and membrane trafficking by interaction with the Golgi apparatus (Kahn *et al.*, 1992). Arf is a myristoylated alpha/beta protein that is made up of a β-sheet core surrounded by α-helices (Amor *et al.*, 1994). Arfs undergo a myristoyl-GTP switch to regulate membrane binding (Randazzo *et al.*, 1995). The structure of the non-myristoylated protein suggests that there is a hydrophobic groove between two β-strands to accommodate the myristoyl group in its "off" state (Amor *et al.*, 1994). Upon activation of the protein by GTP

binding, Arfs have increased membrane binding affinity (Randazzo *et al.*, 1995). The myristoyl group itself is not sufficient for membrane binding (Haun *et al.*, 1992); however, the presence of the myristoyl group increases protein helical content and produces a new hydrophobic face for increased membrane binding (Harroun *et al.*, 2005). The actual molecular details of the switch have not yet been elucidated but extensive evidence suggests that Arfs undergo a myristoyl-GTP switch.

To summarize, myristoyl switches are found in many different proteins that have diverse functions. In general, very little data on the molecular details and basis for the switches has been collected. Hisactophilin provides and interesting opportunity to understand molecular characteristics of the myristoyl switch.

1.4 – Hisactophilin

1.4.1 – Chemical Properties and Function of Hisactophilin

Hisactophilin is an actin binding protein found in the highly motile amoeboid cells of the slime mold *Dictyostelium discoideum* (Schleicher *et al.*, 1995). *D. discoideum* is a model organism that has been used extensively to study cytoskeletal structure and dynamics. Remarkably, the sophisticated mechanism of cytoskeletal rearrangement that allows for the organism's high motility is extremely similar to those of higher organisms (reviewed in Schleicher *et al.*, 1995). Actin binding proteins, such as hisactophilin, act by polymerizing or depolymerizing actin filaments or by cross-linking actin filaments to each other or to membranes (Schleicher *et al.*, 1995). In the case of hisactophilin, the protein binds to actin in a pH dependent manner (Scheel *et al.*, 1989).

Hisactophilin is a histidine-rich protein found to exist free in the cytoplasm as well as being membrane bound (Scheel *et al.*, 1989). Also, this protein exists in two isoforms (denoted as HisI (13.5kDa) and HisII (13.7kDa)), both of which are myristoylated and very similar in sequence and function (Hanakam *et al.*, 1995). The difference in the two isoforms involves a small variation in amino acid sequence; however, the N-terminal myristoylation consensus motifs for the two isoforms are identical (Hanakam *et al.*, 1995). Both isoforms consist of 118 amino acids, of which 31 are histidine for HisI and 36 for HisII. This high histidine content gives the isomers isoelectric points of 6.9 for HisI and 7.1 for HisII. Also, the two isoforms can form hetero- and homodimers. Lastly, the isomers are substrates of a membrane associated threonine/serine kinase; phosphorylation of hisactophilin has been proposed to have some regulatory role in its membrane interaction or in actin binding (Hanakam *et al.*, 1995).

The covalently bound myristoyl group is crucial for the binding of hisactophilin to membranes (Behrisch *et al.*, 1995). This binding is thought to function by way of a myristoyl-histidine switch (Hanakam *et al.*, 1996a), which is modulated by cytoplasmic pH levels or possibly by phosphorylation (Hanakam *et al.*, 1996b). *In vivo* studies have shown that membrane binding increases upon a decrease in cytoplasmic pH (Hanakam *et al.*, 1995). Other evidence for a pH dependent myristoyl-histidine switch for membrane binding is also based upon structural evidence determined by NMR (Habazettle *et al.*, 1992a; Hanakam *et al.*, 1995). Figure 1.9 shows a model for membrane binding and possible actin coupling mechanism (Hanakam *et al.*, 1995).

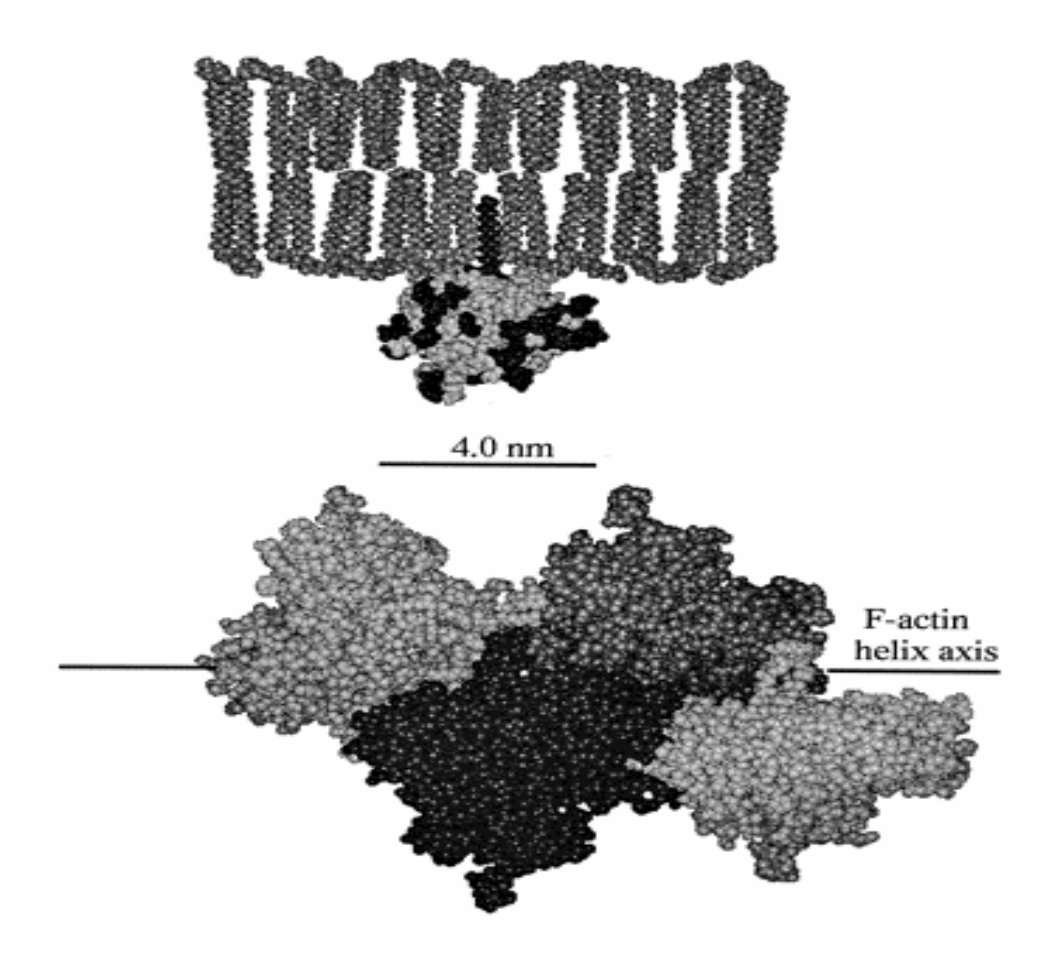

Figure 1.9 - Model of hisactophilin insertion into the inner lipid layer of the plasma membrane. Histidine residues (coloured dark) are thought to be involved in pH dependent actin binding. Model of F-actin shows relative sizes - indicating a possible location for hisactophilin binding (Hanakam *et al.*, 1995).

1.4.2 – Structure of Non-myristoylated Hisactophilin

The three-dimensional structure of non-myristoylated hisactophilin has been solved by NMR spectroscopy (Habazettl *et al.*, 1992a). The structure of hisactophilin is unlike any of the examples described earlier, since it is an all beta protein whereas the others were mostly alpha helical proteins with some amount of beta structure present. Hisactophilin is a member of the beta trefoil superfold which consists of the cytokines (including interleukin-1β (IL-1β)), basic and acidic fibroblast growth factors (FGF), ricin B-like, agglutinin, kunitz inhibitors and hisactophilin (Figure 1.10) (Murzin *et al.*, 1995). These proteins have less than 10% sequence homology, but nevertheless retain the same overall fold (Murzin *et al.*, 1992). There are, however, residues within the proteins that are conserved to allow for the high similarity in folds (Xu and Xiao, 2005; Murzin *et al.*, 1992). These minor sequence similarities have led Ponting and Russel (2000) to the conclusion that β-trefoil proteins may have descended from a common protein ancestor.

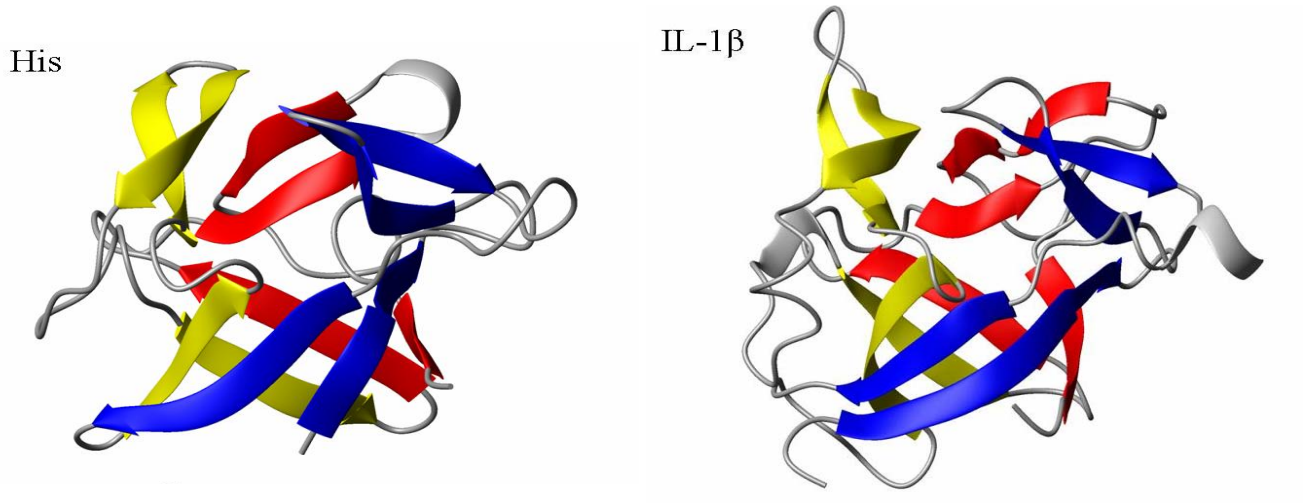

Figure 1.10 – Comparison of Hisactophilin (left) and IL-1β (right) structure

The structure of the β-trefoil fold in hisactophilin consists of twelve β-strands organized into three similar four-stranded trefoil units, as illustrated in Figure 1.11. Each of the trefoil units consists of a β-β-β-loop-β motif where the first and fourth β-strands form an anti-parallel β-sheet. Three of these β-sheets (one from each trefoil unit) make up a β-barrel and the remaining β-strands cover one end of the β-barrel in a triangular hairpin triplet (Figure 1.11). Of the many histidine residues, 90% reside on the surface of the protein in loops and turns, and are highly exposed to solvent (Figure 1.12). The histidines generally have pK_a values of 6.8 (Hammond *et al.*, 1998), consistent with the pH dependence of the proposed myristoyl-histidine switch. That is, a slight decrease in intracellular pH would cause large portions of the protein surface to become positively charged by protonation of the histidines and allow for favourable interactions with negatively charged membranes and actin.

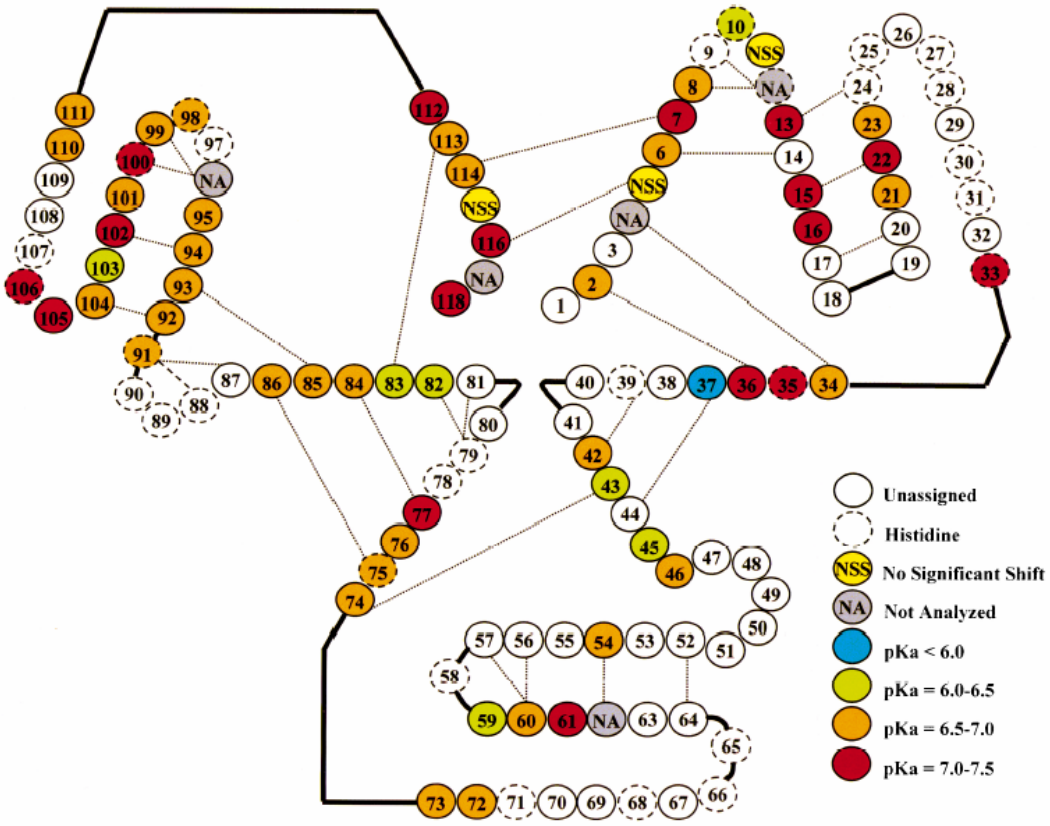

Figure 1.11 – Two-dimensional representation of the tertiary structure of hisactophilin. Each residue is depicted by a circle with the corresponding residue number inside. Colour coding represents the different pKa values for each amino acid. Hydrogen bonds between residues are shown by dotted lines. From this figure the β-trefoil structure is clearly evident. The six β-strands in the centre make up the β-barrel and the six around the outside make up the β-hairpin triplet. (Hammond *et al.*, 1998).

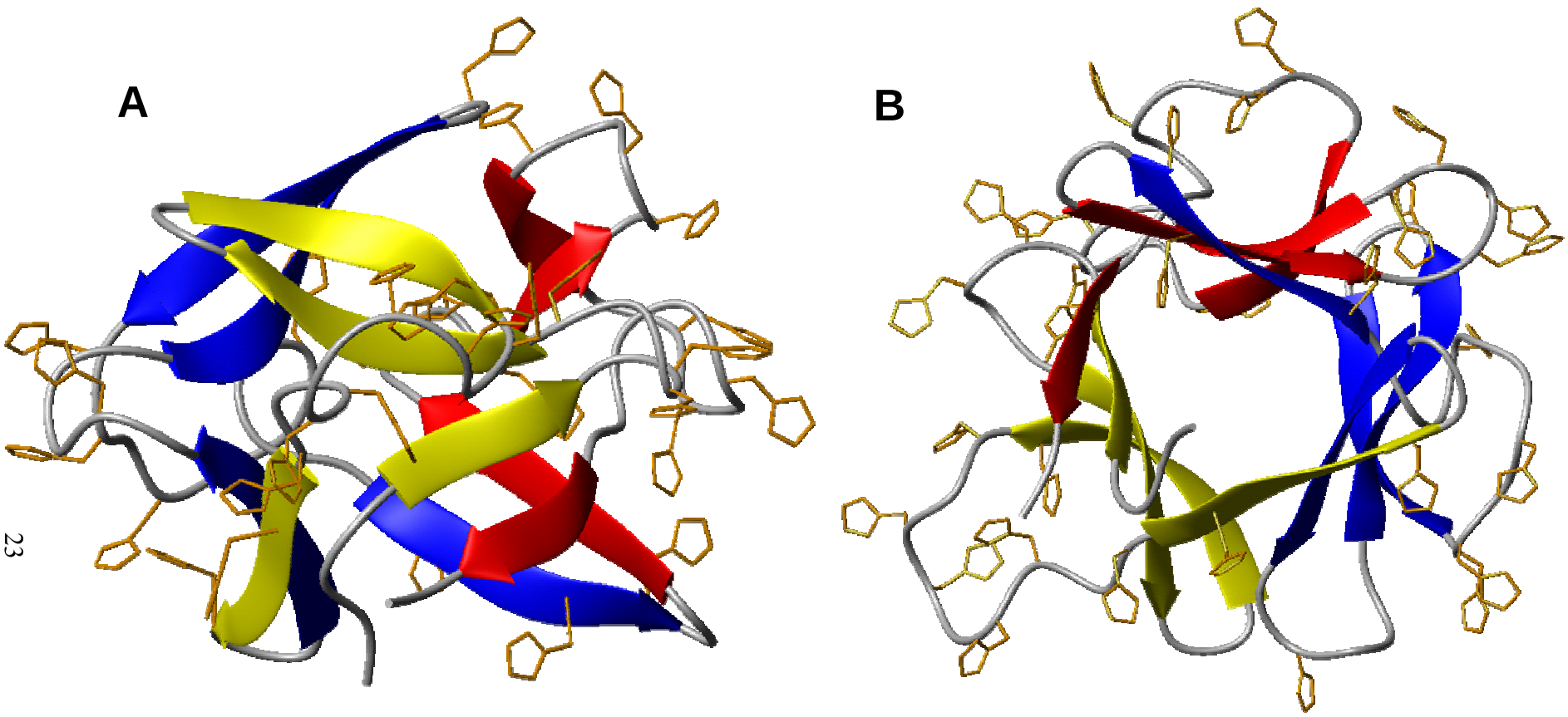

Figure 1.12 – Side view (A) and top view (B) of hisactophilin ribbon diagrams with highlighted histidine residues.

The structural aspects of this study were based upon the structure of the non-myristoylated form of the protein; it was assumed that the structure of myristoylated hisactophilin will be similar. Circular Dischroism (CD) spectroscopy data have been collected for both isoforms of hisactophilin and compared to the CD spectrum of the non-myristoylated protein (Figure 1.13). CD spectra were nearly identical, suggesting that myristoylation has little effect on the secondary structure of the protein (Hanakam *et al.*, 1996b). This is similar to data obtained for other proteins, described above, that also showed structure was not greatly affected by myristoylation.

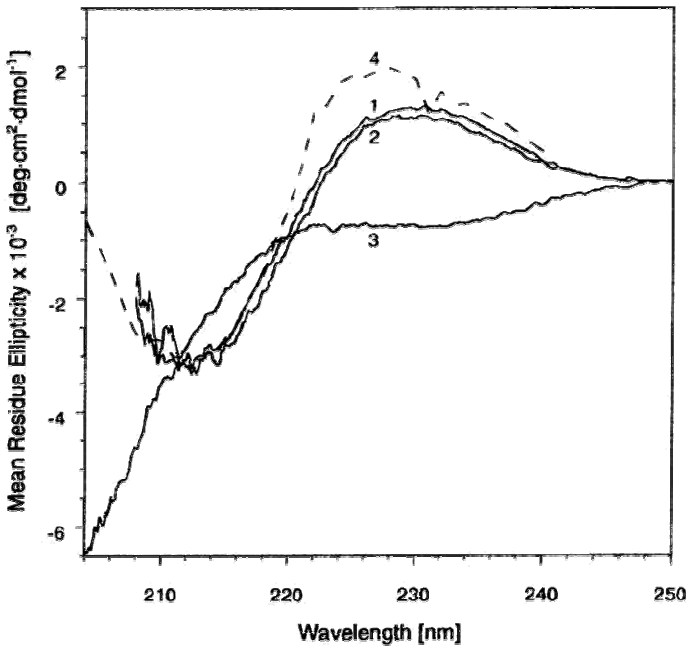

Figure 1.13 – CD spectra of myristoylated and non-myristoylated hisactophilin Solid lines represent 50/50 (mole/mole) myristoylated HisI/HisII at (1) pH 8; (2) pH 6; (3) pH 3. Dotted line (4) represents the spectrum of non-myristoylated hisactophilin. Spectra are nearly identical (Hanakam, 1996).

1.4.3 – Stability and Folding Studies of non-Myristoylated Hisactophilin

The stability and folding of non-myristoylated hisactophilin has been characterized in detail previously in our group. It was determined that the unfolding of non-myristoylated hisactophilin is greater than 90% reversible for urea induced unfolding, and at least 80% reversible for thermal denaturation (Liu *et al.*, 2001). The denaturation data can be well fit using a two-state transition model. From these denaturation studies, hisactophilin was found to have moderate and fairly constant stability from pH 7.7 to 9.7; however, below pH 7.7 stability decreases dramatically due to protonation of the histidine residues (Figure 1.14) (Liu *et al.*, 2001).

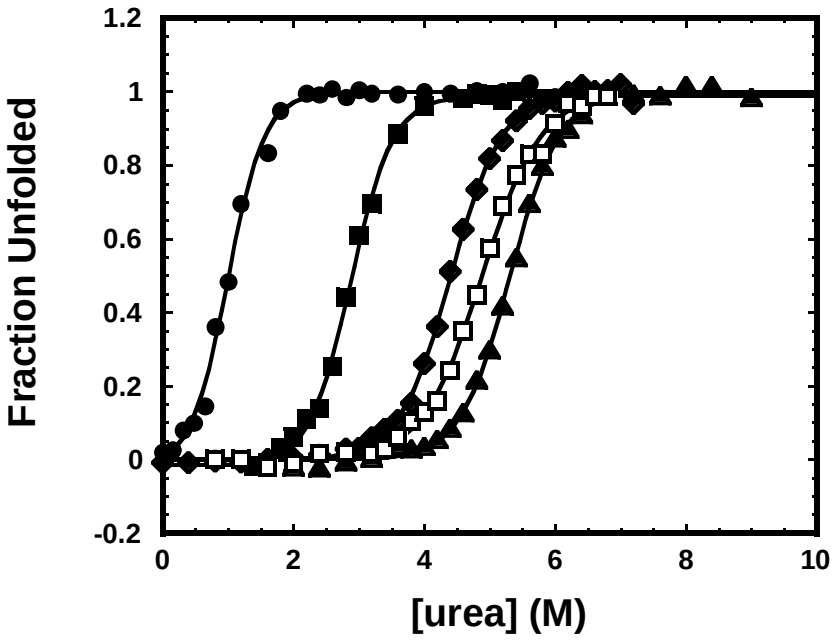

Figure 1.14 – Fluorescence-monitored denaturation curves of hisactophilin. Curves are measured for pH 5.7 (●), pH 6.7 (■), pH 7.7 (□), pH 8.7 (▲) and pH 9.7 (♦), displayed in terms of the fraction of unfolded protein. Hisactophilin stability increases markedly from pH 5.7 to 7.7, and then remains relatively constant from pH 7.7 to 9.7 (Liu *et al.*, 2001).

The folding kinetics of non-myristoylated hisactophilin have also been studied using optical probes as well as quenched flow hydrogen-deuterium exchange methods. The slowly exchanging amides of hisactophilin tend to be similar to those found in IL-1β, another β-trefoil protein, and may be conserved among this superfold (Houliston, 2002). In most cases of β-trefoil proteins, the folding is relatively slow and occurs via formation of intermediates. In the case of hisactophilin, the folding is much faster and apparently follows a two-state model, except under the most stabilizing solution conditions (Liu *et al.*, 2002). In this case, the folding intermediate for hisactophilin was found to resemble the IL-1β intermediate, but differs from that of FGF (Liu *et al.*, 2002). These differences are thought to be due to the differences in non-conserved loops that are involved in protein function.

1.5 – Experimental Objectives

The majority of studies on the molecular basis of myristoyl switches have been concerned with characterizing calcium-myristoyl switches whereas, as discussed above, hisactophilin is thought to bind reversibly to membranes by means of a pH dependent myristoyl switch. A number of *in vivo* studies on the modified protein have been completed to study the function of hisactophilin; however, the structure and stability of the protein have only been characterized using the recombinant non-myristoylated protein. This study focuses on the effects of myristoylation on hisactophilin structure and stability. To achieve this, a co-expression system was used to produce recombinant myristoylated hisactophilin in *E. coli*. Unfortunately, despite a number of optimization

experiments, this expression system yielded only 85% myristic acid incorporation and, which required a new purification protocol to separate myristoylated and non-myristoylated protein. Initial characterization of the structural changes caused by myristoylation has been undertaken using homonuclear and heteronuclear NMR. In addition, preliminary studies on the stabilizing effects of myristoylation were obtained by urea denaturation. The molecular consequences of myristoylation on protein stability and structure, as well as the molecular basis for pH dependent myristoyl switch will be discussed.

CHAPTER 2 – PREPARATION OF RECOMBINANT MYRISTOYLATED HISACTOPHILIN BY A DUAL PLASMID EXPRESSION SYSTEM IN *E. COLI*

2.1 – Introduction

The hisactophilin gene (cDH516) was initially sub-cloned into the plasmid pIMS5 and is designated pHisI (Simon et al., 1988); however, this plasmid contains 4 additional amino acids at the N-terminus of the protein (Habazettl et al., 1992a). These additional amino acids will cause a significant decrease in NMT activity due to N-terminal specificity of NMT. The inserted amino acid codons were deleted from the original plasmid by site-directed mutagenesis, yielding a plasmid designated pHW (Wong, 2002) (For plasmid map refer to Figure 2.1). pHW contains an IPTG-inducible Ptac promoter, b-lactamase for ampicillin resistance and the pBR322 origin of replication (Scheel et al., 1989; Wong, 2002).

For this project, three plsamids encoding different isoforms of NMT were available for testing their ability to myristoylate hisactophilin (Figure 2.1). The first NMT plasmid, pBB131, encodes the *Saccharomyces cerevisiae* NMT1 or yeast NMT1 (yNMT) for expression in *E. coli* (Duronio et al., 1990). Another NMT plasmid that is available for the myristoylation of hisactophilin encodes for human NMT. There are, however, two genetically distinct human NMTs which are denoted as hNMT1 and hNMT2 (Giang and Cravatt, 1998). Genes for hNMT1 and hNMT2 have been sub-cloned onto plasmids and were designated pHV641 and pHV644 respectively (Van Valkenburgh and Kahn, 2002). Along with cloning the human NMT genes, Van Valkenburgh and Kahn (2002) attempted to increase levels of myristoylation by increasing the expression of bacterial methionine aminopeptidase (MAP). Since the N-

terminal methionine of the protein must be cleaved prior to myristoylation, an insufficient level of MAP could lead to a decrease in protein myristoylation. To remedy this, the hNMT plasmids were modified by the insertion of the bacterial MAP gene (Van Valkenburgh and Kahn, 2002). These plasmids are denoted as pHV738 (hNMT1+MAP) and pHV739 (hNMT2+MAP). All of the NMT plasmids discussed are based upon the same parent plasmid and therefore have similar expression properties. That is all the NMT plasmids contain the p15A origin of replication and possess kanamycin resistance. Also, the NMT plasmids contain the IPTG inducible Ptac promoter for NMT expression; in the case of pHV738 and pHV739 MAP expression is endogenous (Duronio et al., 1990; Van Valkenburgh and Kahn, 2002). The NMT plasmids and hisactophilin plasmid (pHV and pHW, Figure 2.1) have different but compatible origins of replication.

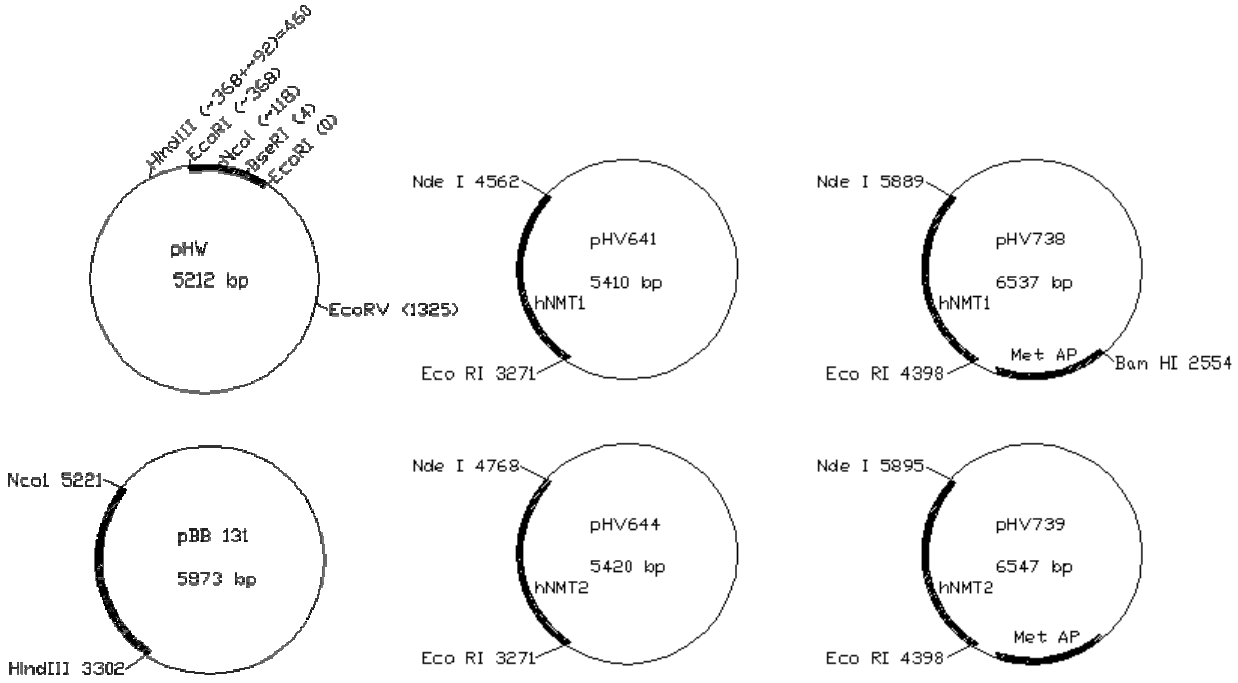

Figure 2.1 – Plasmids used for preparing myristoylated hisactophilin.
Restriction sites for pBB131 (encoding yeast NMT), pHW (encoding hisactophilin), human NMT1 (pHV641), human NMT1+MAP (pHV738), human NMT2 (pHV644) and human NMT2+MAP (pHV739). Coding sequences for various genes are shown by thick lines (Wong, 2002)

E. coli does not have endogenous NMT activity; therefore, to achieve myristoylation of a recombinant protein, a co-expression system is required (Duriono et al., 1990). These two plasmids encode or confer different antibiotic resistances (ampicillin for pHW and kanamycin for NMT), but use the same IPTG inducible Ptac promoter for expression. To allow for myristoylation, a co-expression system was created and the success of myristoylation was monitored by a slight modification to the protocol outlined by Knoll et al. (1995), which is described below.

The co-expression system for myristoylation was accomplished with *E. coli* cells, which were transformed with a plasmid encoding NMT and pHW by electroporation. Electroporation is a highly efficient (nearly 80%) means of transforming plasmid DNA into bacterial cells, as noted in the protocol outlined by Miller and Nikoloff (1995). Electroporation involves a structural rearrangement of the cell membrane caused by the application of a short electric field pulse. This electric field causes pore formation and the driving force to transport plasmids into the cell (Weaver, 1995). Upon transformation, simultaneous resistance to ampicillin (pHW plasmid) and kanamycin (NMT plasmid) was selected by plating transformed cells on media containing ampicilin and kanamycin (Sambrook *et al*., 1989). The plasmids of the transformed cells were induced and myristic acid incorporation was monitored using radioactive [^{3}H]myristic acid. Myristic acid penetrates across the plasma membrane by simple diffusion (Knoll and Gordon, 1993) and is then activated by the acyl-CoA synthetase fadD located on the inner membrane of the bacterial cell (Duronio et al., 1990). Cells were harvested by centrifugation and whole cell lysate was analyzed by SDS-PAGE and fluorography for the presence of myristoylated hisactophilin.

Fluorography was employed to visualize the radioactively labeled [^{3}H]myristic acid to ensure its covalent attachment to hisactophilin. Fluorography was used rather than simple autoradiography due to the low energy of tritium β-particles. Autoradiography is the direct exposure of the radioactive material to an x-ray film. This method of developing radioactively labeled gels is relatively straightforward; however, in this case, the energy of the emitted β particles is so low that they do not have sufficient energy to penetrate the acrylamide gel and contact the x-ray film. To remedy this problem associated with autoradiography, fluorography is used for most low energy β-emitters (Strahler *et al.*, 1989). Fluorography allowed for sufficient exposure under more tractable time frames. Fluorography involves the addition of a scintillant to the acrylamide gel which will absorb the energy of the radiation and re-releases the energy as fluorescent light (Strahler et al., 1989). This fluorescent light then can be easily visualized on x-ray film. In most cases, the scintillant 2,5-diphenyloxazole (PPO) is used and is introduced to the gel by way of dimethylsulfoxide (DMSO); however, for this work, a commercial fluorographic cocktail was used to simplify the process.

2.2 – Materials and Methods

2.2.1 – Plasmid Preparation

All plasmids were prepared by using a FlexiPrep™ Kit from GE Healthcare Life Sciences (Piscataway, NJ) according to the manufacturer's directions. Plasmids coding for hisactophilin (pHW1 and pHW3) were obtained from Hannah Wong. The pBB131 plasmid was obtained from Dr. Jeffery Gordon (Washington University School of Medicine). The plasmids encoding for hNMT along with those encoding Arf were graciously donated by Dr. Richard Kahn (Emory University, School of Medicine).

2.2.2 – Media preparation

LB media was prepared by dissolving 20g of LB (BioShop Canada Inc., Burlington, ON) in 1L of distilled deionized water (ddH_2O) and autoclaving. LB-agar plates were prepared by adding 15g of agar (BioShop Canada Inc.) to 1L of LB media and autoclaved to dissolve the agar. The LB-agar was then cooled to 50^oC using a water bath prior to adding ampicilin (100μg/mL) and kanamycin (30μg/mL). After adding antibiotics, approximately 30mL was poured into sterile plastic Petri dishes and allowed to set. Plates were stored at 4^oC; prior to use plates would be equilibrated at 37^oC.

2.2.3 – Preparation of Electrocompetent Cells and Transformation

Cell stocks (TG2 and BL21(DE3)) were made competent by inoculating 10mL of LB media and incubated at 37^oC with 200 rpm of shaking overnight. 5mL of this overnight culture was then used to inoculate 500mL of LB media which was allowed to grow to mid-log phase with an A_{600} of 0.7 at 37^oC with shaking at 200 rpm. Once cells

had reached mid log phase, they were placed on ice for approximately 20 minutes. Cells were harvested by centrifugation at 4000g for 15 minutes and at 4^{o}C. The supernatant was removed and the cells were washed by resuspending in 500mL of ice cold sterile 10% glycerol (EMD Pharmaceuticals, Durham, NC). The cells were collected again by centrifugation and the wash was repeated with 250mL and 20mL of the glycerol. The competent cells were resuspended in a final volume of 2mL of 10% glycerol, flash frozen in liquid nitrogen as 80uL aliquots and stored at -80^{o}C.

Plasmids coding for a target protein and hNMT2 were co-transformed into competent *E. coli* cells (strain TG2 for Hisactophilin and BL21(DE3) for hArf) by electroporation. The electroporation was performed with 40μL of competent *E. coli* cells mixed with 1μL of prepared plasmid which coded for the protein and 1μL of prepared plasmid which coded for hNMT2. This mixture was incubated on ice for 1 minute and transferred to a sterile electroporation cuvette with 0.1 cm electrode gap (Bio-Rad Laboratories, Hercules, CA) . The electroporation was performed using a Bio-Rad Gene Pulser (Bio-Rad Laboratories) and operated according to the manufacturers directions for the electroporation of *E. coli*. Immediately after electroporation, the transformed cells were added to 1mL of SOC (2% bacto-tryptone, 0.5% bacto-yeast extract, 10mM NaCl, 1.5mM KCl, 10mM Mg_2Cl, 10mM $MgSO_4$, 20mM glucose) and incubated at 37^{o}C with 200 rpm shaking for 1 hour to allow the cells to build antibiotic resistance. The transformed cells were then plated on agar plates containing 100μg/mL ampicillin (BioShop Canada Inc.) and 30μg/mL kanamycin (BioShop Canada Inc.) and incubated at 37^{o}C, overnight.

2.2.4 – Preparation of Radioactively Labeled [^{3}H]-Myristoylated Protein

Single colonies were isolated and used to inoculate 10mL LB cultures (containing 100μg/mL ampicillin and 30μg/mL kanamycin) incubated at 37^{o}C and 200 rpm shaking overnight. 150μL of the overnight culture was used to inoculate 15mL LB cultures (containing ampicillin and kanamycin) which were allowed to grow to A_{600} of 0.7 at 37^{o}C with shaking at 200 rpm. Once the cells reached an A_{600} of 0.7, both plasmids (coding for protein and NMT) were induced, simultaneously, with a final concentration of 1mM IPTG (BioShop Canada Inc.). Immediately, a 2mL aliquot of the induce cells was distributed to 200μCi of [^{3}H]myristic acid (Perkin Elmer Life Sciences, Inc., Boston, MA) which was prepared in a sterile 15mL falcon tube. [^{3}H]Myristic acid was prepared by drying 200μL of the stock solution (0.100μCi/mL [^{3}H]myristic acid) under nitrogen (which was filtered through a 0.2μm filter). The 2mL radioactive cultures were allowed to grow for 1.5 hours at 37^{o}C with 200rpm shaking. The cells were then harvested by centrifugation (4000g for 10 minutes) and the supernatant was removed by aspiration. The pellets were stored at -20^{o}C

.

2.2.5 – SDS-PAGE and Fluorography

Pellets were resuspended in 100μL of 1x SDS-PAGE loading buffer (125mM Tris pH 6.8, 4% SDS, 20% glycerol, 10% 2-mercaptoethanol). Samples were boiled for 10 minutes and gently centrifuged to collect water droplets. 4.5μL of each sample were loaded onto a 0.75mm thick, 10cm, self cast, 15% SDS-PAGE gel and run with a constant current of 8mA until the dye front reached the end of the gel (~3 hours). SDS-PAGE was performed using a Mighty Small II Gel Electrophoresis Unit (Pharmacia

Biotech Inc. San Francisco, CA). The gel was stained with coomassie brilliant blue R-250 (Sigma Chemical Company, St. Louis, MO).

Fluorography was performed by following the protocol set forth by Strahler *et al*. (1989). After the gel had been destained it was rinsed with ultra pure water filtered with a milliQ water system (Millipore Ltd., Bedford, MA) and treated with the commercial fluorographic cocktail, Amplify™ Fluorographic Reagent (Amersham Biosciences, Piscataway, NJ) for 30 minutes at room temperature and gentle agitation. The Amplify was decanted; the gel was rinsed with water and dried on Whatman No. 1 filter paper (VWR, Mississauga, ON) in a Bio-Rad model 443 slab dryer (Bio-Rad Laboratories) for 1.5 hours at 60°C. The x-ray film, Hyperfilm™ MP high performance autoradiography film (Amersham Biosciences) was cut to the same size as the gel (in complete darkness) and pre-flashed using an orange O2 filtered (Pentax Imaging Company, Westminster, CO) flash. In order for the film to have an absorbance at 540nm wavelength between 0.10 and 0.2 (after development) the flash was placed 90cm from the film and covered with 1 piece of Whatman No. 1 filter paper (VWR). After pre-flashing, the film was positioned against the gel and taped into an autoradiography cassette; the cassette was then placed into a lightproof bag stored at -80°C for the duration of the exposure. After a 10 day exposure, the X-ray film was warmed to room temperature prior to development. Under the safety light the film was immersed for 2 minutes with constant shaking in the Kodak GBX developer solution (Amersham Biosciences). This was followed by an approximately 15 second rinse with water and 4 minutes in the Kodak GBX fixer solution (Amersham Biosciences) with intermittent shaking. The film was then rinsed for at least 15 minutes and hung to dry.

2.3 – Results and Discussion

2.3.1 – Plasmid Expression in *E. coli*

All plasmids used for co-expression were checked for expression of the desired proteins in both TG2 and BL21(DE3) cell lines. Each plasmid was transformed into *E. coli*, induced with IPTG and whole cell lysate was analyzed by SDS-PAGE before and after induction. For each plasmid, bands increased in intensity after induction were seen and have expected molecular weight.

Figure 2.2 shows that the hisactophilin band runs slower than one would expect based on its known molecular weight of 13.5kDa. This is most likely due to the high number of histidine residues that are present in this protein. In addition, the pHW1 plasmid seems to have a rather leaky expression, as a fairly intense hisactophilin band is apparent prior to induction. It is difficult to ascertain if the NMT proteins also have leaky expression as the NMT band is in a crowded region of the gel. This may be problematic for achieving high yields of myristoylated protein since hisactophilin will be produced in the absence of the NMT protein and therefore myristoylation will not occur. In addition, as we discuss in the following chapter, myristic acid is not added to the initial media, so even if the NMT protein has a similar leaky expression (which may be expected for plasmids with similar promoters) the excess myristic acid will not be available for incorporation to these proteins being produced prior to induction.

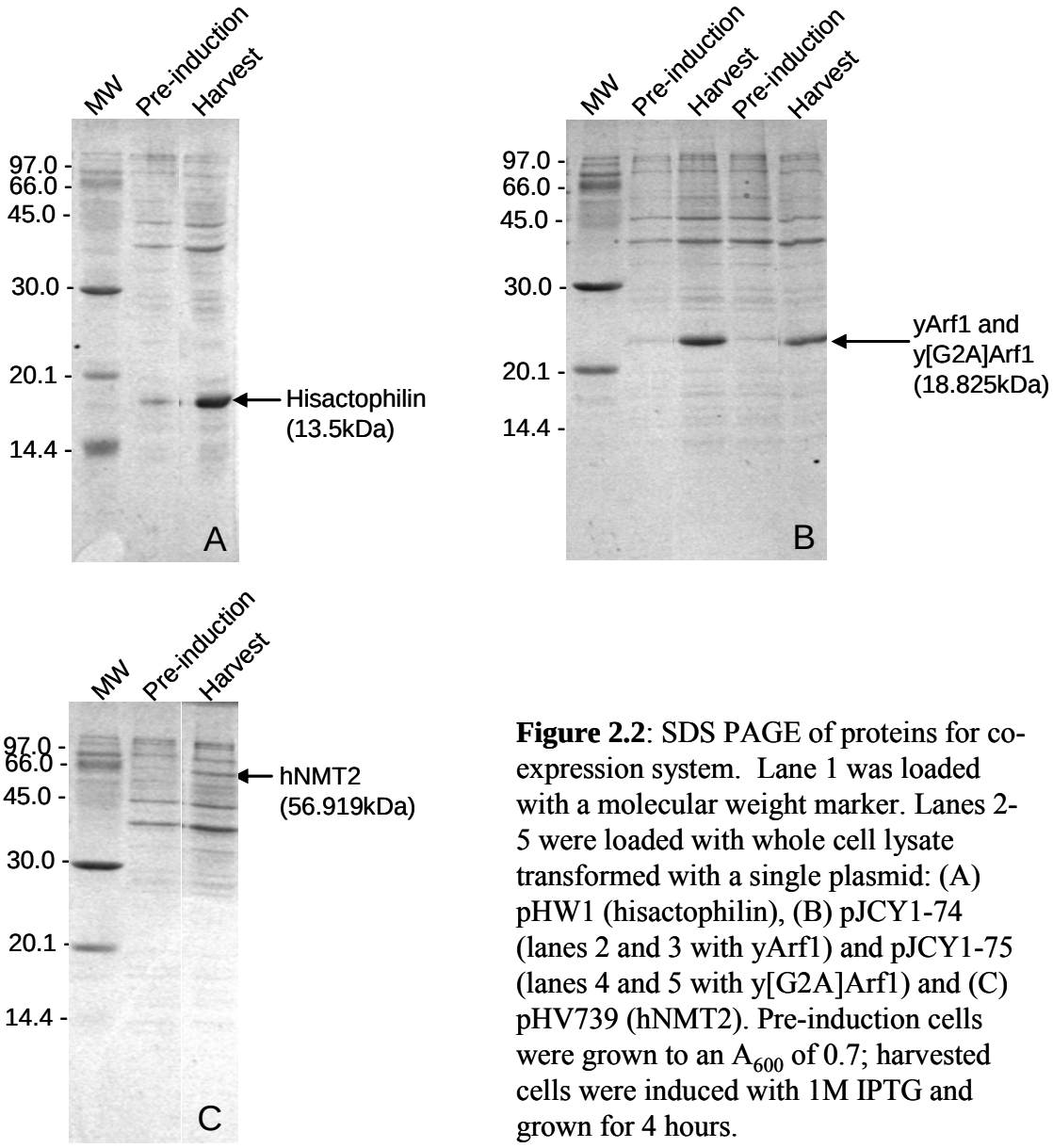

Figure 2.2: SDS PAGE of proteins for co-expression system. Lane 1 was loaded with a molecular weight marker. Lanes 2-5 were loaded with whole cell lysate transformed with a single plasmid: (A) pHW1 (hisactophilin), (B) pJCY1-74 (lanes 2 and 3 with yArf1) and pJCY1-75 (lanes 4 and 5 with y[G2A]Arf1) and (C) pHV739 (hNMT2). Pre-induction cells were grown to an A_{600} of 0.7; harvested cells were induced with 1M IPTG and grown for 4 hours.

2.3.2 – Verification of Co-Expression System by Radioactive Labeling

To produce myristoylated hisactophilin through a recombinant system in *E. coli,* a dual expression system of plasmids pHW1 (hisactophilin) and pHV739 (hNMT2 and MAP) was prepared in TG2 cells. The plasmid pHV739 was chosen for two reasons. Firstly, previous studies have shown that yNMT1 either does not myristoylate hisactophilin or does so at very low levels that were not detected by the methods that were employed previously to monitor incorporation (Wong, 2000). In addition the yNMT1 has the lowest sequence homology to hisactophilin's cognate NMT (the *D. discoideum* NMT). On the other hand, hNMT2 has the highest sequence homology to the *D. discoideum* NMT. In addition to coding for hNMT2, the pHV739 plasmid also codes for bacterial MAP. The additional MAP that will be produced from the plasmid should ensure that all N-terminal methionine is cleaved from the hisactophilin and allow for maximum levels of myristoylation.

To determine whether hisactophilin was properly myristoylated by the co-expression system, a number of controls were implemented. The first negative control consisted of the preparation of an *E. coli* TG2 cell line that carried only the pHW1 plasmid and a cell line that carried only the hNMT2 plasmid. For a positive control, the co-expression system was tested using the pHV739 (hNMT2) plasmid with a plasmid of a known NMT substrate. In this case, the plasmids used encode for yeast Arf1 which is designated as pJCY1-74; this system has already been successful in other studies (Duronio et al., 1990; Van Valkenburgh and Kahn, 2002). In addition to this plasmid which expresses Arf1, another negative control was applied using an NMT plasmid co-expressed with a plasmid designated pJCY1-75, which expresses a gly2-ala mutation of the yeast Arf1 (yeast [G2A]Arf1) protein. This mutation does not allow for

myristoylation because of the absence of N-terminal glycine. Like pHW, these plasmids confer ampicillin resistance; however, they have the ColE1 origin of replication and utilize the T7 promoter. Due to the T7 promoter of these plasmids, *E. coli* BL21(DE3) cells were needed to allow for expression.

Figure 2.3 shows that hisactophilin can be myristoylated using the co-transformed *E. coli* system. The control experiments (lanes 1, 4 and 6) show no incorporation of the radioactively labeled [^{3}H]myristic acid into the target proteins, while there is obvious incorporation of myristic acid with the yArf1 (lane 5) and hisactophilin (lane 2) seen in the fluorograph (figure 2.2 B). In addition, the fluorograph also shows high intensity signals for all lanes in the lower portion, which correspond to unused [^{3}H]myristoyl-CoA present in the whole cell lysate. Also, there are some low levels of myristoylation for other proteins indigenous to *E. coli* and happen to fit the somewhat loose consensus motif of hNMT2.

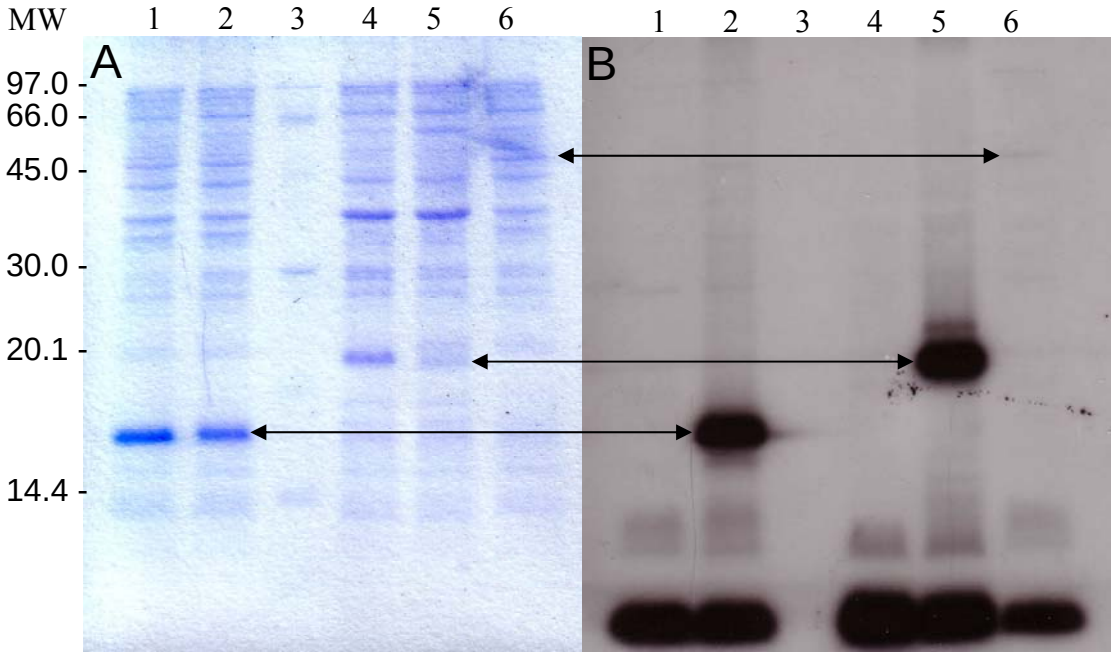

Figure 2.3: Visualization of myristoylation using a radioactively labeled ^{3}H myristic acid assay. (A) 15% SDS PAGE of myristoylated proteins; controls and (B) resulting x-ray film from fluorography. Lanes were loaded with whole cell lysate of cells transformed with the following plasmids: (1) pHW (hisactophilin only control), (2) pHW and pHV739 (myristoylated hisactophilin), (3) molecular weight marker, (4) pJCY1-75 and pHV739 (y[G2A]Arf1 negative control), (5) pJCY1-74 and pHV739 (myristoylated yArf1) and (6) pHV739 (hNMT2 only). Arrows indicate ^{3}H myristic acid incorporation for hisactophilin, Arf1 and a weak band corresponding to the migration of hNMT2. The large bands at the bottom of the fluorgram represent unincorporated ^{3}H-myrsitoyl CoA.

2.4 – Summary

The radioactively labeled [^{3}H]myristic acid test preparations clearly demonstrate that hisactophilin can be myristoylated using a dual plasmid system in *E. coli*. *E. coli* TG2 cells transformed with pHW1 (hisactophilin) and pHV739 (hNMT2 with MAP) allows for significant myristoylation of hisactophilin. In order to perform structural studies of the protein the preparation was scaled up for large scale purified of myristoylated hisactophilin, described in the following chapter.

CHAPTER 3 – OPTIMIZATION OF SCALED-UP PREPARATION AND PURIFICATION OF MYRISTOYLATED HISACTOPHILIN

3.1 – Introduction

In most cases, myristoylated proteins are purified in the same manner as their non-myristoylated forms because the two forms of the protein behave in a similar manner (Knoll *et al.*, 1995); however, in some cases, such as for hisactophilin, additional purification steps are required to separate unmodified protein (Fisher *et al.*, 2000; Haun *et al.*, 1992). Therefore, myristoylated hisactophilin has been purified previously in the same manner as non-myristoylated hisactophilin, with an additional purification step required to separate myristoylated and non-myristoylated forms of the protein. The purification protocol is a slight modification of that previously described by Scheel *et al.* (1989).

Myristoylated protein can be purified from a natural system or through an over expression system in *E. coli* (as outlined in section 1.1). An over expression system will result in higher protein yields compared to a natural system; however, the production of myristoylated protein in *E. coli* requires a dual expression system (*i.e.* one plasmid for target protein expression and one for NMT expression), because *E. coli* does not have endogenous NMT activity, which often results in a low efficiency of myristoylation. This has been found for some proteins such as $G_o\alpha$, recoverin and Arf proteins (Knoll *et al.*, 1995, Ray *et al*., 1992 and Khan *et al*., 1992, Yonemoto *et al.*, 1993); this was also found to be also true for the myristoylation of hisactophilin. Low levels of myristoylation have been speculated to be caused mainly by low solubility of the myristic acid in the bacterial cell environment (Van Valkenburgh and Kahn, 2002). In some

cases, to correct for poor solubility it may be necessary to substitute myristic acid with shorter acyl chains or myristic acid analogs (Van Valkenburgh and Kahn, 2002). A solution to the problem of low levels of myristoylation has been found through modification of induction times, inducer concentrations and growth temperatures. First, induction times and inducer concentration may need to be manipulated to find a good balance for optimal myristoylated protein (Randazzo and Kahn, 1995; Knoll *et al.*, 1995). A decreased temperature of incubation to decrease protein expression and lower the stress on the bacterial system may also be necessary (Knoll *et al.*, 1995). NMTs function well at 24^{o}C to 37^{o}C (Knoll *et al.*, 1995) and lowering the temperature to between 24^{o}C and 30^{o}C in some cases can increase myristoylation by 30% (Van Valkenburgh and Kahn, 2002). Therefore, variations in temperature, induction times and inducer concentration were examined to determine conditions for optimal myristoylation of hisactophilin.

In addition to the above growth conditions, the type of myristoyl substrate used may also have an affect on incorporation. A study of recoverin showed an increase in the level of myristoylation from 80% with myristic acid to 95% with sodium myristate; in addition, the total protein yield also doubled with the use of sodium myristate as opposed to myristic acid (Desmueles *et al.*, 2006). Since myristic acid is insoluble in water it is dissolved in ethanol prior to adding to cell cultures; the concentration of ethanol was suggested to be a cause for the low protein yields. Sodium myristate, on the other hand, is slightly soluble in water and ethanol is not required.

Another reason for possible low levels of myristoylation may be due to both plasmids pHW (for hisactophilin expression) and pHV738 (for hNMT1 expression), contain promoters which are induced by IPTG (see Figure 2.1 for plasmid maps). In

most cases of proteins that have been successfully myristoylated in *E. coli*, the target protein gene and the NMT gene are controlled by different promoters and use different inducing material (Knoll *et al.*, 1995). Since myristoylation is a co-translational modification, the protein NMT must be present and complexed with myristoyl-CoA prior to hisactophilin transcription to allow for the modification to occur. Since both plasmids were induced simultaneously, some hisactophilin was not myristoylated. This problem has been encountered previously in a study which attempted to prepare myristoylated recoverin (Yonemoto *et al.*, 1993). This problem has not been overly evident since the promoters in this system were somewhat leaky (as was discussed in section 2.3.1). That is, some NMT protein was produced prior to induction of hisactophilin.

The use of non-species-specific NMT may also be a reason for incomplete myristoylation of proteins (Knoll *et al.*, 1995). This type of problem has been seen for the myristoylation of human Arf proteins (Randazzo and Kahn, 1995; Van Valkenburgh and Kahn, 2002). This incompatibility is possible since, as stated in Chapter 1 (Section 1.2), the *D. discoideum* NMT has low sequence homology to both human NMTs and the commonly used yeast NMT. Also, comparing the phylogeny of various NMTs from different organisms, the NMT of *D. discoideum* is quite unique in its structure (Maurer-Stroh *et al.*, 2002) which may be a reason for decreased levels of myristoylation.

To separate myristoylated hisactophilin from non-myristoylated hisactophilin reverse-phase high pressure liquid chromatography (RP-HPLC) was employed. Previous studies have demonstrated that myristoylated and non-myristoylated hisactophilin can be resolved using RP-HPLC as illustrated in Figure 3.1 (Hanakam *et al*., 1995). The use of denaturing organic solvents for protein purification is not often employed; fortunately as

shown in this chapter hisactophilin refolds in a non-denaturing buffer with little protein loss.

The level of myristoylation is an important aspect for a large scale preparation of myristoylated hisactophilin, but total protein yield is also important. The growth conditions used in the protocol outlined in this chapter yielded relatively high level of myristoylation efficiency; however, total protein yield is low. Preliminary experiments to increase the total protein yield were conducted and discussed briefly. The purification protocol was examined closely to ensure that there was no significant loss in protein yield during each stage of purification.

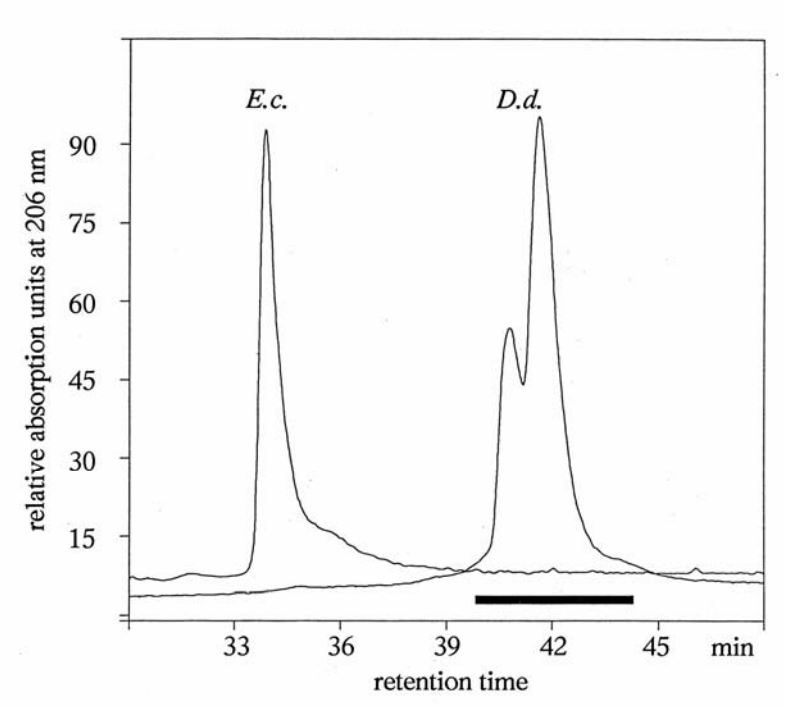

TFigure 3.1: T Comparison of myristoylated hisactophilin purified from *Dictyostelium* cells (*D.d.*) with non-myristoylated hisactophilin expressed in *E. coli* (*E.c.*). The proteins were run under identical conditions on a reversed-phase column with a linear acetonitrile gradient. Image from Hanakam *et al*. (1995).

3.2 – Materials and Methods

3.2.1 – Media and Substrate Preparation

Recombinant protein was prepared, depending upon the application, using rich media or M9 minimal media. Rich media was prepared by dissolving 20g of LB media (BioShop Canada Inc., Burlington, ON) in 1L of deionized and distilled water and autoclaving for 30 mintues. M9 minimal media (48mM Na_2HPO_4, 22mM KH_2PO_4, 8.5mM NaCl, 2mM $MgSO_4$, 0.1mM $CaCl_2$, 2% Glucose, 5μg/L Thiamine HCl, 0.5g/L NH_4Cl) was prepared from a 10x stock solution of M9 salts (480mM Na_2HPO_4, 220mM KH_2PO_4 and 85mM NaCl) diluted with distilled deionized water and autoclaved. After sterilization of the M9 salts, stock solutions of autoclaved 1M $MgSO_4$ and 0.1M $CaCl_2$ and stock solutions of filter sterilized (0.2μm filter) 0.05% Thiamine HCl, 20% Glucose and antibiotics (final concentration of 100μg/mL ampicillin and 30μg/mL kanamycin) were added to the media. Lastly, 0.5g/L of NH_4Cl was added directly to the media prior to inoculation.

Myristoylation substrates were prepared using either myristic acid or sodium myristate. Myristic acid stock solutions were prepared by dissolving myristic acid in methanol to a final concentration of 200mM and stored at -20^{o}C until needed. Sodium myristate stock solution was prepared by dissolving sodium myristate in sterilized water at 50^{o}C for 1 hour to a final concentration of 20mM. Sodium myristate solutions were prepared fresh for each growth and stored at 45^{o}C until added to the media.

3.2.2 – Preparation of Myristoylated Hisactophilin in Rich Media

To begin the preparation of myristoylated hisactophilin *E. coli* TG2 or BL21 (non DE3, *i.e.* they lack the T7 polymerase) cells were transformed with pHW1 (hisactophilin) and pHV738 (hNMT1+MAP) according to methods outlined in Chapter 2 (see Section 2.2.3). Single colonies of the double transformed cells were then used to inoculate 10mL of LB media with ampicillin (100ug/mL) and kanamycin (30ug/mL) which was incubated at 37^{o}C with 200 rpm shaking overnight. The entire 10mL overnight culture was then used to inoculate 1L of LB media (with ampicillin and kanamycin) which was again incubated at 37^{o}C and 200 rpm shaking until the cells had reached an A_{600} of approximately 0.2. At this point sodium myristate was added to a final concentration of 200μM and continued incubation. The culture was incubated for approximately 1 hour until it reached mid-log phase with an A_{600} of 0.7; the cells were then induce with IPTG to a final concentration of 1mM. Cells were allowed to grow for 5-7 hours before harvesting by centrifugation at 5000g for 10 minutes at 4^{o}C. Cell pellets were stored at -20^{o}C overnight or at -80^{o}C if longer storage times were needed.

3.2.3 – Preparation of Myristoylated Hisactophilin in M9 Minimal Media

Protein that was prepared in M9 minimal media for ^{15}N labeling was achieved in a similar manner as above but with some minor modifications. Double transformed *E. coli* BL21 cells were used to inoculate 10mL LB (with ampicillin and kanamycin) cultures incubated overnight at 37^{o}C with 200 rpm shaking. The 10mL LB overnight culture was then used to inoculate an intermediate culture of 100mL of M9 minimal media (with ampicillin and kanamycin and ammonium chloride). The intermediate culture was incubated at 37^{o}C with 200rpm of shaking until it reached an A_{600} of 0.7. 10mL of the

intermediate culture was used to inoculate 1L of M9 minimal media and then incubated at 37°C with 200rpm of shaking. Once the culture reached an A_{600} of approximately 0.4, sodium myristate was added to a final concentration of 200μM and incubation continued at 37°C. After approximately 1 hour, the culture reached mid-log phase with an A_{600} of 0.7 and was induced with IPTG to a final concentration of 1mM. Cells were allowed to grow for 7 hours before harvesting by centrifugation at 5000g for 10 minutes at 4°C. Cell pellets were stored at -20°C overnight or at -80°C if longer storage times were needed.

3.2.4 – Optimization of Myristoylation

Optimization of myristoylation and protein yield experiments followed similar methods but with modifications in the following parameters: NMT isoforms, growth temperature, IPTG concentration, substrate (myristic acid or sodium myristate) and substrate concentration. The protein concentration was determined by absorbance measurements at 280nm using an extinction coefficient of 0.330 for a 1mg/mL hisactophilin solution (Liu *et al.*, 2001).

3.2.5 – Purification of Myristoylated Hisactophilin

All of the optimization experiments used the following for protein purification protocol. The harvested cells (from 3L of media) were resuspended on ice in 25-50mL of buffer A (20mM Tris pH 8.0, 1mM EDTA). Cells were lysed using an EmulsiFlex-C5 homogenizer (Avestin Inc., Ottawa, ON) at a pressure of at least 17000psi according to the manufacturer's directions. To extract membrane-bound hisactophilin, the lysate was incubated with 0.5% CHAPS (BioShops Canada Inc.) with constant stirring at 4°C for 2

hours. After incubation the cell debris was collected by centrifuging the lysate at 50000g for 25 minutes at 4°C. The supernatant was collected and filtered using a 0.4μm filter.

Initially, a crude purification of the protein is achieved by anion exchange chromatography. Anion exchange chromatography was performed at 4°C. The 50mL cell lysate was loaded at 3mL/min onto a self-packed 2.5×50cm DEAE-Sepharose Fast Flow (Sigma Chemical Company, St. Louis, MO) anion exchange column pre-equilibrated with 2L of buffer A (20mM Tris pH 8.0, 1mM EDTA) using the BioLogic LP chromatography system (Bio-Rad Laboratories, Hercules, CA). The column was washed with 90mL of buffer A at 2mL/min. The protein was eluted using a 0-100% buffer B (20mM Tris pH 8.0, 1mM EDTA and 400mM NaCl) linear salt gradient over 700mL at 2mL/min. Hisactophilin elutes between 140-240mM NaCl. Fractions identified by SDS-PAGE to contain hisactophilin were collected and concentrated to approximately 7.5mL using a 3kDa cutoff YM-3 Amicon (Millipore, Billerica, MA) filter.

The second step of purification was achieved using size exclusion chromatography. A 5×60cm G75-Superdex Size Exclusion column (Pharmacia, Piscataway, NJ) was equilibrated with 1 column volume (approximately 300mL) of size exclusion buffer (150mM Tris pH 8.0, 1mM EDTA, 1mM DTT) using a BioCad Sprint Perfusion Chromatography System (Perceptive BioSystems, Ramsey, MN). The concentrated fractions from anion exchange chromatography were diluted to 15mL with a 2× size exclusion buffer and injected onto the column over 3 injections using a 5mL loop. The protein was eluted with size exclusion buffer at 3ml/min. Fractions identified by SDS-PAGE to contain hisactophilin were exchanged into ultra pure water using a 1000×

dilution with a 3kDa cutoff YM-3 Amicon filter and the protein was concentrated to 15mL using the Amicon filter. The protein was further concentrated to 1mL using a 3kDa cutoff YM-3 Centriprep® Centrifugal Filter (Millipore).

To separate myristoylated hisactophilin from non-myristoylated hisactophilin reverse phase HPLC was employed. The protein was loaded onto a Bondapak RPC18 column (15-20μm 25x100mm) (Waters, Milford, MA) using a Waters 600 HPLC Pump and Gradient Controller equipped with a 996 Photodiode Array Detector (Waters) and a 1mL sample loop. The column was pre-equilibrated with 5-10 column volumes (250-500mL) of a 98:2 mixture of solvent A (0.1% trifluoracetic acid in water) and solvent B (0.1% trifluoracetic acid in acetonitrile). Protein was eluted at a flow rate of 10mL/min with a linear gradient of 2-62% B in A over 60 minutes (*i.e.* 1% per minute). The eluted myristoylated protein was collected and immediately dialyzed against 25mM ammonium carbonate, concentrated with a 3kDa cutoff YM-3 Amicon filter and flash frozen in liquid nitrogen. Protein was stored at -80^{o}C.

Calculation of percent yield after each stage of purification was achieved collecting aliquots of each stage and analyzed by SDS- PAGE as outlined in Section 2.2.5. The intensity of bands for each lane was then analyzed and peaks corresponding to hisactophilin were integrated using the ImageJ (U. S. National Institutes of Health, Bethesda, MA) software package.

3.2.6 – Circular Dichroism Spectroscopy

CD measurements were performed using a J715 spectrapolarimeter (Jasco Inc., Easton, MD) with a 1mm path-length cuvette. Temperature was kept constant at 25^{o}C using an Elfin Model ELDC5D4 Peltier-controlled sample cell (Jasco Inc. Easton, MD).

Protein samples were prepared by dialyzing into 25mM ammonium carbonate (after RP-HPLC) and dilution to a final protein concentration of 20μM (0.25mg/mL). Denatured samples were prepared using lyophilized protein reconstituted in 20mM acetic acid at the same concentration. Scans were acquired with 1mm path-length cuvette over a wavelength range of 280-190nm with a step of 0.5nm; data were collected as an average of 5 scans and no further processing was completed.

3.2.7 – Mass Spectrometry

Mass spectrometry samples were prepared by diluting a 2× protein sample in H_2O with a 0.4% TFA in acetonitrile for a final protein concentration of approximately 7μM. Samples were analyzed using a Micromass Q-TOF Ultima™ Global instrument (supplied by the University of Waterloo Mass Spectrometry Facility) using electrospray ionization.

3.3 – Results and Discussion

3.3.1 – Purification of Recombinant Myristoylated Hisactophilin

Previously, purification of recombinant non-myristoylated hisactophilin was achieved using a two step process consisting of DEAE anion exchange chromatography followed by size exclusion chromatography (Liu, 1999). With the incorporation of a myristoyl group into the protein, it was necessary to add an additional reverse phase HPLC purification step. This purification step is necessary to separate myristoylated hisactophilin from non-myristoylated hisactophilin since not all hisactophilin produced was myristoylated. Incomplete myristoylation may be caused by the leaky expression of hisactophilin as well as incompatibilities of hNMT with hisactophilin (as discussed above).

Both myristoylated and non-myristoylated hisactophilin co-elute during anion-exchange chromatography at a relatively low salt concentration. Figure 3.2 illustrates that both forms of the protein co-elute at between 140-220 mM salt. The fractions collected during this first step of purification show only the presence of a small number of high molecular weight proteins remain. These high molecular weight proteins are easily separated from hisactophilin using size exclusion chromatography. This second stage of protein purification yields a highly pure mixture of myristoylated and non-myristoylated hisactophilin. The myristoyl group only adds an additional mass of 228Da to the protein which did not to allow for differentiation of the two forms of the protein by this separation method (Figure 3.3).

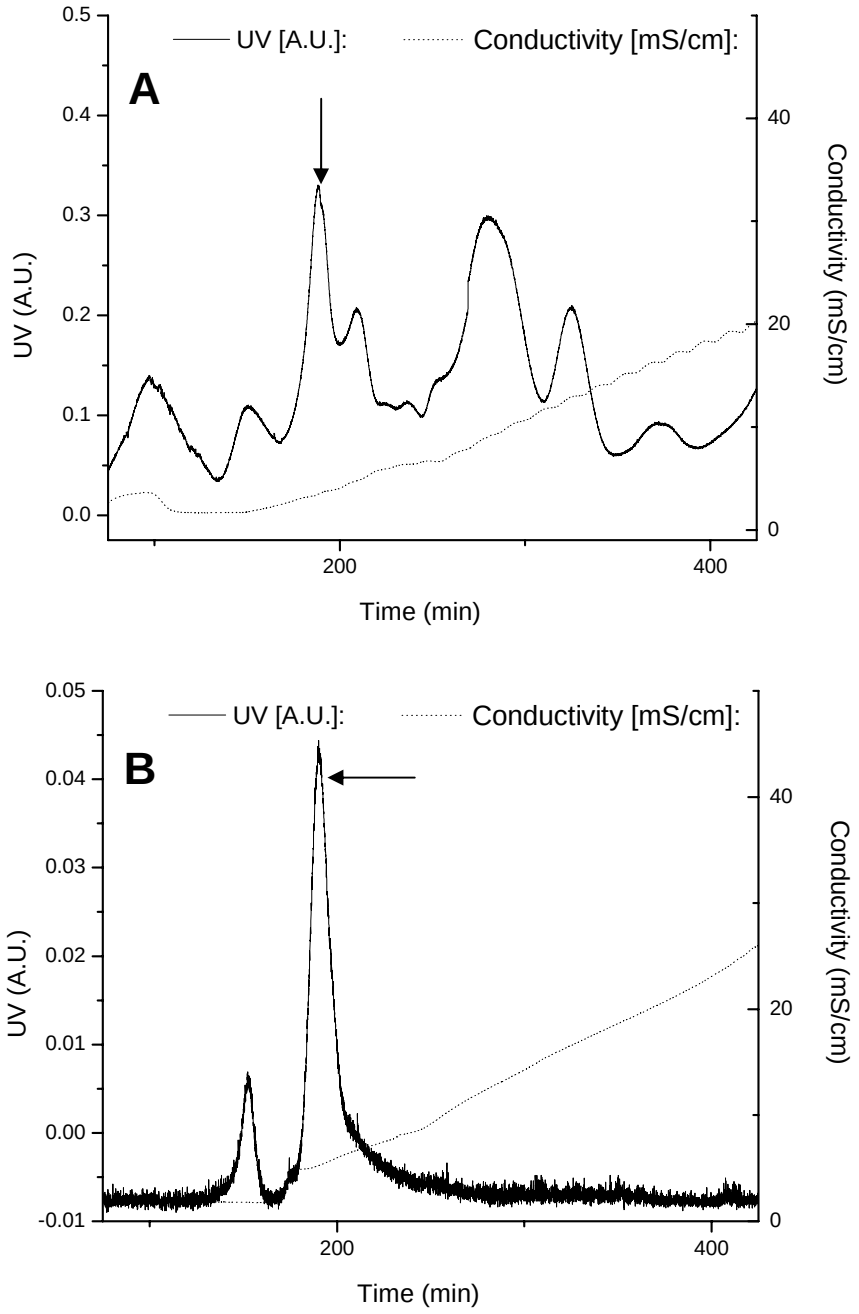

Figure 3.2: DEAE anion exchange elution profiles for myristoylated hisactophilin preparation. (**A**) Typical elution profile of myristoylated hisactophilin from whole cell lysate. (**B**) Elution of a standard pure non-myristoylated hisactophilin sample. Arrows indicate the location of hisactophilin.

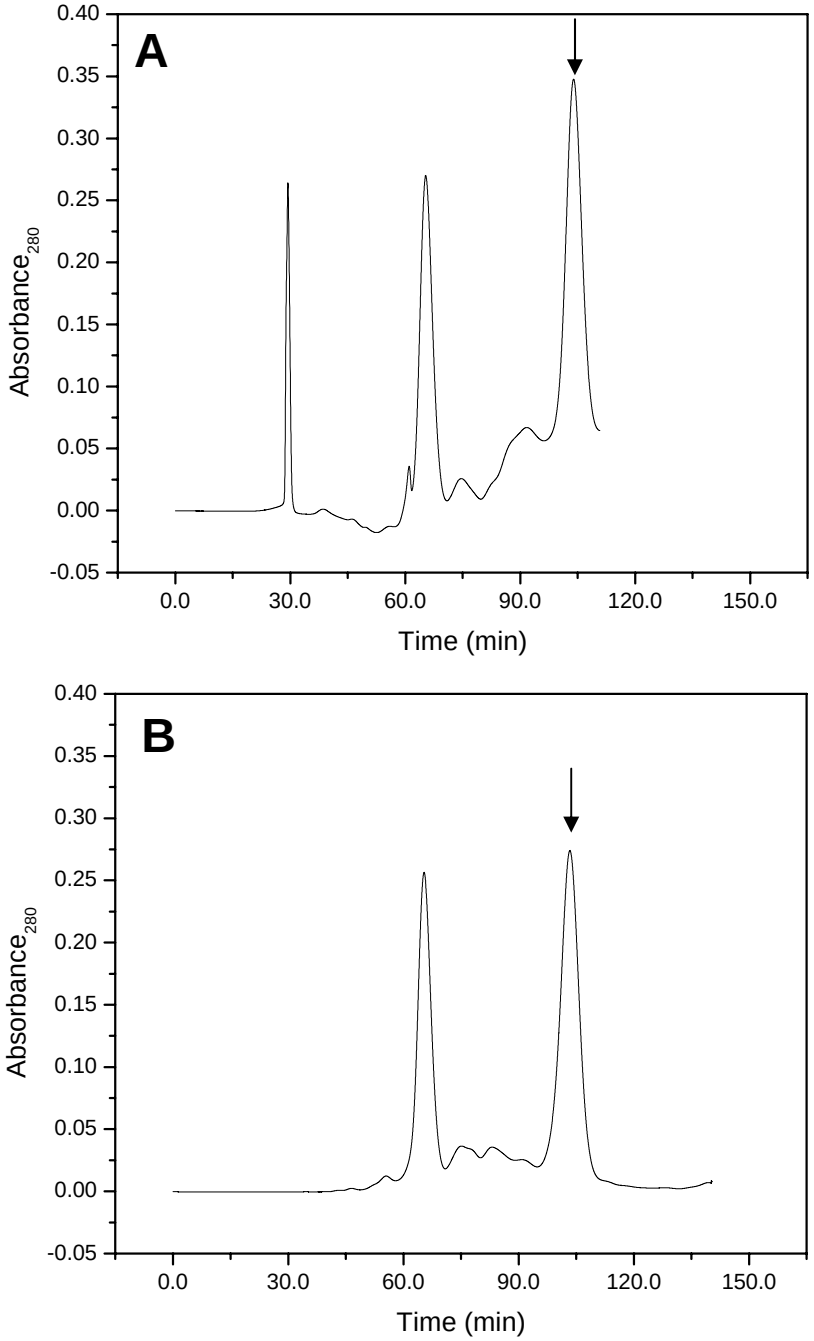

Figure 3.3: Size exclusion chromatography for the purification of hisactophilin. The elution curves are from a purification of (**A**) non-myristoylated hisactophilin and (**B**) myrisotylated hisactophilin. Arrows indicate that the elution of both myristoylated and non-myristoylated protein are the same with a retention time of 103 minutes.

Furthermore in SDS-PAGE both myristoylated and non-myristoylated forms of the protein migrate at the same rate (Figure 3.4A). Likewise, native PAGE also shows no differences in the manner in which they migrate (Figure 3.4B). The gels, along with the above purification protocol, are a good indication that the presence of the myristoyl group does not significantly alter the overall physical characteristics of the protein.

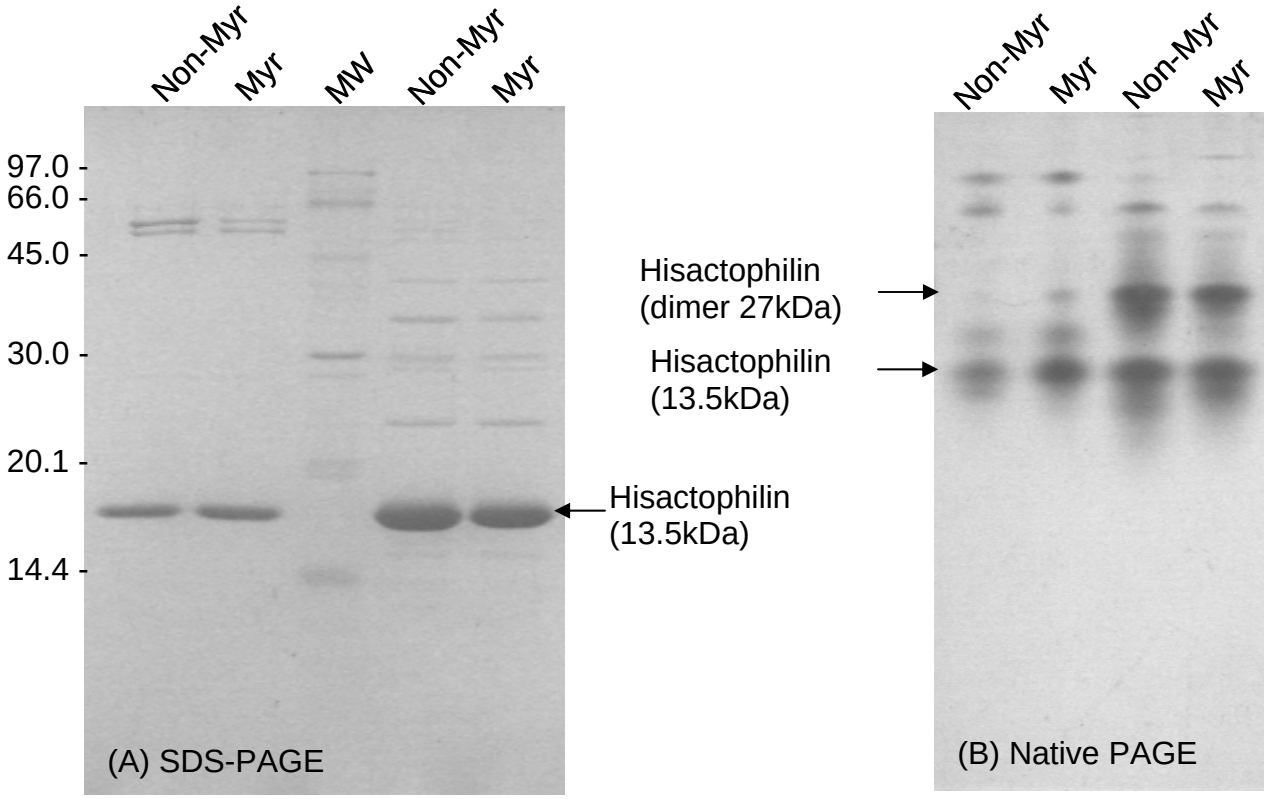

Figure 3.4: Fractions collected from DEAE anion exchange column. (**A**) Two different fractions were analyzed by SDS-PAGE for both non-myristoylated (Non-Myr) and myristoylated (Myr) hisactophilin preparations. Each fraction shows a number of higher molecular weight proteins which were separated by size exclusion chromatography. (**B**) Same fractions run on a native-PAGE. Note that neither SDS- or native-PAGE show different migration for myristoylated and non-myristoylated protein. MW represents the molecular weight marker.

Separation of myristoylated and non-myristoylated forms of the protein was initially attempted, unsuccessfully, under non-denaturing conditions by hydrophobic interaction chromatography (results not shown). However, the denaturing conditions of C18 reverse-phase HPLC proved to be sufficient for the separation. This method of separation has been employed for the purification of other myristoylated proteins which have low-efficiency of myristoylation (Hughes *et al*., 1995). In the reverse-phase HPLC elution profiles of myristoylated hisactophilin there are three well resolved peaks with a retention time between 30 and 45 minutes (Figure 3.5A). The non-myristoylated form of the protein elutes with a retention time of 33.2 minutes, whereas, the myristoylated form of the protein has a retention time of 43.1 minutes; these retention times are similar to those found previously by Hanakam *et al*. (1998) and was confirmed by mass spectrometry (Appendix 1). The myristoylated form of the protein will have a much higher hydrophobicity due to the myristoyl group and therefore will elute later. The third peak in the elution profile has a retention time of 40.3 minutes and is most likely hisactophilin that has been modified with an acyl chain other than myristate. The activity of hNMT is not highly selective for myristoyl CoA and may attach other fatty acids (Bhatnagar *et al.*, 1999). This elution profile was also observed protein was prepared without excess sodium myristate (*i.e.* hisactophilin preparation using dual transformed system without adding sodium myristate). Although myristic acid is a rare cellular fatty acid, *E. coli* has some endogenous myristic acid available for myristoylation to occur in the absence of excess sodium myristate (Gordon *et al.*, 1991).

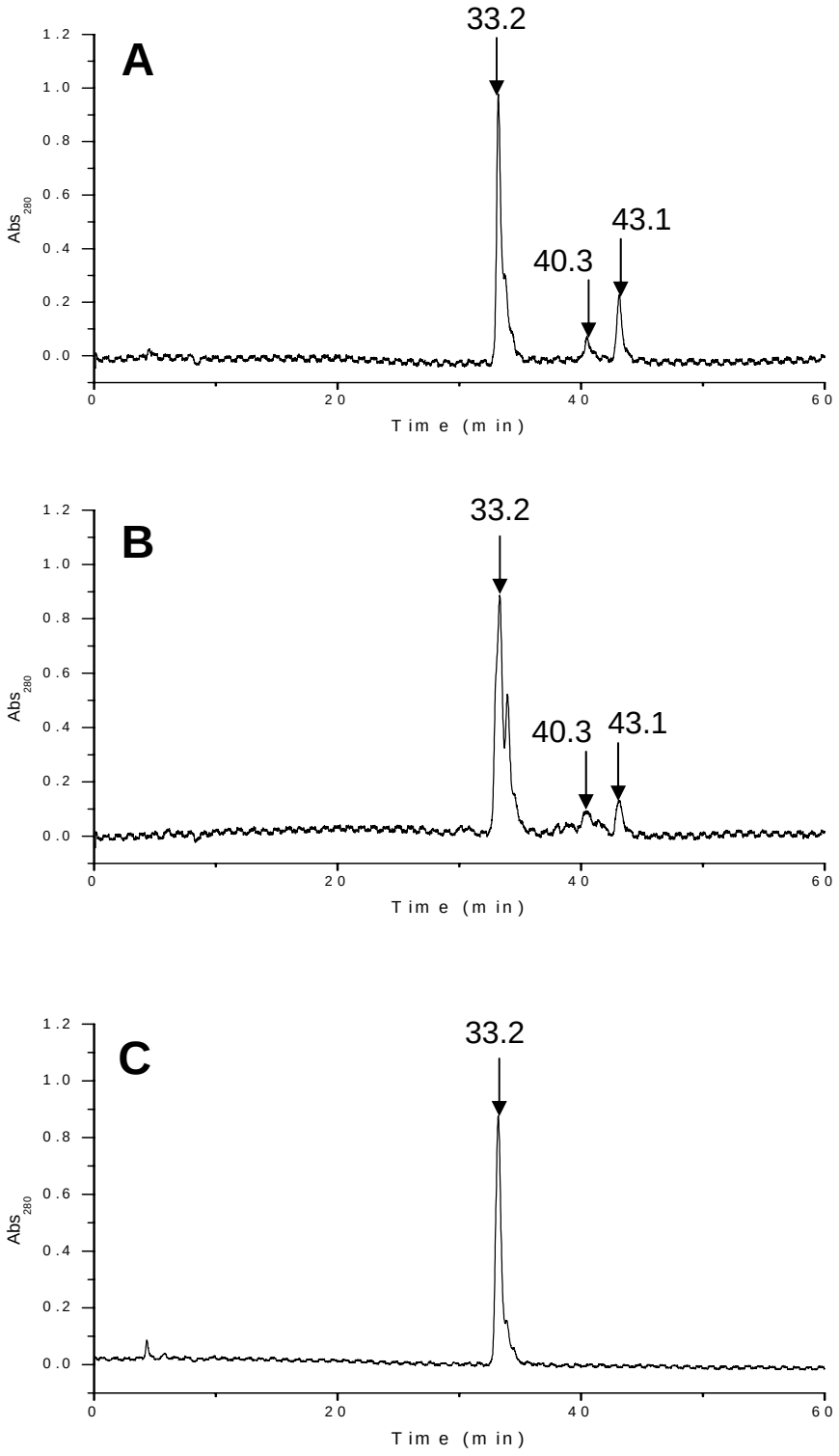

Figure 3.5: C18 RP-HPLC purification of hisactophilin. (**A**) Myristoylated hisactophilin preparation with hNMT2 indicating retention times for non-myristoylated protein (33.2min), acylated protein (40.3min) and myristoylated protein (43.1min). (**B**) Hisactophilin preparation with hNMT2 but no additional myristic acid substrate indicating same retention times as A; myristoylated protein has a much lower incorporation rate. (**C**) Non-myristoylated hisactophilin preparation indicating elution of only non-myristoylated protein (33.2min).

In this case (Figure 3.5B), the elution profile still shows the presence of three well resolved peaks corresponding to non-myristoylated hisactophilin, myristoylated hisactophilin and a third acylated hisactophilin. Only when hisactophilin is prepared using a system lacking NMT (Figure 3.5C), there is one distinct peak corresponding to the non-myristoylated form of the protein.

It was important to ensure that after separating denatured myristoylated and non-myristoylated forms of hisactophilin by reverse phase chromatography that the protein can refold to its native state in a non-denaturing buffer. Non-myristoylated hisactophilin has been shown previously to refold with high reversibility under many solution conditions (Lui *et al*, 1999). The refolding of myristoylated hisactophilin was verified, initially by circular dichroism spectroscopy, and later confirmed by NMR (see Section 4.3). In most cases, the myrsitoylated and non-myristoylated forms of a protein yield nearly identical CD spectra (Resh, 1999), which is also true for hisactophilin (see Figure 1.13 for CD spectra of myristoylated and non-myristoylated hisactophilin) (Hanakam, 1996). From Figure 3.6 it is clear that hisactophilin undergoes renaturation after dialysis into non-denaturing buffers.

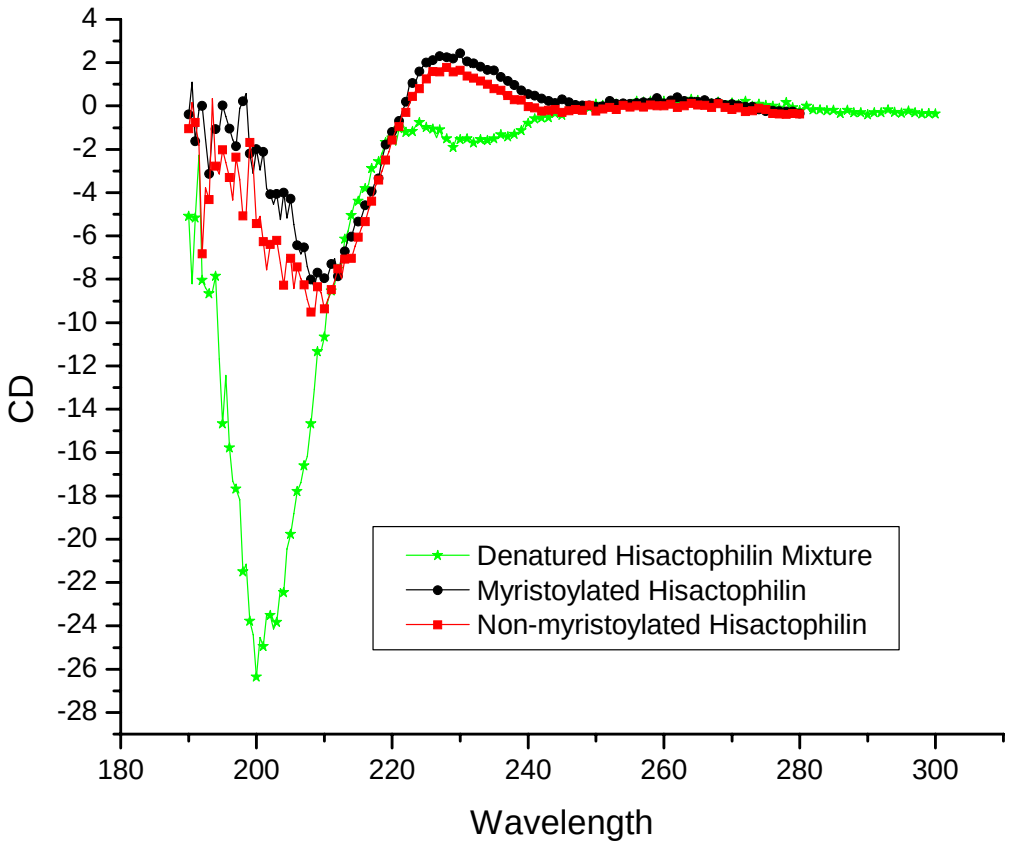

Figure 3.6: Circular Dichroism Spectra of myristoylated, non-myristoylated and denatured hisactophilin. Results are displayed as raw CD (A.U.) data with no processing. Myristoylated and non-myristoylated scans are nearly identical. In addition, dialyzing protein into ammonium carbonate causes the protein to refold after exposure to the denaturing conditions of C18 RP-HPLC.

3.3.2 – Optimization of Myristoylation and Total Protein Yield

Reverse phase HPLC was required for the purification, but also provides a means to monitor levels of myristoylation. The myristoylation levels were simply determined by integrating the area of the peaks within the elution curve to calculate the percent myristoylation. This, along with yield of purified protein, was used to determine conditions for obtaining the best possible yield of myristoylated hisactophilin from this system by manipulating a number of different growth parameters. The parameters investigated included: growth temperature, IPTG concentration, NMT isoform, substrate, substrate concentration and growth media. The results of these optimization experiments are summarized in Table 3.1 and are further discussed below.

3.3.2.1 – Growth Temperature

In some cases levels of protein myristoylation have been increased significantly by lowering the growth temperatures (Van Valkenburgh and Kahn, 2002). For hisactophilin, a decrease in the growth temperature for the cells caused a significant decrease in the level of myrisoylation. Protein prepared at 37^{o}C (with hNMT2, 200μM myristic acid and 1mM IPTG) was 22% myristoylated, which decreased to 15% at 30.5^{o}C and as low as 5% at 24^{o}C (Figure 3.7A and 3.8). In most cases a decrease in temperature will slow down protein expression, which in turn puts less stress on the cells and allows for an increased level of myristoylation (Van Valkenburgh and Kahn, 2002).

Table 3.1: Summary of all growth parameters tested for optimization of myristoylation of hisactophilin

Growth Parameters										
Cells	**Media**	**NMT**	**Substrate**	**[Substrate]** (μM)	**Temperature** (^{o}C)	**[IPTG]** (mM)	**Induction Time** (hrs)	**%**	**Total Hisactophilin** (mg/L of prep)[a]	**Total Myristoylated Hisactophilin** (mg/L of prep)[a]
TG2	LB	hNMT2	Myristic Acid	200	37	1	7	22	*27*	*5.8*
TG2	LB	hNMT2	Myristic Acid	200	30.5	1	10.5	17	*33*	*5.6*
TG2	LB	hNMT2	Myristic Acid	200	24	1	13.5	5	*48*	*2.4*
TG2	LB	hNMT2	Myristic Acid	200	37	0.5	10	17	*24*	*4.0*
TG2	LB	hNMT2	Myristic Acid	200	37	0.25	10	19	*20*	*3.8*
TG2	LB	hNMT2	Myristic Acid	200	37	0.1	12	4	*14*	*0.6*
TG2	LB	hNMT2	Myristic Acid	200	24	0.1+0.1	12	2	*16*	*0.3*
TG2	LB	hNMT1	Myristic Acid	200	37	1	4	49	*7.8*	*3.8*
TG2	M9	hNMT1	Myristic Acid	200	37	1	5	12	*3.3*	*0.4*
BL21	LB	hNMT1	Sodium Myristate	200	37	1	4	84	13.6	11.4
BL21	M9	hNMT1	Sodium Myristate	200	37	1	7	58	5.7	3.3
BL21	M9	hNMT1	Sodium Myristate	80	37	1	7	56	*5.6*	*3.2*

[a] Mass of total protein was calculated from preliminary experiments and needs to be verified for accuracy

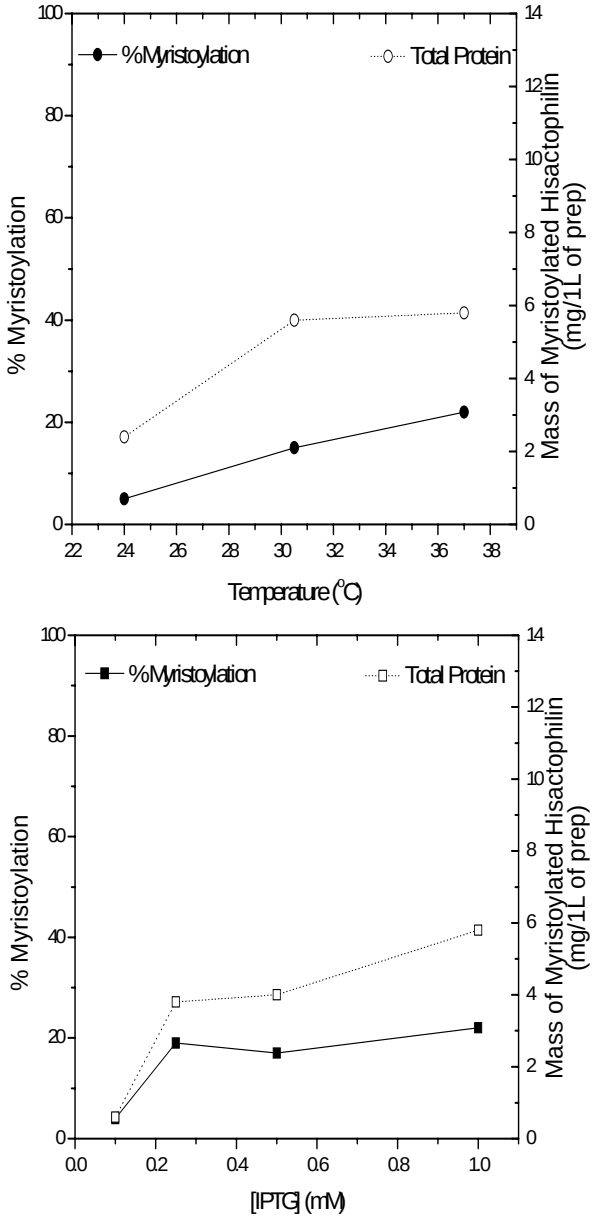

Figure 3.7: Optimization of myristoylation for hisactophilin. (A) optimization of temperature. (B) Optimization of IPTG concentration. It appears to have the highest incorporation of myristoyl along with highest protein yield cells should be grown at 37P^{oP}C and induced with 1mM IPTG.

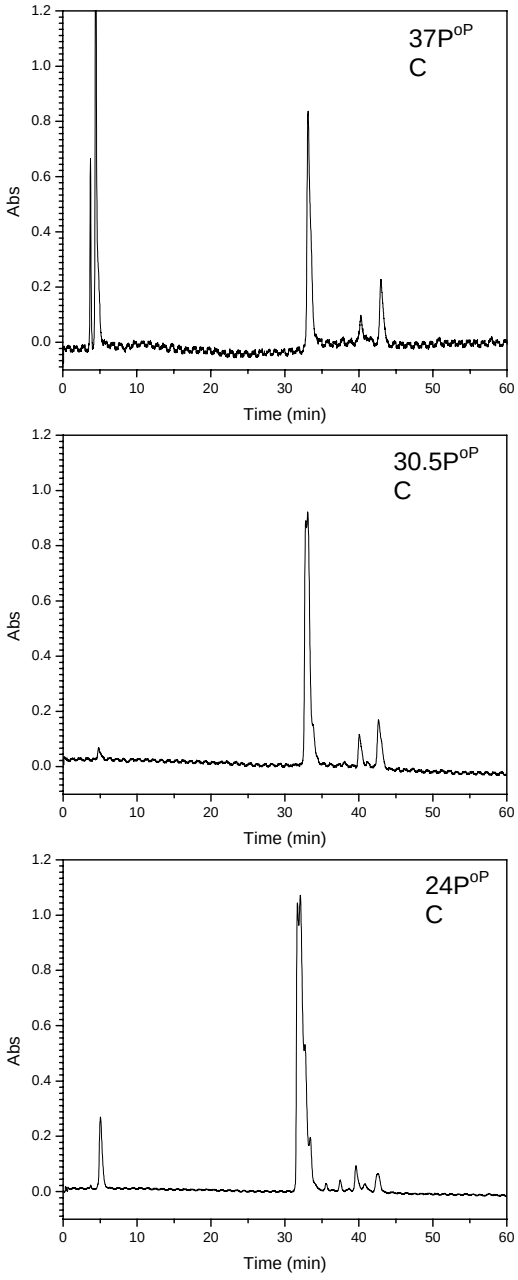

Figure 3.8: HPLC Elution profiles of myristoylated hisactophilin preparation at various temperatures. Myristoylation levels decrease with temperature. Also note that at 24P^{oP}C has a different elution profile as described in the text

In addition to a decreased level of myristoyl incorporation at 24°C, RP-HPLC elution curves also showed the presence of additional contaminating peaks with retention times around 40 minutes (Figure 3.8C). These additional peaks may be caused by the incorporation of a number of different acyl chains other than myristic acid being incorporated into the protein by NMT.

3.3.2.2 – IPTG Concentration

For a similar reason as above for temperature, the concentration of IPTG added to induce the production of protein influences the levels of myristoylation. A decrease in IPTG concentration caused a decrease in the levels of myristoylation. Protein prepared with 1mM IPTG (with hNMT2, 200μM myristic acid and at 37°C) showed the highest level of incorporation of 22% whereas decreasing IPTG to 0.1mM decreased the incorporation to a mere 4%. However, a two-fold decrease in IPTG concentration to 0.5mM resulted in only minor suppression of myristoylation with levels of incorporation at 17% and further decrease to 0.25mM IPTG gave a myristoylation level of 19% (Figure 3.7B). This implies that the concentration of IPTG above 0.25mM does not have a large affect on the level of myristoylation.

3.3.2.3 – NMT Isoform

Although the hNMT2 system could be used for preparing myristoylated hisactophilin (as shown in Section 2.3.2) it gave rather low levels of incorporation. Hisactophilin prepared with hNMT2 (200μM myristic acid, 1mM IPTG and at 37°C) had only 22% incorporation (Figure 3.9A). On the other hand, the hNMT1 system (200μM myristic acid, 1mM IPTG and at 37°C) gave a much higher level of myristoylation at

49% (Figure 3.9B). Unfortunately, from preliminary results the system using hNMT1 has a much lower total protein yield. These results were calculated from a single purification and were allowed to grow for different induction times therefore these values need to be verified by further experimentation.

3.3.2.4 – Myristoyl Substrate

The use of myristic acid as a substrate has a two-fold negative impact on the level of myristoylation. According to studies on the preparation of myristoylated recoverin, the methanol used to solubilize myristic acid decreases total protein yield and, additionally, water soluble sodium myristate has a higher efficiency of incorporation (Desmueles *et al*., 2006). This study also shows an increase in both total protein yield and level of myristoylation when using sodium myristate as opposed to myristic acid. The level of myristoylation increases from 49% with myristic acid to 84% with sodium myristate (Figure 3.9C and Table 3.1). Likewise, the total protein yield increases total protein yield from 7.8 mg to 13.6 mg per 1L of media when using sodium myristate.

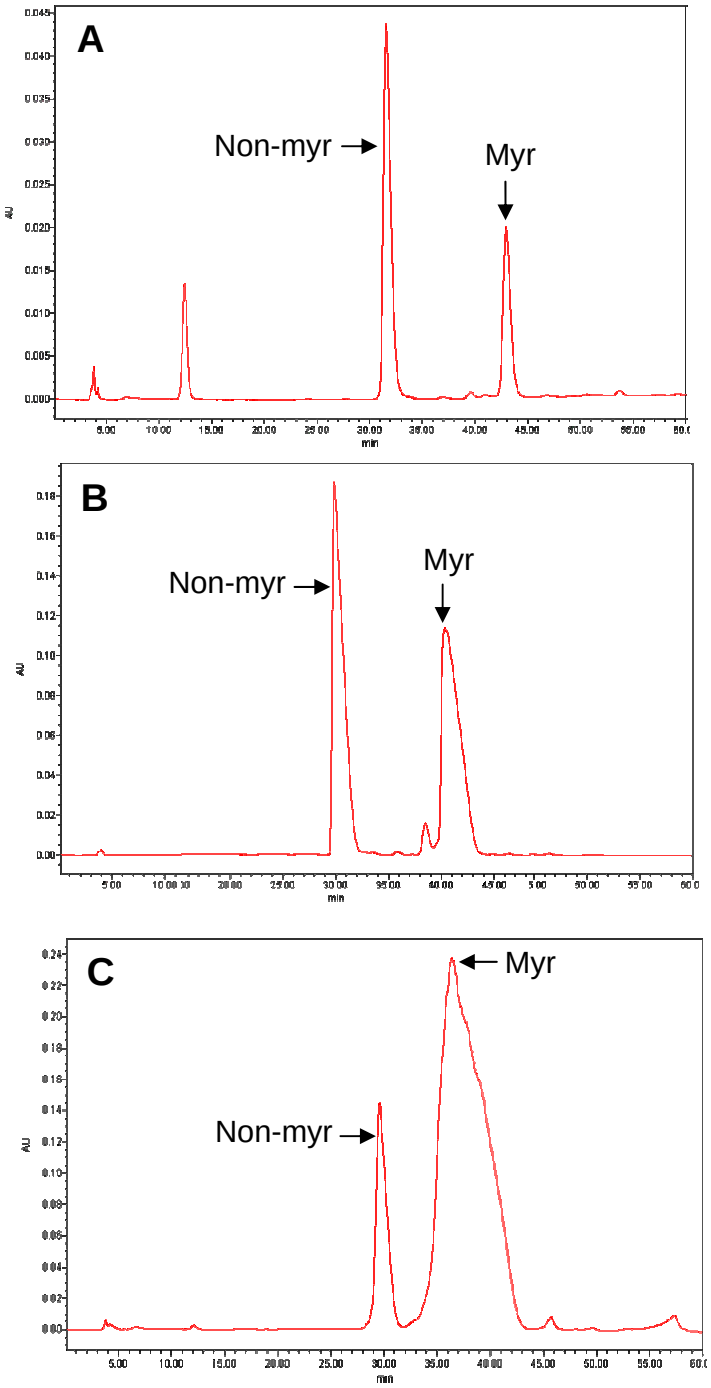

Figure 3.9: HPLC elution curve of myristoylated hisactophilin for various growth conditions. (**A**) Co-expression system with hNMT2 and myristic acid (22% myristoylation), (**B**) Co-expression system with hNMT1 myristic acid (49% myristoylation) and (**C**) Co-expression system with hNMT1 and sodium myristate (84% myristoylation.

3.3.2.5 – M9 Minimal Media

Detailed structural analysis of myristoylated hisactophilin (described in the following chapter) required the preparation of ^{15}N-labeled protein. ^{15}N-labeled myristoylated hisactophilin was prepared by combining the above procedure for preparing myristoylated protein with established procedures for preparing ^{15}N-labeled non-myristoylated hisactophilin using ^{15}N-enriched minimal media (Houliston, 2002). Using M9 minimal media (containing ^{15}N-labeled ammonium chloride as the sole nitrogen source) also had an impact on the level of myristoylation and the total protein yield. The use of M9 minimal media caused the level of myristoylation to drop to 58% incorporation as opposed to 84% when grown for rich LB media. In addition, minimal media only yields 3.3 mg of total protein per 1L of media. Although it would be preferable to have a higher yield, this yield was sufficient to pursue NMR studies, described in the next chapter.

3.3.3 – Percent Yield for Purification Stages of Myristoylated Hisactophilin

In order to ensure that the protocol outlined for the purification of myristoylated hisactophilin the total protein percent yield for each stage of purification was checked. As there is no simple activity assay available, the percent yield for each stage of hisactophilin purification was measured by monitoring SDS-PAGE band intensities. At each stage of purification an aliquot was taken. Analysis of band intensity shows that for both preparation in rich LB media (Figure 3.10) and M9 minimal media (Figure 3.11) have minor loss of the total protein during each stage of purification detailed in Table 4.2. RP-HPLC has, as expected, a much higher loss of protein since only 85% in rich media and 58% in minimal media was myristoylated.

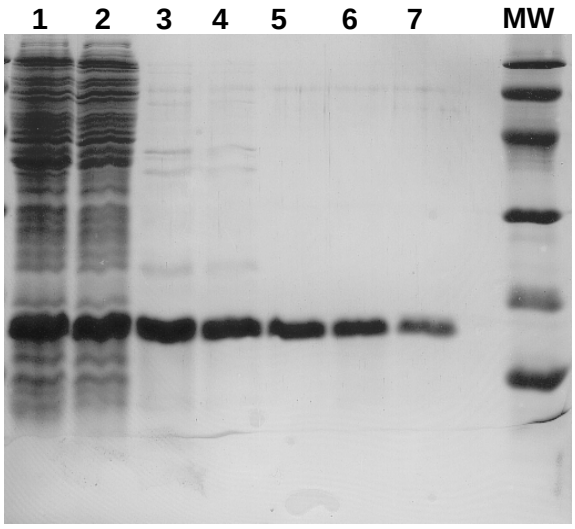

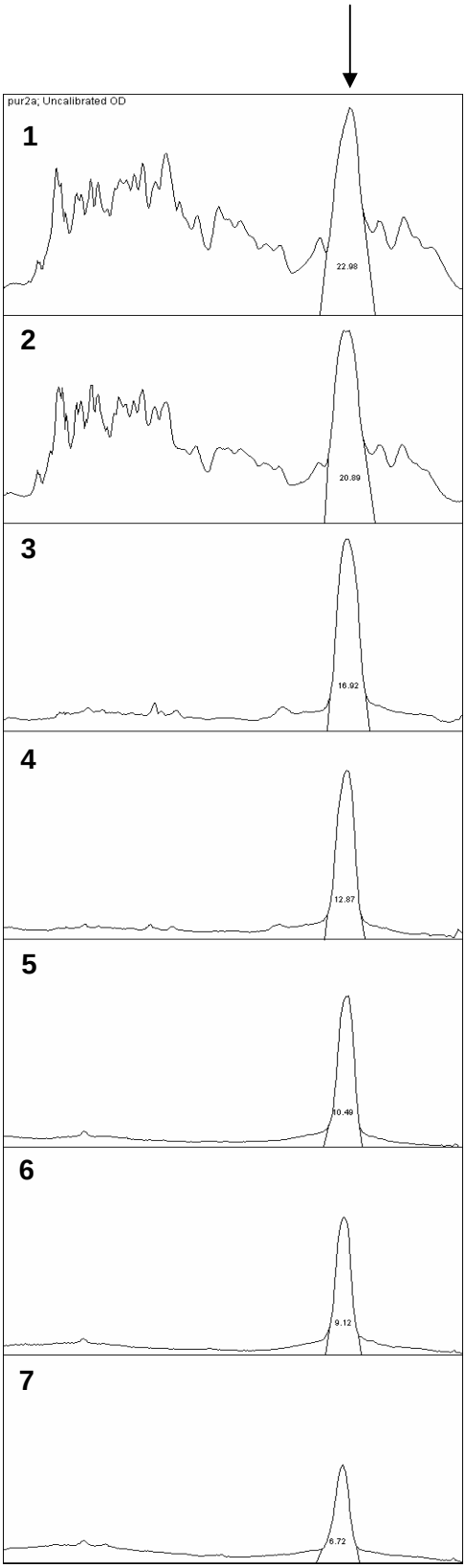

Figure 3.10: Percent yield determination for myristoylated hisactophilin purification in rich LB media. Above shows the gel of each stage of purification collected. Right is the histogram of the band intensity for each corresponding lane of the gel. The stages of purification are: (1) whole harvested cells, (2) cell lysate, (3) fractions from DEAE anion exchange, (4) dialysis into size exclusion buffer, (5) fractions from size exclusion, (6) dialysis into water and (7) fractions from HPLC.

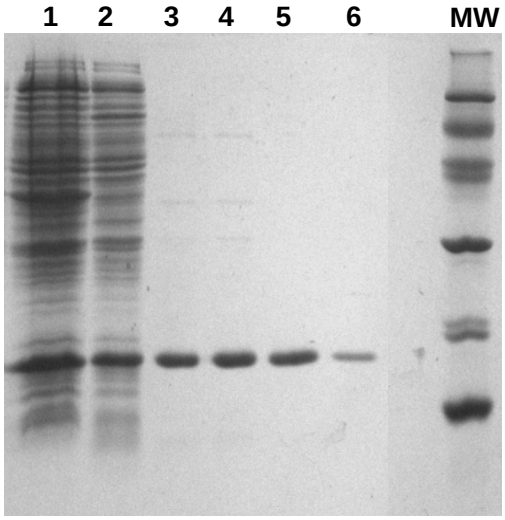

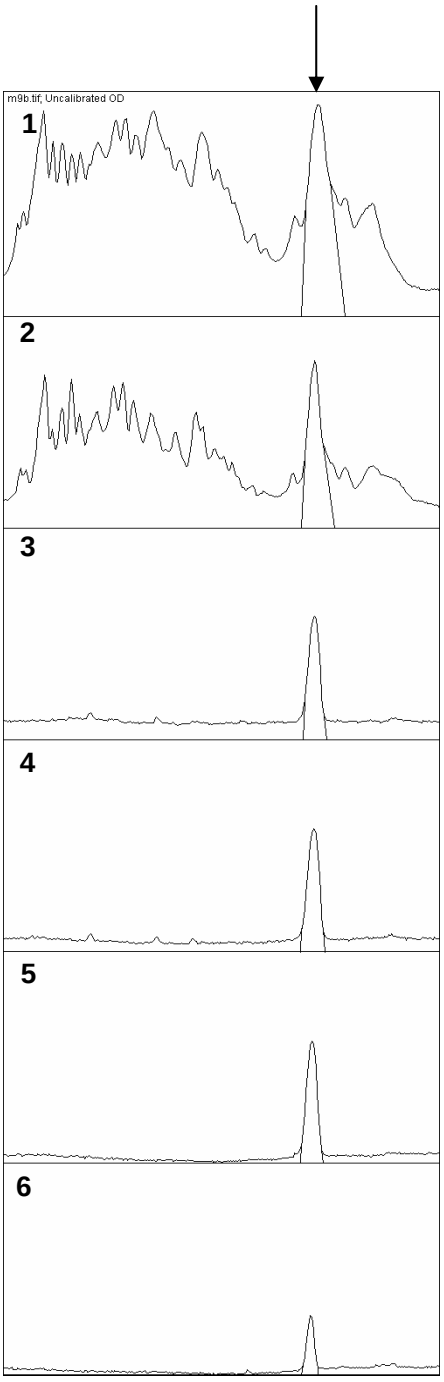

Figure 3.11: Percent yield determination for myristoylated hisactophilin purification in M9 minimal media. Above shows the gel of each stage of purification collected. Right is the histogram of the band intensity for each corresponding lane of the gel. The stages of purification are: (1) whole cells, (2) cell lysate, (3) fractions from DEAE anion exchange, (4) dialysis into size exclusion buffer, (5) fractions from size exclusion, (6) fractions from HPLC.

Table 3.2: Purification of myristoylated hisactophilin in LB and M9 minimal media

	Stage of Purification	% Area from Integration[a]	Total Hisactophilin (mg/1L of cells)	% Yield
	Rich LB Media			
1	Whole cells	22.7	23.0	100
2	Cell lysate	20.7	21.2	91.2
3	DEAE anion exchange	17.3	18.4	76.3
4	Dialysis 1[b]	12.9	15.5	57.1
5	Size exclusion	10.5	14.0	46.5
6	Dialysis 2[c]	9.3	13.2	40.9
7	RP-HPLC	5.6	11.4	24.8
	M9 Minimal Media[c]			
1	Whole cells	20.6	6.9	100.0
2	Cell lysate	18.7	6.3	91.0
3	DEAE anion exchange	14.2	5.2	69.2
4	Dialysis 1[b]	12.3	4.8	59.6
5	Size Exclusion	11.2	4.5	54.5
7	RP-HPLC	3.6	3.3	17.4

[a] Values are calculated from an average of two separate purifications
[b] First dialysis into size exclusion buffer
[c] Second dialysis into water; this was not collected for the M9 minimal media purification

The purification of protocol outlined has only minor losses of protein for each stage of purification. For each purification (LB rich media and M9 minimal media) cell lysis showed an approximately 10% loss of protein. This is similar for the dialysis steps, which is most likely caused by protein sticking to the filter membranes used. DEAE anion exchange chromatography has the highest level of protein loss at nearly 20%. On the other hand, RP-HPLC looses very little protein as the loss of protein is caused by separation of non-myristoylated from myristoylated protein.

3.4 – Summary

Overall, the optimization experiments undertaken yielded a protocol with relatively high levels of myristoylation (86%); unfortunately, this protocol also had low total protein yield. Further optimization experiments could be undertaken using hNMT2 which may have given higher total protein yield but low myristoylation levels. However, this protocol does produce sufficient amounts of protein for characterization of the effects of myristoylation of hisactophilin.

To extract structural effects of myristoylation of hisactophilin using NMR methods the protein must be uniformly ^{15}N-labeled. To achieve this labeling, *E. coli* BL21 cells carrying the pHW plasmid and the hNMT plasmid need to be grown in M9 minimal media. To ensure proper labeling, $^{15}NH_4Cl$ is used as the sole nitrogen source. These modifications to the protocol outlined above for the myristoylation of hisactophilin will yield uniformly ^{15}N-labeled hisactophilin with a covalently-bound, myristic acid group. Although it would be preferable to have a higher yield preparing protein in M9 minimal media, the yield was sufficient to pursue NMR studies, described in the next chapter.

CHAPTER 4 – EFFECTS OF MYRSITOYLATION ON THE STRUCTURE AND STABILITY OF HISACTOPHILIN

4.1 – Introduction

4.1.1 – Nuclear Magnetic Resonance of Myristoylated Hisactophilin

The structural changes incurred by the myristoylation of hisactophilin were monitored by multidimensional, multinuclear solution NMR. To determine structure by solution NMR, relatively high concentrations (in the mM range) of protein are needed, and thus the protein being studied must be highly soluble. Non-myristoylated hisactophilin is sufficiently soluble for NMR experimentation (Habazettl *et al.*, 1992a); also, myristoylated hisactophilin is likely to be sufficiently soluble since it can be found in rather high concentrations in the cytosol (Hanakam *et al.*, 1995). However, during preparation of myristoylated hisactophilin samples the solubility appears very low at a pH below 6.7; above this pH we are able to prepare relatively concentrated solutions of myristoylated protein sufficient for NMR experiments.

The first step in determining the structure of a protein by NMR is the determination of sequence specific resonance assignments. In most cases, resonance assignments are determined through a variety of multidimensional and multinuclear NMR experiments (Bax *et al.*, 1994; Kay, 1997). However, since the structure of non-myristoylated hisactophilin has already been solved by NMR, the resonance assignments have already been determined and are available. The assignments were made using ^{1}H and ^{15}N homo- and heteronuclear multi-dimensional methods (Habazettl *et al.*, 1992b) which were also sufficient for the sequence specific resonance assignments for myristoylated hisactophilin.

The known resonance assignments for non-myristoylated hisactophilin were very useful as a starting point for assigning the myristoylated form, since numerous resonances had similar chemical shifts in both forms of the protein. The assignments for myristoylated hisactophilin will provide the basis for analyzing the structural consequences of myristoylation by NMR. The most important of these structural data are distance restraints determined by NOESY (Van Holde, 1998). These distance restraints are obtained from NOESY cross-peaks that arise from spins that are far apart in sequence but close enough (within 5Å) structurally to allow for the through-space NOE interaction (Wuthrich, 1986). Also, a great deal can be determined from NOE experiments about the secondary-structure of the protein. Each of the different secondary structures that are present within proteins yields characteristic patterns of repeating NOE cross-peaks (Wuthrich, 1986). For example, β-strands will have relatively strong sequential $C_\alpha H/NH$ cross-peaks (Van Holde, 1998). This information on secondary structure is useful for the comparison of the two forms of the protein. Also, NOE crosspeaks for the methyl of the myristoyl group will be of particular interest for defining the location of the myristoyl group in the protein.

It is expected that the membrane binding properties of hisactophilin operate in conjunction with some type of myristoyl switch that is most likely pH dependent (Hanakam *et al.*, 1996b). The presence of this switch was determined by monitoring the structure of myristoylated hisactophilin over a variety of different pH values. As the pH is varied, the structure of hisactophilin may change as the myristoyl switch moves from an "on" (membrane-binding) to "off" (non-binding) position.

4.1.2 – Stability of Myristoylated Hisactophilin

The final stages of this project were to determine the stability and folding of myristoylated hisactophilin. The conformational stability of a protein is determined through denaturation by comparing the free energy of the folded state with the free energy of the denatured state. The conformational stability of the protein may then be defined as the change in free energy for the following equation:

$$\text{folded (native)} \leftrightarrow \text{unfolded (denatured)}$$

The conformational stability of a protein is then defined as $\Delta G(H_2O)$ for chemical denaturation and $\Delta G(25^{O}C)$ for thermal denaturation (Pace *et al.*, 1989).

The stability and folding of non-myristoylated hisactophilin have been determined previously (Liu *et al.*, 2001). The stability of the myristoylated protein was investigated using similar methods to those described by Liu *et al.* (2001). The thermodynamic stability of myristoylated hisactophilin was determined using urea denaturation curves. Urea-induced unfolding of hisactophilin was monitored by far-UV CD measurements. In order to perform denaturation experiments of myristoylated hisactophilin, the denaturation process must be at equilibrium and must be reversible, as is required for all thermodynamic measurements (Pace *et al.*, 1989). Liu *et al.* (2001) have determined that urea induced unfolding of non-myristoylated hisactophilin is greater than 90% reversible while thermal denaturation is at least 80% reversible (Liu *et al.*, 2001). This data were then used to compare the stability of myristoylated hisactophilin to non-myristoylated hisactophilin as well as the stability of other β-trefoil proteins. To monitor the physical properties of the protein during urea denaturation, many different optical probes may be used, such as UV difference spectroscopy, fluorescence, CD, or NMR (Pace, 1986).

However, for this study, only preliminary denaturation experiments using CD have been completed.

4.1.3 – Circular Dichroism Spectroscopy

Secondary structural changes occurring during urea denaturation can be monitored conveniently using CD spectroscopy. This technique exploits the optical activity that arises in small molecules due to the presence of asymmetric carbons (Woody, 1996). The optical activity associated with proteins is highly dependent upon the molecular conformation (Woody, 1996). Since this technique is sensitive to the molecular conformation of the peptides, it is also sensitive in monitoring changes in secondary structure of proteins (Manning, 1989). Monitoring these changes in secondary structure caused by denaturing the protein will be used to produce denaturation curves.

Monitoring denaturation by CD utilizes a polarization of light known as circular polarized light to determine the secondary structure of a peptide (Woody, 1996). Circular polarized light, unlike planar polarized light, rotates with the frequency of the radiation (Woody, 1996). This type of polarized light can be rotating in either a clockwise or counterclockwise direction and is labeled by convention as right-circular polarized and left-circular polarized light respectively (Woody, 1996).

Most biological macromolecules have optical activity which will cause them to absorb only one direction of circular polarized light (Woody, 1996). During an experiment, a sample is exposed to alternating left- and right-circular polarized light and the absorbance of each is measured (Manning, 1989). The difference in these absorbencies is defined as the circular dichroism (ΔA). When the CD is collected over a

range of wavelengths in the far UV, (~180-260nm) it will produce a CD spectrum which is unique to the secondary structure of that protein (Berndt, 1996).

Native non-myristoylated hisactophilin has a characteristic CD spectrum similar to what is expected of an all β-protein (Figure 4.1). The native spectrum (no denaturant) contains broad minima at 209nm and 200nm and a maximum at 227nm (Liu *et al.*, 2001). The CD spectrum of native non-myristoylated hisactophilin is nearly identical to that of myristoylated hisactophilin (as was seen in the previous chapter Figure 3.5) (Liu *et al.*, 2001; Hanakam *et al.*, 1996b); therefore, similar parameters were used to monitor denaturation.

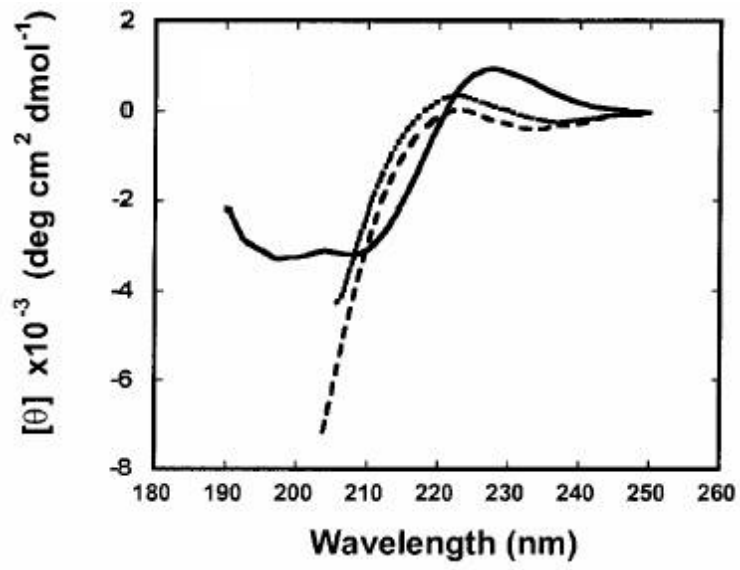

Figure 4.1 – CD Spectra of non-myristoylated hisactophilin. Spectra obtained of protein in 0M Urea (solid line), 3M urea (dashed line) and 8M urea (dotted line) (Liu *et al.*, 2001)

4.2 – Materials and Methods

4.2.1 – Protein Preparation

Protein was prepared as described in section 3.2.3 and purified as described in section 3.2.6 with the following modifications for preparation of ^{15}N-labelled protein. Protein used in ^{15}N-edited NMR experiments was prepared using minimal media with unlabeled NH_4Cl in the intermediate culture and 0.5g/L of $^{15}NH_4Cl$ (Cambridge Isotope Laboratories, Andover, MA) added directly to 1L growth cultures. Following purification protein was lyophilized in 25mM ammonium carbonate.

Unlabeled myristoylated and non-myristoylated (prepared as before without co-expression or RP-HPLC) protein samples for homonuclear NMR experiments were prepared by dissolving 15mg of unlabeled lyophilized protein in 500µL of 50mM potassium phosphate buffer at pH 6.7 with 10% D_2O; this produced a final protein concentration of 2.2mM and a final pH of 6.78 for the myristoylated protein and 6.81 for the non-myristoylated sample. A second myristoylated sample was prepared with the same parameters as above using 100% D_2O for amide exchange information.

^{15}N-labeled protein for heteronuclear experiments was prepared by dissolving 19.5mg of lyophilized protein in 500µL of 50mM potassium phosphate buffer at pH 6.7 with 10% D_2O; the final protein concentration was 2.9mM and a final pH of 6.81. Sample pH was determined using a Calomel Glass Micro pH Electrode (Thermo Electron Co., Beverly, MA) with no correction for isotope effects.

4.2.2 – NMR

All NMR experiments were performed using at 303.0K on a Bruker Avance DMX 600MHz spectrometer equipped with an inverse $^{1}H/^{13}C/^{15}N$ triple resonance xyz gradient probe (Bruker, Billerica, MA)

4.2.2.1 – ^{1}H Homonuclear NMR of Myristoylated and non-Myristoylated Hisactophilin

One dimensional homonuclear spectra were obtained using excitation sculpting for water suppression for all protein samples (Hwang and Shaka, 1995). ^{1}H-^{1}H TOCSY experiments were conducted with a τ_m of 46.04ms (16 cycles) for both myristoylated and non-myristoylated hisactophilin. A total of 64 scans were performed collecting 4096 points in the direct dimension and 512 points in the indirect dimension. ^{1}H-^{1}H NOESY experiments were conducted with a τ_m of 125ms for both myristoylated and non-myristoylated hisactophilin. A total of 80 scans were performed collecting 4096 points in the direct dimension and 512 points in the indirect dimension. Complete pulse sequences can be found in Appendix 2.

4.2.2.2 – Multidimensional Heteronuclear NMR of Myristoylated Hisactophilin

3D ^{15}N-edited TOCSY experiments were performed using a τ_m of 55.25ms (9 cycles). 3D ^{15}N-edited NOESY experiments were performed using a τ_m of 150ms. Detailed pulse sequences can be found in Appendix 2.

HSQC spectra were obtained at various pH values by titrating ^{15}N-labeled protein with 0.5M NaOH (BioShops). Approximately 4-10uL of NaOH was needed to raise the pH by 0.2-0.4 pH units; HSQC spectra were obtained at pH values of 6.81, 7.04, 7.24, 7.67 and 8.01.

4.2.3 – Analysis of NMR Data

All NMR data was processed using Felix97 Software (MSI Inc.) using an Indigo II workstation (Silicon Graphics, Increase). A square sinebell apodization function was applied to the directly acquired dimension. Indirect dimension were linear predicted to twice the original data size, a square sine bell function was applied to the resulting indirect FID and zero filled to the nearest 2^n data points.

Sequence specific resonance assignments were completed with CARA v.1.8.1 developed by the Institute of Molecular Biology and Biophysics at ETH Zurich. The free software can be downloaded from http://www.nmr.ch. All protein figures were created using MolMol 2K.2 (Institute of Molecular Biology and Biophysics at ETH, Zurich).

4.2.4 – Chemical Denaturation of Myristoylated Hisactophilin

Denaturation curves were prepared at different pH values by unfolding myristoylated hisactophilin in a series of urea concentrations. A 9M urea (BioShops) stock solution was prepared gravimetrically in a volumetric flask and stored until needed at -80^{o}C. All buffers were prepared gravimetrically in volumetric flask using glycine (BioShops) for pH 8.7, potassium phosphate (BioShops) for pH 7.7 and 6.7 and MES (Sigma) for pH 5.7. A 10× protein stock solution was prepared by dissolving lyophilized protein in the appropriate buffer. The protein solution was then diluted in a combination of urea and water to yield a final protein solution of 0.2mg/mL myristoylated hisactophilin in 50mM buffer, 1mM EDTA (BioShops), 1mM DTT (Bioshops) and desired urea concentration ranging between 0-9M as outlined in Appendix 3. The samples were allowed to equilibrate for approximately 3 hours before taking CD measurements at 227nm in a 1mm cuvette on a J715 spectrapolarimeter (Jasco Inc.) at

25^{o}C. Midpoints were calculated by fitting data to a two state model using OriginPro v.7.5 (OriginLab Corporation, Northhampton, MA)

4.3 – Results and Discussion

4.3.2 – Structural Studies of Myristoylated Hisactophilin

Although the 1D proton NMR spectra of proteins are rather crowded, some structural data can often be extracted. A comparison of 1D proton NMR spectra of myristoylated and non-myristoylated hisactophilin (Figure 4.2) shows similar dispersion of signal with some obvious differences. Firstly, well resolved downfield amide peaks (10.0ppm to 11.0ppm) move upon myristoylation. The spectrum for the non-myristoylated protein shows four well-resolved peaks which have previously been assigned to the amide protons of I85 (δ 10.375ppm), L45 (δ10.273ppm), F6 (δ 10.130ppm) and S8 (δ10.017ppm). Figure 4.3 illustrates the amide protons of I85, L45 and F6 are situated on β-strands 9, 5 and 1 (which are all part of the beta barrel) and are on the interior of the protein. S8 also faces the interior of the protein but is in a turn connecting β-strands 1 and 2. The downfield shift of these protons is most likely caused from heavy hydrogen bonding in β-strands and in a turn. In contrast, the spectrum of the myristoylated protein shows only two well resolved peaks in this region with one peak shifted further downfield (δ 10.706ppm) than any peaks for the non-myristoylated form. Since I85, L45 and F6 are located on β-strands this would suggest that there is a change in the hydrogen bonding network of the beta barrel caused by myristoylation of the protein. Although it appears that I85, L45 and F6 have shifted significantly it appears that the peak corresponding to S8 of the non-myristoylated protein remains unchanged; this suggests that S8 does not have a significant change due to myristoylation of the protein. Although all of these residues face the core of the protein, S8 is not located within the beta-barrel but is located in a turn.

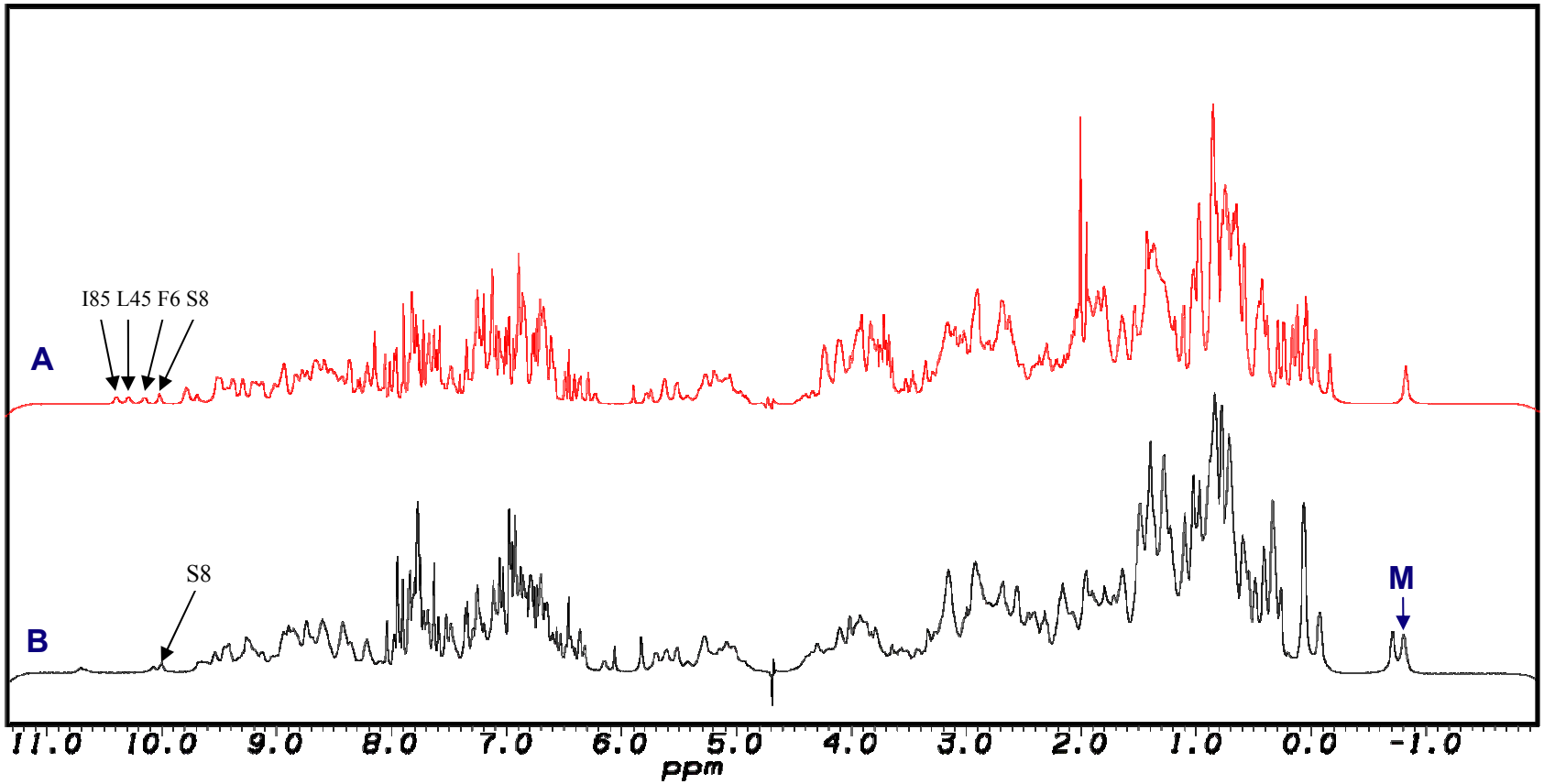

Figure 4.2: Comparison of 1D NMR spectra of (**A**) non-myristoylated hisactophilin and (**B**) myristoylated hisactophilin. Resonance for the putative methyl of the myristoyl group is indicated (**M**).

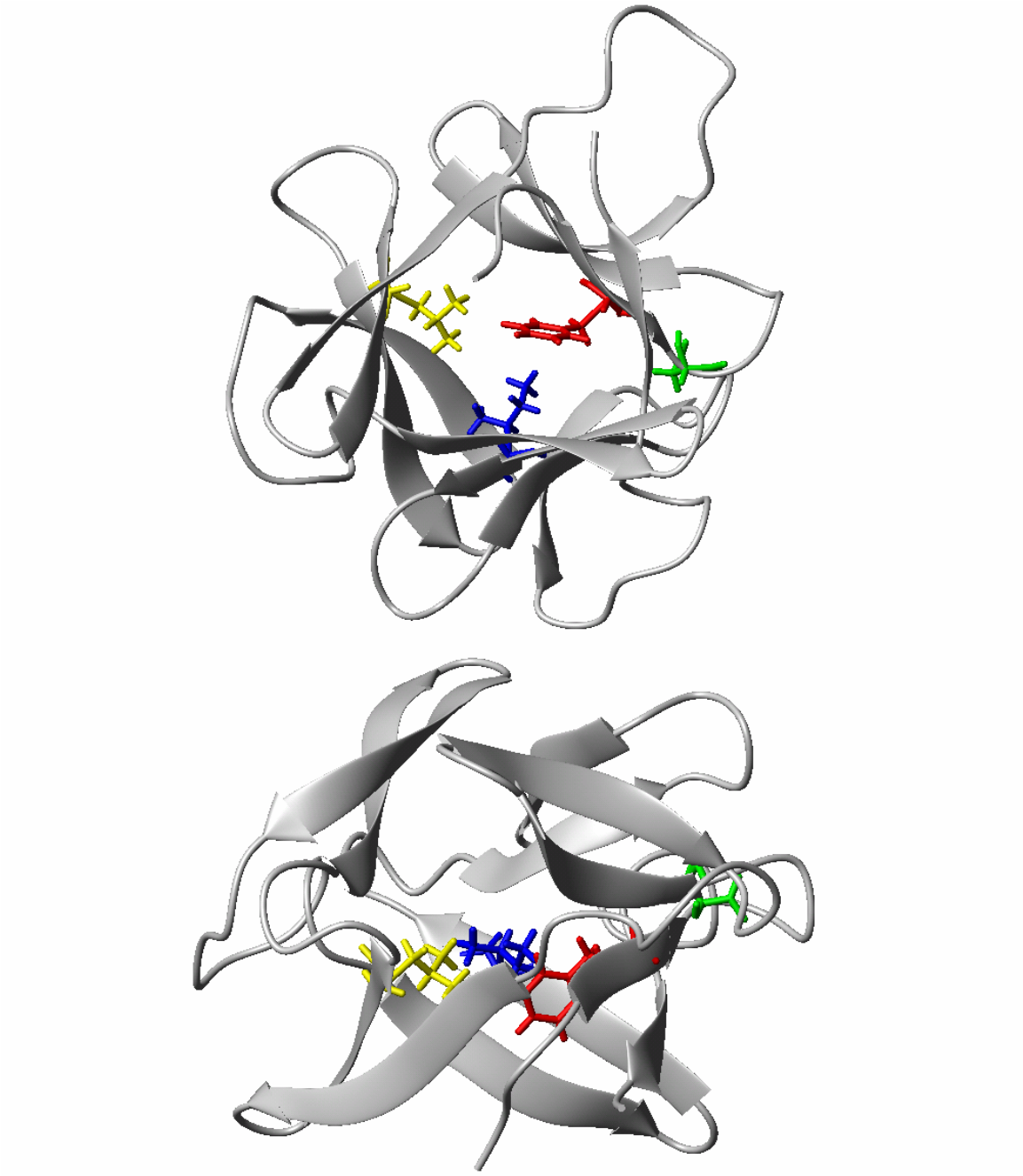

Figure 4.3: Ribbon diagram of non-myristoylated hisactophilin highlighting various residues. The figure shows (A) a bottom view of the protein looking down the beta barrel and (B) a side view of the protein. Residues highlighted are F6 (red), S8 (green), L45 (yellow) and I85 (blue). Figure was created with MolMol using pdb code 1hcd.

Since S8, is not affected by myristoylation this indicates that there is a change in the packing of the beta-barrel and, most likely, not a significant change in the packing of the hairpin triplet – although this is difficult to interpret from only one residue and is further addressed by heteronuclear experiments (see below).

In addition to well defined downfield peaks, both 1D ^{1}H spectra share a well resolved peak upfield at approximately -0.8ppm. Previous assignments for non-myristoylated hisactophilin have indicated that this peak arises from the δCH_3 group of I85 located within the core of the beta barrel. Methyl groups are expected to resonate in the range of 0-2ppm (Wuthrich, 1989). Analysis of the structure of non-myristoylated hisactophilin shows that I85 is situated close to the aromatic ring of F6 and due to ring current shifts the δCH_3 peak resonates significantly upfield. Since this peak does not shift significantly upon myristoylation the δCH_3 of I85 likely remains packed near the ring of F6. The spectrum of the non-myristoylated protein has one upfield peak at -0.803ppm; however, an obvious difference is the presence of two upfield peaks with a chemical shift of -0.732ppm and -0.824ppm in the spectrum of myristoylated hisactophilin. These two peaks are not a splitting of the single peak found in the spectrum of non-myristoylated hisactophilin. Since these peaks resonate upfield similar to the δCH_3 of I85, it is likely that these protons are in a very similar local environment and are also affected by the ring current of F6. Homonuclear TOCSY and NOESY experiments demonstrate clear intra-residue and sequential crosspeaks indicated that the chemical shift of I85 has not changed significantly; whereas these experiments suggest the new upfield peak is due to protons of the myristoyl group.

2D ^{1}H-^{1}H TOCSY (Figure 4.4) and NOESY (Figure 4.5) were adequate for the determination of a small number of residue assignments but more importantly for assigning myristoyl resonances. In the homonuclear TOCSY of non-myristoylated hisactophilin the δCH_3 of I85 peak at -0.803ppm has two strong TOCSY crosspeaks which were previously assigned to the γCH_2 protons (at -0.09ppm and 0.93ppm). The δCH_3 peak also shows a weaker crosspeak with the β proton (at 1.277ppm). Comparing this spectrum with that of the myristoylated protein there are now two sets of upfield peaks at slightly different chemical shifts. A resonance at -0.732ppm shows a similar TOCSY pattern to that of δCH_3 of I85, with crosspeaks to two putative γCH_2 protons at 0.369ppm and 1.321ppm. A second resonance -0.824ppm has two overlapping TOCSY crosspeaks at -0.118ppm and -0.025ppm, these peaks are significantly shifted from those in the non-myristoylated protein. ^{15}N edited 3D TOCSY and NOESY experiments confirm that the peak at -0.732ppm is the δCH_3 of I85 and the crosspeaks at 0.369ppm and 1.321ppm are the γCH_2 protons of I85. Thus, the new upfield resonance at -0.824ppm and related resonances at -0.118ppm and -0.025ppm likely arise from the myristoyl group. Other aliphatic resonances in the protein core that might resonate in this region have been assigned (by 3D heteronuclear TOCSY and NOESY experiments – see below), and the resonances are not clearly associated with any other possible side chain. We have tentatively assigned the most upfield resonance to the methyl group of the myristoyl moiety and the other resonances to CH_2 groups; however, these assignments should be confirmed by further experiments.

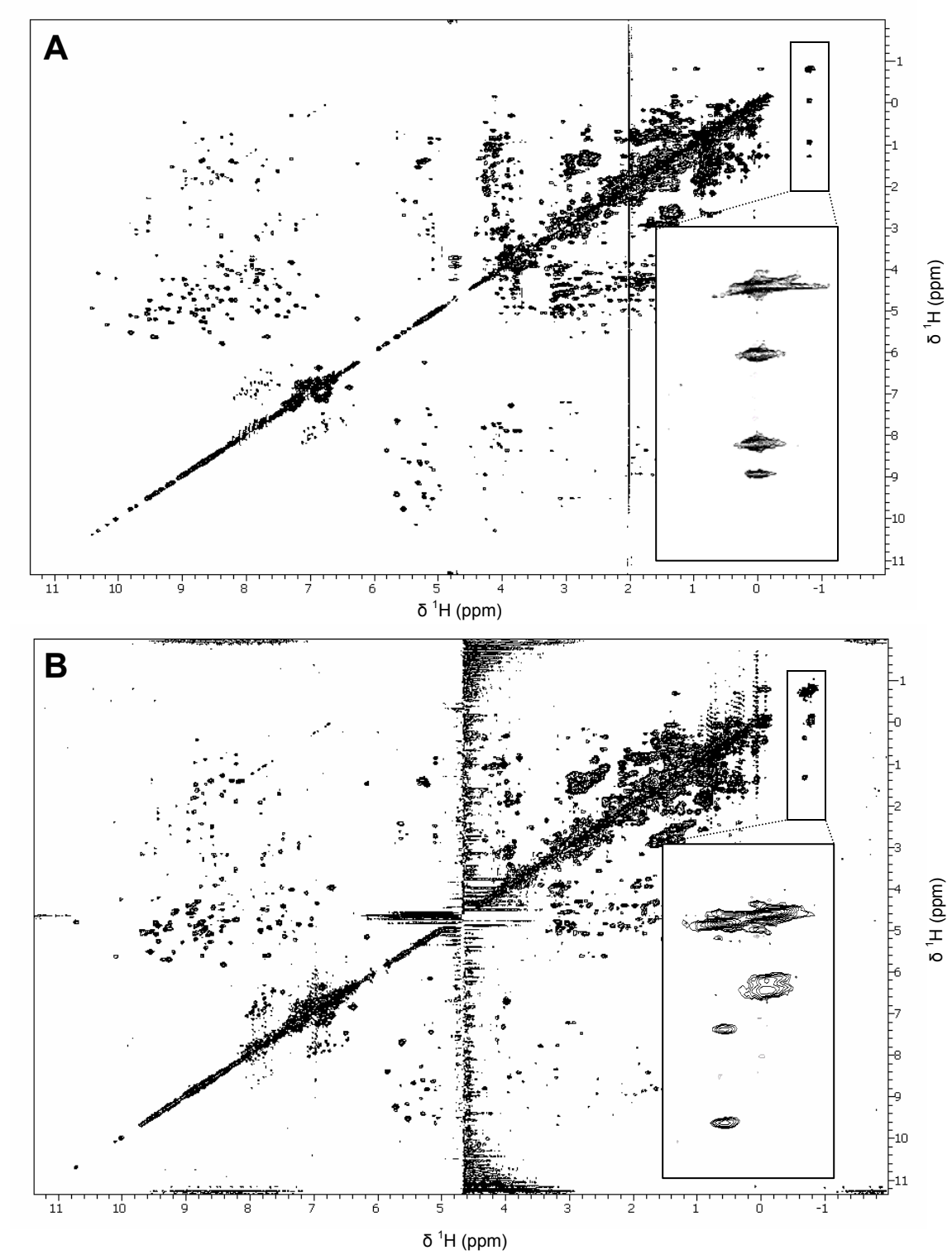

Figure 4.4:^{1}H-^{1}H TOCSY of (A) non-myristoylated and (B) myristoylated hisactophilin. Inlays show a magnification of peaks used to assign the δCH_3 of I85 and the methyl of the myristoyl moiety as discussed in the text.

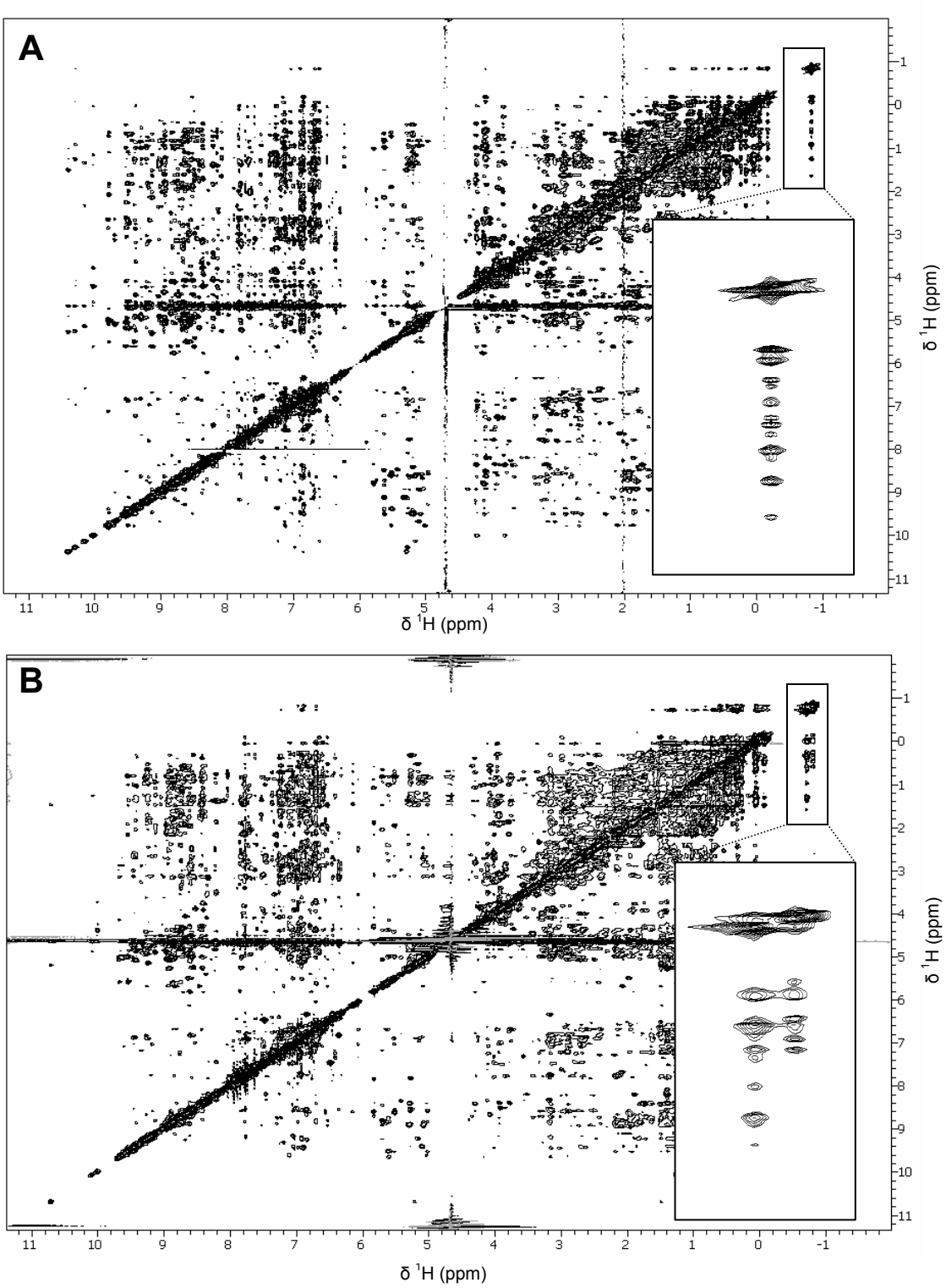

Figure 4.5: ^{1}H-^{1}H NOESY of (A) non-myristoylated and (B) myristoylated hisactophilin. Inlays show a magnification of peaks used to assign the δCH_3 of I85 and the methyl of the myristoyl moiety as discussed in the text.

^{15}N-edited 3D TOCSY and NOESY experiments allowed for nearly complete sequence specific residue assignments to be deduced and for a further understanding of the structural consequences of myristoylation. From CD and fluorescence experiments, which indicated that myristoylated hisactophilin has an overall similar structure as non-myristoylated hisactophilin (Figure 3.5), one might expect only minor changes in the HSQC spectrum and assignments could be made very easily; however, as seen in Figure 4.6, myristoylation appears to have caused significant chemical shift changes for many residues. A direct comparison of the HSQC spectra of myristoylated and non-myristoylated hisactophilin suggests that there are only a few large changes in chemical shift but numerous minor changes in chemical shift. Hisactophilin amide proton chemical shifts are very highly sensitive to pH (Hammond *et al*., 1998), thus small differences in pH may be related to some of the observed differences in the spectra of the myristoylated (pH 6.81) and non-myristoylated (pH ~6.7) protein.

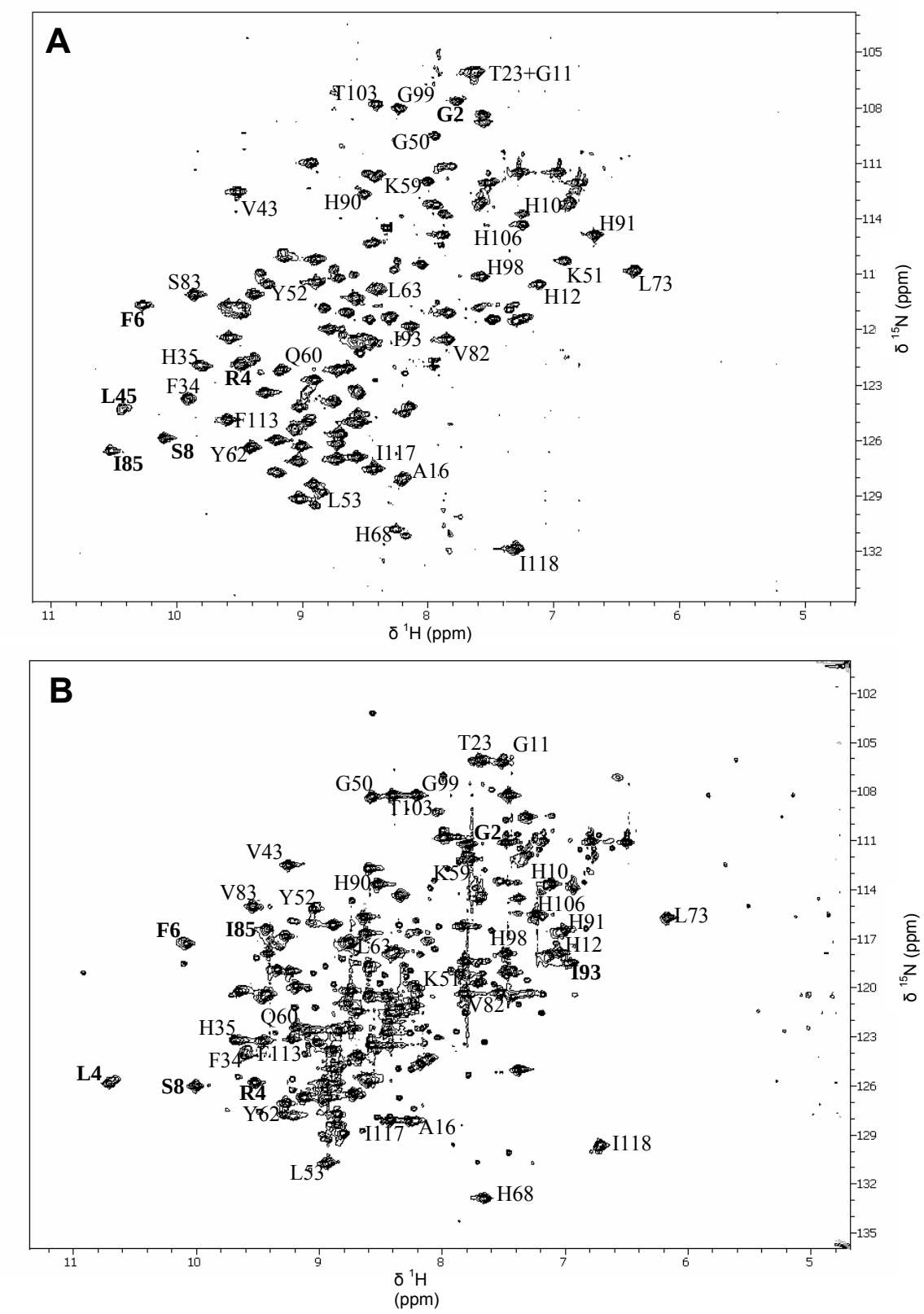

Figure 4.6: ^{15}N-edited HSQC of (A) non-myristoylated and (B) myristoylated hisactophilin. Some of the assigned residues have been labeled to show the significant rearrangement caused by myristoylation.

Another factor complicating the assignment process is the presence of two sets of peaks of different intensities for the myristoylated protein. The lower intensity peaks most likely represent a contaminating species and not a second conformation of the protein. If these lower intensity peaks represent a different conformation of the protein one would expect their intensities to change with pH due to the likelihood that hisactophilin undergoes a pH dependent myristoyl switch; however, the intensity of these smaller peaks remain constant over a varying pH range (Figure 4.7). This suggests that these weak peaks must be a contaminating species present after purification. From the previous chapter (section 3.3.1), the purification of myristoylated hisactophilin during reverse phase HPLC yields a small peak with a retention time similar to that of myristoylated hisactophilin, which was assumed to be hisactophilin acylated with something other than myristoyl. This additional acylated protein may have co-eluted with the myristoylated protein.

Despite these complications in determining the sequence specific residue assignments nearly all of the assignments were completed. Through the use of ^{15}N-editied 3D TOCSY to determine spin systems and ^{15}N-editied 3D NOESY experiments for through space information 85% of the residues were assigned, the same as for the non-myristoylated protein (see Appendix 4 for all assignments made). Assignments for residues located on large loops (such as residues 25-32) or within tight turns (such as residues 40-41, 57-58 and 80-81) are often difficult to determine using only ^{15}N labeling techniques (Wuthrich, 1989). Fortunately, since the myristoyl group lies within the centre of the beta-barrel, most likely there will be little change in the unassigned residues situated in peripheral parts of the structure

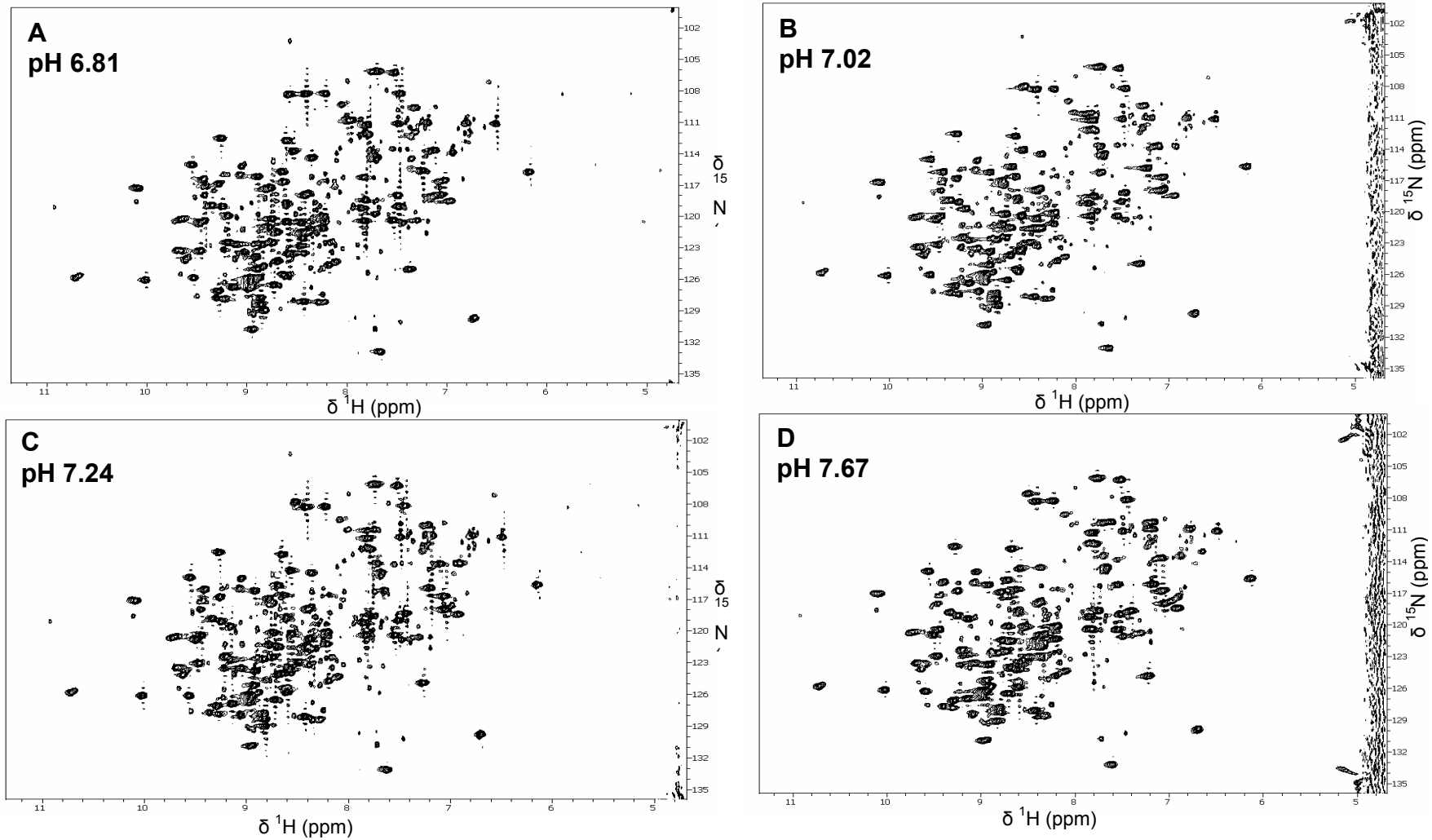

Figure 4.7: ^{15}N-edited HSQC spectra of myristoylated hisactophilin at a variety of different pH values. HSQC spectra were obtained at (A) pH 6.81, (B) pH 7.02, (C) pH 7.24 and (D) pH 7.67. Note that the weaker intensity peaks do not change intensity with pH.

A summary of the changes in chemical shift (seen in Figure 4.8) shows that large changes in chemical shift are concentrated in several regions of the sequence. The changes in proton chemical shifts (Figure 4.8 A) appear to be distributed throughout the entire sequence compared to changes in nitrogen chemical shift (Figure 4.8 B); however, as mentioned above, the changes in proton shift may be also affected by pH differences. Perturbations in chemical shift are localized in the residues of the beta barrel, most prominently in beta-strands 6, 8 and 9. Likewise, there are large perturbations at the N and C termini of the protein. From these regions of structural rearrangement it is evident that the myristoyl moiety sits somewhere within the beta barrel which is further confirmed by NOE analysis below.

Mapping the degree of chemical shift perturbation onto the 3D structure of the non-myristoylated protein for each residue (Figure 4.9) allows for a much better understanding of the location of the myristoyl group when it is sequestered within the protein, as well as regions of structural changes. The most significant chemical shift perturbations are concentrated around I85. Minor changes in chemical shift also appear to be localized to the beta barrel and residues of the hairpin triplet that cap off the beta barrel. This suggests that the myristoyl group lies within the beta barrel which has also caused a change in the packing of the protein core near the top of the beta barrel.

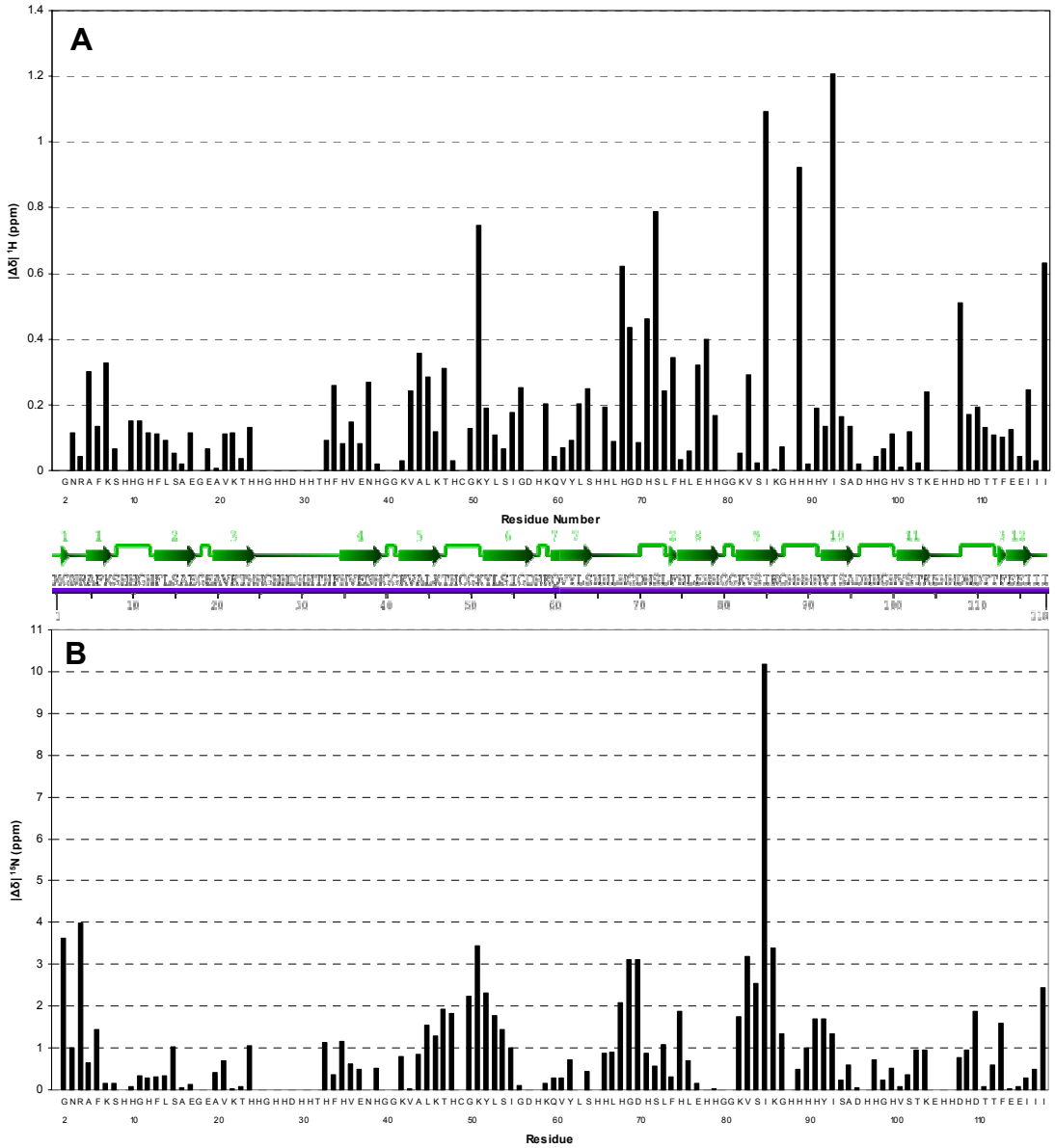

Figure 4.8: Histogram of the changes in (**A**) amide proton chemical shift and (**B**) nitrogen chemical shift caused by myristoylation of hisactophilin. Changes in chemical shift are calculated as the absolute value of the change. Also, shown are the secondary structural elements for the amino acid sequence.

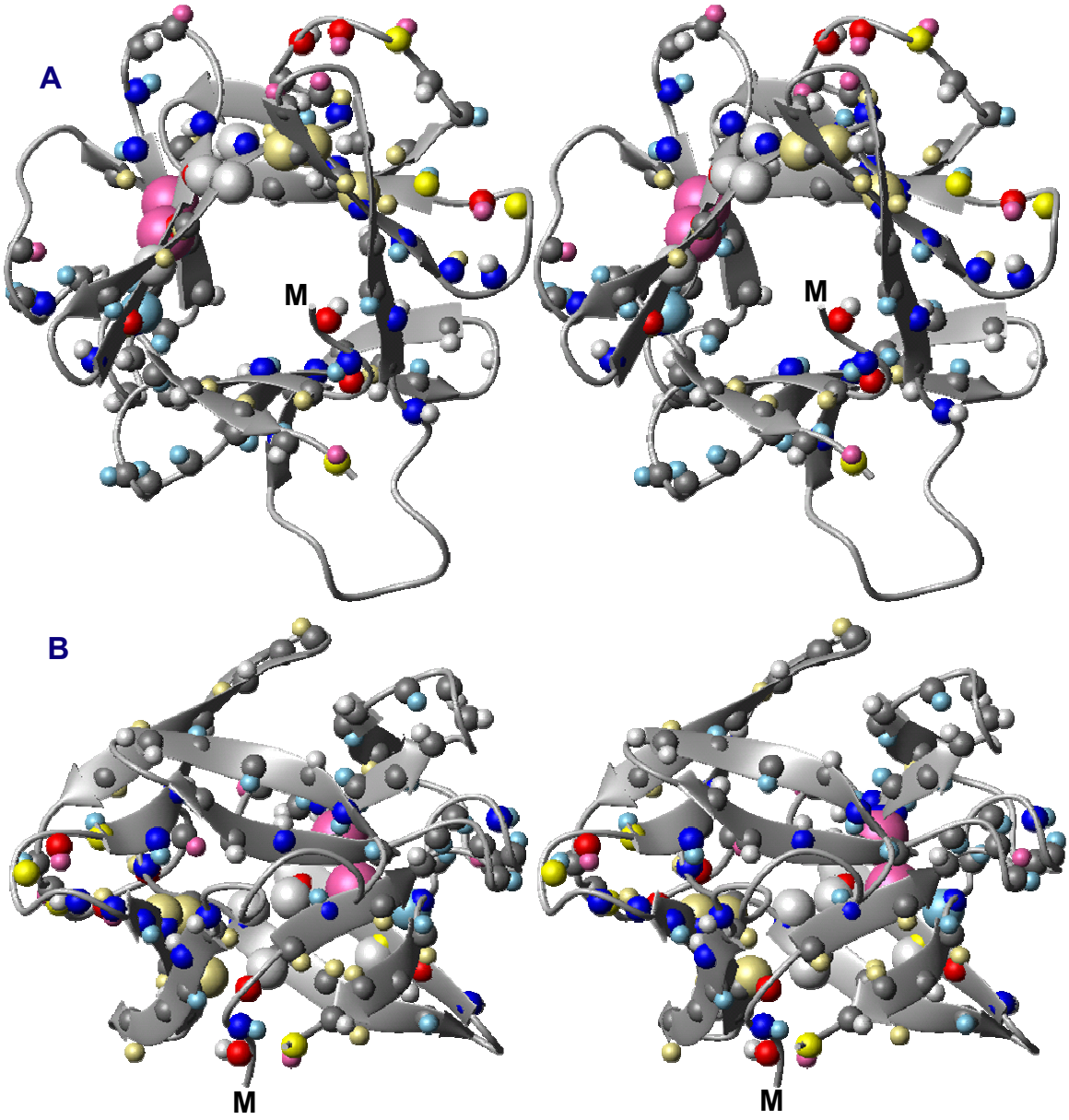

Figure 4.9: Side (**A**) and top view (**B**) for stereo ribbon diagrams of non-myristoylated hisactophilin indicating the degree of chemical shift change caused by myristoylation. See the legend (right) for colour scheme. Inflated spheres represent those amide protons which show NOE crosspeaks to the putative methyl of the myristoyl group; the magnitude of inflation corresponds to the intensity of the NOE. The N-terminus and point of attachment of the myristoyl group is also indicated (**M**)

Atom	Degree of Change	Δδ range (ppm)
N	No Change	< 1.00
H_N	No Change	< 0.100
N	Small	1.00 – 2.00
H_N	Small	0.100 - 0.200
N	Medium	2.00 – 3.00
H_N	Medium	0.200 – 0.400
N	Large	> 3
H_N	Large	> 0.4

In support of this, strong NOEs are found between the methyl of the myristoyl group and the amide protons of I85 and V86 and S87. Similarily, a strong NOE is observed between the amide proton of I93 and the myristoyl group. This indicates that the myristoyl group is sequestered deep within the beta barrel and close to I93 which is located within the hairpin triplet capping off the beta barrel. A number of weak NOEs are also evident which link the methyl of the myristoyl moiety with the amide protons of S84, F74, H75, L76, H94, F113, E114, K45 and T46. These weak NOEs may only be spectral artifacts caused by spin diffusion, overlapping resonances in the myristoyl chain or may be due to movement of the myristoyl group within the beta barrel. Since hisactophilin is thought to function with pH dependent myristoyl switch, the myristoyl group itself cannot be a static structural element and may have some motion to allow for the switch to operate. In order for the myristoyl group to pack this far within the beta-barrel there must be some rearrangement of the N-terminus; consistent with this, G2 and R4 experience significant perturbations in chemical shift (Figure 4.8 and 4.9).

4.3.2 – Stability of Myristoylated Hisactophilin by Urea Denaturation

Preliminary denaturation experiments were performed to obtain a better understanding of the stability of the myristoylated form of hisactophilin. Despite its rather unusual core structure, non-myristoylated hisactophilin is a relatively stable protein (Lui *et al*., 2001); adding a myristoyl group to the core may be likely to affect the overall stability of the protein. Although the denaturation studies performed were only preliminary, information about the stability of the protein can be extracted from these experiments. A comparison of the midpoints of the denaturation curves (which were

found to remain constant over time) allows for a qualitative understanding of protein stability.

From the denaturation curves for myristoylated hisactophilin (Figure 4.10) it is evident that a decrease in pH causes a decrease in stability; this is similar to previous results obtained for the non-myristoylated form of the protein. There is only a minor change in stability from pH 8.7 to 7.7 and a much more substantial decrease when the pH is decreased to 6.7 or 5.7. Again this trend is similar to that of non-myristoylated protein hisactophilin (Lui *et al*., 2001). Although the relation of pH and stability are similar for both forms of the protein, overall the myristoylated form of the protein is more stable. This is similar to what was found through denaturation studies on the myristoylated protein frequenin (Muralidhar, 2005). At pH 7.7 and 8.7, the midpoints of the denaturation curves are nearly 1M higher for the myristoylated protein than for the non-myristoylated protein. In contrast, at pH 5.7 and 6.7 the midpoints of the curves are only ~0.3M higher for myristoylated protein. This trend seems logical since the myristoyl switch is thought to occur somewhere around pH 6.7. At high pH values where the myristoyl moiety is sequestered deep in the beta barrel may cause an increase in stability by allowing for better packing of the protein core. Whereas, at low pH hisactophilin associates with membranes (Hanakam *et al*., 1996); the myristoyl group has been proposed to extend away from the protein and penetrate the hydrophobic interior of the plasma membrane (Hanakam *et al*., 1998). The relatively smaller stabilization of the protein at low pH may favour switching at low pH.

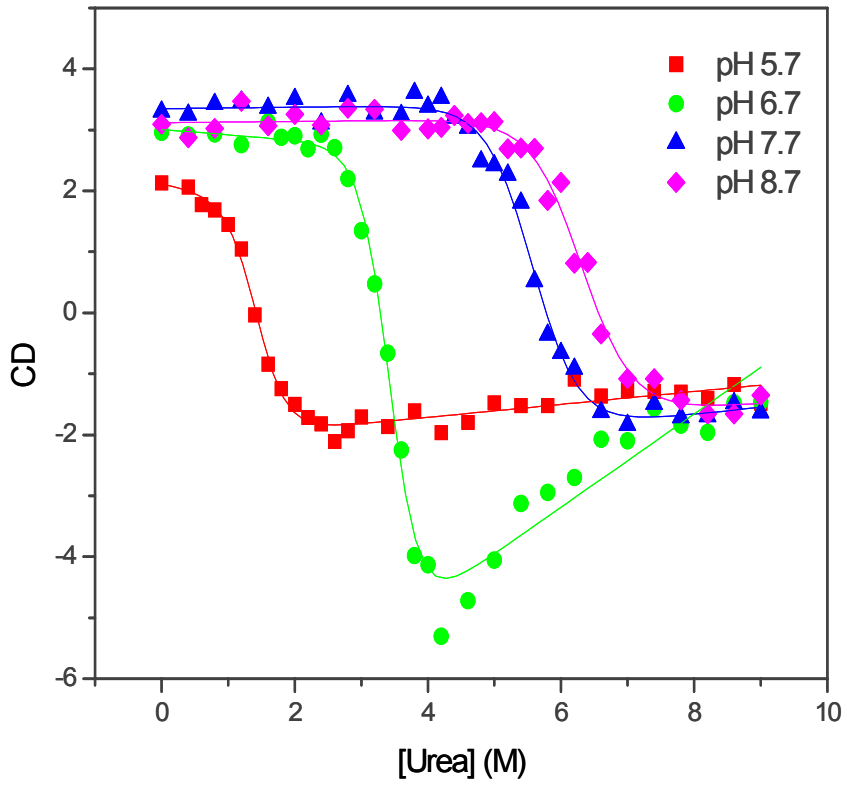

Figure 4.10: CD-monitored urea denaturation curves of myristoylated hisactophilin for pH 5.7 (■), pH 6.7 (●), pH 7.7 (▲) and pH 8.7 (♦). Data was fit to a two state model using the linear extrapolation method according to Liu *et al.* (2001). Data fitting at pH 6.7 may not be reliable due to skewed *m* values.

Table 4.1: Comparison of protein stability for myristoylated and non-myristoylated hisactophilin determined by urea denaturation

pH	Myristoylated	Non-myristoylated[a]	ΔC_{mid} (M)
	C_{mid} (M)[b]	C_{mid} (M)	
5.7	1.44 ±0.06	1.02 ±0.02	0.42
6.7	3.43 ±0.04	3.10 ±0.05	0.33
7.7	5.58 ±0.05	4.31 ±0.01	1.27
8.7	6.32 ±0.09	5.18 ±0.03	1.14

[a] Data was taken from Liu *et al.* (2001)
[b] Data was fit to a two state model using the linear extrapolation method according to Liu *et al.* (2001)

4.4 – Summary

Overall, the NMR data collected suggests that some structural rearrangement was caused by myristoylation. This structural rearrangement appears to be associated with residues of the interior of the beta-barrel, along with residues of the hairpin triplet that cap off the beta-barrel. This information, along with NOE cross-peaks from the protein to the myristoyl moiety, suggests that the myristoyl group is sequestered deep in the beta-barrel at pH 6.81.

Similar to other myristoylated proteins, hisactophilin demonstrated increased stability when myristoylated. Preliminary denaturation studies showed a significant increase in protein stability at a pH above the assumed pH of switching around 6.7; that is when the myristoyl group is sequestered within the protein. Below this pH value myristoylated hisactophilin was only slightly more stable which may favour switching.

CHAPTER 5 – SUMMARY AND FUTURE WORK

5.1 – Summary

In general, little has been uncovered on effects that co- and post-translational modification have on the structure, stability and folding of a protein; preliminary NMR and denaturation studies of myristoylated hisactophilin were completed to examine these effects. The majority of studies on the molecular basis of myristoyl switches have been conducted on characterizing calcium-myristoyl switches, whereas hisactophilin is thought to bind reversibly to membranes by means of a pH dependent myristoyl switch. This information would be interesting to not only uncover some characteristics of a pH dependent myristoyl switch, but more generally to compare the properties of recombinant proteins and the naturally modified proteins.

This study showed that hisactophilin can be myristoylated using a co-expression system in *E. coli*. That is the expression of hisactophilin (via the pHW plasmid) along with expression of hNMT1 (via the pHV738 plasmid) was successful for the myristoylation of hisactophilin. Through a number of optimization experiments an 86% efficiency of myristoylation was achieved, but the total protein yield was not very high and may require further optimization. The addition of a reverse-phase HPLC purification step to the existing non-myristoylated hisactophilin purification protocol was successful in purifying sufficient amounts of myristoylated protein for preliminary NMR and denaturation studies on myristoylated hisactophilin.

NMR experiments suggested that some structural rearrangement was caused by myristoylation. This structural rearrangement appears limited to the residues of the interior of the beta-barrel, along with residues of the hairpin triplet that cap off the beta-

barrel. This information, along with protein-myristoyl NOE cross-peaks suggest that the myristoyl group is sequestered deep within the beta-barrel at high pH. Like other myristoylated proteins, hisactophilin appears to bind the myristoyl group to a hydrophobic region when the myristoyl switch is in the “off” (non-membrane binding) position.

Also similar to other myristoylated proteins, hisactophilin demonstrated increased stability when myristoylated. Denaturation curves showed a significant increase in protein stability at a pH above the assumed pH of switching around 6.7. Below this pH value myristoylated hisactophilin was only slightly more stable. This difference in stability may favour switching but further experimentation is needed to confirm this.

5.2 – Future Work

5.2.1 – Optimization of Total Protein Yield

The preparation and purification of myristoylated hisactophilin protocol was sufficient for NMR and denaturation experiments performed; however, further optimization of the total protein yield needs to be considered. Preliminary results suggested that use of hNMT1 for the co-expression system yielded the highest total protein yield but rather low levels of myristoylation. In addition, the use of sodium myristate (as opposed to myristic acid) increased not only the total protein yield, but also the level of myristoylation. Sodium myristate was not used for preparation with hNMT1 and may result is significantly increased levels of myristoylation as well as high protein yields. Systematic checking of growth parameters such as time of induction can also be examined to ensure optimal protein yield.

5.2.2 – Stability of Myristoylated Hisactophilin and Energetics of the Myristoyl Switch

The denaturation experiments completed were only preliminary and will be verified and expanded on. One key aspect of characterizing stability by denaturation is to ensure the system is at equilibrium, as is the case for all thermodynamic measurements (Pace *et al.*, 1989). Liu *et al.* (2001) have determined that non-myristoylated hisactophilin is greater than 90% reversible for urea induced unfolding and at least 80% reversible for thermal denaturation (Liu *et al.*, 2001). To determine reversibility of unfolding for myristoylated hisactophilin, the native form of the protein is measured by CD or fluorescence. The protein will then be subjected to a high concentration of denaturant and measured again. The spectrum at this point should resemble that of a

fully denatured protein. Finally, the protein will be exchanged back into a low concentration of urea. If this final spectrum resembles the original spectrum, then denaturation will be considered to be reversible.

In addition to reversibility of denaturation the use of at least a second optical probe is needed to verify the results. Previously, non-myristoylated hisactophilin was analyzed using fluorescence and CD. Further denaturation experiments will allow for not only a better understanding of the stabilizing effects of myristoylation, but potentially an understanding of the energetics of the myristoyl switch. Implementation of careful control experiments may help to uncover the free energy required for the switch to occur – which has not been completed for any myristoylated proteins. The preliminary data collected here suggests that at low pH the protein is less stable which may be the favourable conditions required for the switch to occur and allow for subsequent binding to membranes. A comparison of the free energy for each state of the switch might allow for this.

5.2.3 – Structural Characterization of the Myristoyl Switch

The structural data obtained by NMR strongly suggest that the myristoyl group is sequestered within the beta-barrel of the protein; however, this can be easily confirmed through further experimentation. Assignment of the resonances of myristoyl groups for the myristoylated protein recoverin were achieved through a series of multidimensional heteronuclear NMR experiments of ^{13}C labeled myristoyl group and ^{15}N labeled protein (Tanaka *et al*., 1995). These additional experiments will not only allow for verification of the location of the myristoyl group but also help in a final structure calculation of myristoylated hisactophilin in the myristoyl “off” state.

Our results with myristoylated hisactophilin behaves similar to a study of recoverin where myristoylation of the protein had caused a significant decrease in solubility when the myristoyl switch is in the "off" position (Ames *et al.*, 1997). This would imply that protein solubility is poor under conditions where the myristoyl group is solvent exposed – in the case of myristoylated hisactophilin that is at low pH. To overcome these problems, a number of myristic acid analogs have been developed in an attempt to increase solubility (Knoll *et al.*, 1995; Ames *et al.*, 1997). In the case of recoverin, solubility difficulties were easily overcome by using a myristoyl analog which consisted of an oxygen at position 13 of the fatty acid chain; this analog allowed for sufficient solubility and retained protein function (Ames *et al.*, 1997). Since solubility for myristoylated hisactophilin was poor at low pH values incorporation of a myristoyl analog will be necessary for a full characterization of the structural consequences caused by myristoylation as well as characterization of the switch.

REFERENCES

Ames, J.B., Hendricks, K.B., Strahl, T., Huttner, I.G., Hamasaki, N. & Thorner, J. (2000). Structure and Calcium-Binding Properties of Frq1, a Novel Calcium Sensor in the Yeast *Saccharomyces cervisiae*. *Biochem* **39**, 12149-61.

Ames, J.B., Ishima, R., Tanaka, T., Gordon, J,I., Stryer, L. & Ikura, M. (1997). Molecular mechanics of calcium-myristoyl switches. *Nature* **389**, 198-202.

Ames, J.B., Porumb, T., Tanaka, T., Ikura, M. & Stryer. L. (1994). Amino-terminal Myristoylation Induces Cooperative Calcium Binding to Recoverin. *J Biol Chem* **270**, 4526-33.

Ames, J.B., Tanaka, T., Ikura, M. & Stryer, L. (1995). Nuclear Magnetic Resonance Evidence for Ca^{2+}-induced Extrusion of the Myristoyl Group of Recoverin. *J Biol Chem* **270**, 30909-13.

Ames, J.B., Tanaka, T., Stryer, L. & Ikura, M. (1994). Secondary Structure of Myristoylated Recoverin Determined by Three-Dimensional Heteronuclear NMR: Implications for the Calcium-Myristoyl Switch. *Biochem* **33**, 10743-53.

Ames, J.B., Tanaka, T., Stryer, S. & Ikura, M. (1996). Portrait of a myristoyl switch protein. *Curr Opin Struct Biol* **6**, 432-8.

Amor, J.C., Harrison, D.H., Kahn, R.A. & Ringe, D. (1994). Structure of the human ADP-ribosylation factor 1 complexed with GDP. *Nature* **372**, 704-8.

Bax, A., Vuister, G.W., Grzesiek, S., Delaglio, F., Wang, A.C., Tschudin, R & Zhu, G. (1994). Measurement of Homo- and Heteronuclear J Couplings from Quantitive J Correlation. *Met Emzymol* **239**, 79-105.

Beven, L., Adenier, H., Kichenama, R., Homand, J., Redeker, V., Le Caer, J., Ladant, D. & Chopineau, J. (2001). Ca^{2+}-Myristoyl Switch and Membrane Bindin of Chemically Acylated Neurocalcins. *Biochem* **40**, 8152-60.

Bhatnagar, R.S., Futterer, K., Waksman, G. & Gordon, J.I. (1999). The structure of myrisotyl-CoA:protein N-myristoyltransferase. *Biochimica Et Biophysica Acta* **1441**, 162-72

Burgoyne, R.D. (2004). The neuronal calcium-sensor proteins. *Biochimica Et Biophysica Acta* **1742**, 59-68.

Desmeules, P., Penney, S.E. & Salesse, C. (2006). Single-step Purification of Myristoylated and Nonmyristoylated Recoverin and Substrate Dependence of Myristoylation Level. *Anal Biochem* **349**, 25-32.

Dizhoor, A.M., Ericsson, L.H., Johnson, R.S., Kumar, S., Olshevskaya, E., Zozulya, S., Neubert, T.A., Stryer, L., Hurley, J.B. & Walsh, K.A. (1992). The NH_2 Terminus of Retinal Recoverin Is Acylated by a Small Family of Fatty Acids. *J Biol Chem* **267**, 16033-6.

Duronio, R. J., Jackson-Machelski, E., Heuckeroth, R.O., Olins, P. O., Devine, D.S., Yonemoto, W., Slice, L. W., Taylor, S.S. &Gordon, J.I. (1990). Protein N-myristoylation in *Escherichia coli*: Reconstitiution of a eukaryotic protein modification in bacteria. *Proc Natl Acad Sci USA* **87**, 1506-10.

Duronio, R.J., Rudnick, D.A., Johnson, R.L., Linder, M.E. & Gordon, J.I. (1990). Reconstitution of Protein N-Myristoylation in *Escherichia coli*. *Methods* **1**, 253-63.

Farazi, T.A., Waksman, G. & Gordon, J.I. (2001). The Biology and Enzymology of Protein N-Myristoylation. *J Biol Chem* **276**, 39501-4.

Fisher, J.R., Sharma, Y., Iuliano, S., Piccioti, R.A., Kyrlov, D., Hurley, J., Roder, J. & Jeromin, A. (2000). Purification of myristoylated and nonmyristoylated neuronal calcium sensor-1 using single-stop hydrophobic interaction chromatography. *Protein* **20**, 66-72.

Gangal, M., Clifford, T., Deich, J., Cheng, X., Taylor, S.S. & Johnson, D.A. (1999). Mobilization of a A-kinas N-myristate through an isoform-specific intermolecular switch. *Proc Natl Acad Sci USA* **96**, 12394-9.

Giang, D.K. & Cravatt, B.F. (1998). A Second Mammalian N-Myristoyltransferase. *J Biol Chem* **273**, 6595-8.

Gordon, J.I., Duronio, R.J., Rudnick, D.A., Adams,S.P. & Gokel, G.W. (1991). Protein N-Myristoylation. *J Biol Chem* **266**, 8647-50.

Habazettl J, Gondol D, Wiltscheck R, Otlewski J, Schleicher M, Holak TA. (1992A). Structure of hisactophilin is similar to interleukin-1 beta and fibroblast growth factor. *Nature* **359**, 855-8.

Habazettl J, Schleicher M, Otlewski J, Holak TA. (1992B). Homonuclear three-dimensional NOE-NOE nuclear magnetic resonance/spectra for structure determination of proteins in solution. *J Mol Biol* **228**, 156-69.

Hanakam, F., Eckerskorn, C. Lottspeich, F., Muller-Taubenberger, A., Schafer, W., Gerisch, G. (1995). The pH-sensitive actin-binding protein hisactophilin of *Dictyostelium* exists in two isoforms which both are myristoylated and distributed between plasma membrane and cytoplasm. *J Biol Chem* **270**, 596-602.

Hanakam F, Albrecht R, Eckerskorn C, Matzner M, Gerisch G. (1996A). Myristoylated and non-myristoylated forms of the pH sensor protein hisactophilin II: intracellular shuttling to plasma membrane and nucleus monitored in real time by a fusion with green fluorescent protein. *EMBO J* **15**, 2935-43.

Hanakam F, Gerisch G, Lotz S, Alt T, Seelig A. (1996B). Binding of hisactophilin I and II to lipid membranes is controlled by a pH-dependent myristoyl-histidine switch. *Biochemistry* **35**, 11036-44.

Harroun, T.A., Bradshaw, J.P., Balali-Mood, K. & Katsaras, J. (2005). A structural study of the myristoylated N-terminus of ARF1. *Biochimica et Biophysica Acta* **1668**, 138-44.

Haun, R.S., Tsai, S., Adamik, R., Moss, J. & Vaughan, M. (1992). Effect of Myristoylation on GTP-dependent Binding of ADP-ribosylation Factor to Golgi. *J Biol Chem* **268**, 7064-8.

Houliston, R.S., Liu, C., Singh, L.M.R. & Meiering, E.M. (2002). pH and Urea Dependence of Amide Hydrogen-Deuterium Exchange Rates in the B-trefoil Protein Hisactophilin. *Biochem* **41**, 1182-1194.

Hwang, T.-L. & Shaka, A.J. (1995). Excitation Sculpting in High-Resolution Nuclear Magnetic Resonance Spectroscopy: Application to Selective NOE Experiments. *J Magn Reson Series A* **112,** 275-279.

Jaenicke, R. & Rudolph, R. (1989). Folding Proteins. In *Protein Structure: A Practical Approach*; Creighton, T.E.;Ed., IRL Press at Oxford University Press: Oxford, England, 191-222.

Kahn, R.A., Randazzo, P., Serafini, T., Weiss, O., Cherrie, R., Clark, J., Amherdt, M., Roller, P., Orci, L. & Rothman, J.E. (1992.) The Amino Terminus of ADP-ribosylation factor (ARF) Is a Critical Determinant of ARF Activities and Is a Potent and Specific Inhibitor of Protein Transport. *J Biol Chem* **267**, 13039-46.

Kay, L.E. (1997). NMR methods for the study of protein structure and dynamics. *Biochem. Cell Biol* **75**, 1-15.

Kennedy, M.T., Brockman, H. & Rusnak, F. (1996). Contributions of Myristoylation to Calcineurin Structure/Function. *J Biol Chem* **271**, 26517-21.

Kennedy, M.T., Brockman, H. & Rusnak, F. (1997). Determinants of calcineurin binding to model membranes. *Biochem* **36**, 13579-85.

Kishore, N.S., Lu, T.B., Knoll, L.J., Katoh, A., Rudnick, D.A., Mehta, P.P., Devadas, B., Huhn, M., Atwood, J.L., Adams, S.P., *et al.*. (1991). The substrate specificity of *Saccharomyces cervisiae* myristoyl-CoA:protein-myristoyltransferas. Analysis of myristic acid analogs containing oxygen, sulfur, double bonds, triple bonds, and/or an aromatic residue. *J Biol Chem* **266**, 8835-55.

Knoll, L.J. & Gordon, J.I. (1993). Use of *Escherichia coli* strains containing fad mutations plus a triple plasmid expression system to study the import of myristate, its activation by *Saccharomyces cervisiae* acyl-CoA synthetase, and its utilization by *S. cerevisiae* myristoyl-CoA: protein N-myristoyltransferase. *J Biol Chem* **268**, 4281-90.

Knoll, l.J., Johnson, R., Bryand, M.L. & Gordon, J.I. (1995). Functional Significance of Myristoyl Moiety in N-Myristoyl Proteins. *Met Enzymol* **250**, 405-35.

Ladant, D. (1995) Calcium and Membrane Binding Properties of Bovine Neurocalcin δ Expressed in *Escherichia coli*. *J Biol Chem* **270**, 3179-85.

Liu C. (1999). Thermodynamic and kinetic folding studies of hisactophilin, a beta-trefoil protein. Masters Thesis, University of Waterloo.

Liu C., Chu D, Wideman RD, Houliston RS, Wong HJ, Meiering EM. (2001). Thermodynamics of denaturation of hisactophilin, a beta-trefoil protein. *Biochemistry* **40**, 3817-27.

Liu C., Gaspar JA, Wong HJ, Meiering EM. (2002). Conserved and nonconserved features of the folding pathway of hisactophilin, a beta-trefoil protein. *Protein Sci* **11**, 669-79.

Lugtenberg, B., Peters, R., Bernheimer, H. & Berendsen, W. (1976). Influence of cultural conditions and mutations on the composition of the outer membrane proteins of Escherichia coli. *Mol Gen Genet* **147**, 251-202.

Manning, M.C. (1989). Underlying Assumptions in the Estimation of Secondary Structure Content in Proteins by Circular Dichroism Spectroscopy – A Critical Review. *Pharma Biomed Anal*. **7**, 1103-1119.

McLaughlin, S. & Aderem, A. (1995). The myristoyl-electrostatic switch: a modulator of reversible protein-membrane interaction. *J Int Biomet Soc* **20**, 272-6

Miller, E.M. & Nikoloff, J.A. (1995). *Escherichia coli* Elictrotransformation. *Met Mole Biol*, **47**,105-13.

Muralidhar, D., Jobby, M.K., Krishnan, K., Annapurna, V., Chary, K.V.R., Jeromin, A. & Sharma, Y. (2005). Equilibrium unfolding of neuronal calcium sensor-1: N-terminal myristoylation influences unfolding and reduces the protein stiffening in the presence of calcium. *J Biol Chem.* In Press

Murin, A.G., Lesk, A.M. & Chothia, C. (1992). beta-Trefoil fold. Patterns of structure and sequence in the Kunitz inhibitors interleukins-1 beta and 1 alpha and fibroblast growth factors. *J Mol Biol* **223**, 531-43.

Murzin, A.G., Brenner, S.E., Hubbard, T. & Chothia, C. (1995). SCOP: A Structural Classification of Proteins Database for the Investigation of Sequences and Structures. *J Mol Biol* **247**, 536-40.

O'Callaghan, D.W., Ivings. L., Weiss, J.L., Ashby, M.C., Tepikin, A.V. & Burgoyne, R.D. (2002). Differential Use of Myristoyl Groups on Neuronal Calcium Sensor Proteins as a Determinant of Spatio-temporal Aspects of Ca^{2+} Signal Transduction. *J Biol Chem* **277**, 14227-37.

Pace, C.N. (1986). Determination and analysis of urea and guanidine hydrochloride denaturation curves. *Met Enzymol* **131**, 266-80.

Pace, C.N. (1990). Measuring and increasing protein stability. *Trends Biotech,* **8,**93-8

Pace, C.N., Shirley, B.A. & Thomson, J.A. (1989). Measuring the conformational stability of a protein. In *Protein Structure: A Practical Approach*; Creighton, T.E.;Ed., RL Press at Oxford University Press: Oxford, England, 311-29.

Plum, G.E. & Breslauer, K.J. (1995). Calorimetry of proteins and nucleic acids. *Curr Opin Struct Biol.* **5**, 682-90.

Privalov, P.L. & Potekhin, S.A. (1986). Scanning Microcalorimetry in Studying Temperature-Induced Changes in Protein. *Met Enzymol*, **131**, 4-51.

Randazzo, P.A. & Kahn, R.A. (1995). Myristoylation and ADP-Ribosylation Factor Function. *Met Enzymol* **250**, 394-405.

Randazzo, P.A., Terui, T., Sturch, S., Fales, H.M., Ferrige, A.G. & Kahn, R.A. (1995). The Myristoylated Amino Terminus of ADP-riobsylation Factor 1 Is a Phospholipid- and GTP-sensitive Switch. *J Biol Chem* **270**, 14809-15.

Rasband, W.S., ImageJ, U. S. National Institutes of Health, Bethesda, Maryland, USA, http://rsb.info.nih.gov/ij/, 1997-2006.

Resh, M. D. (1999). Fatty acylation of proteins: new insights into membrane targeting of myristoylated and palmitoylated proteins. *Biochimica et Biophysica Acta* **1451,** 1-16.

Rudnick, D.A., McWherter, C.A., Rocque, W.J., Lennon, P.J., Getman, D.P. & Gordon, J.I.(1991). Kinetic and Structural Evidence for a Sequential Ordered Bi Bi Mechanism of Catalysis by *Saccharomyces cerevisiae* Myristoyl-CoA:Protein N-Myristoyltransferase. *J Biol Chem* **266**, 9732-9.

Rusnak, F. & Mertz, P. (2000). Cacineurin: Form and Function. *Phys Rev* **80**, 1483-1510.

Scheel, J., Ziegelbauer, K., Kupke, T., Humbel, B.M., Noegel, A.A., Gerish, G. & Schleicher, M. (1989). Hisactophilin, a histidine-rich actin-binding protein from Dictyostelium discoideum. *J Biol Chem* **264**, 2832-9.

Schmid, F.X.(1989). Spectral Methods of Characterizing Protein Conformation and Conformational Changes. In *Protein Structure: A Practical Approach*; Creighton, T.E.;Ed., IRL Press at Oxford University Press: Oxford, England, 251-84.

Senin, I.I., Vaganova, S.A., Weiergraber, O.H., Ergorov, N.S., Philippov, P.P. & Kock, K. (2003). Functional Restoration of the Ca^{2+}-myristoyl Switch in a Recoverin Mutant. *J Mol Biol* **330**, 409-18.

Simon, M. N., Mutzel, R., Mutzel,H. & Veron, M. (1988). Vectors for expression of truncated coding sequences in *Esherichia coli*. *Plasmid* **19**, 94-102.

Strahler, J.R., Kuick, R. & Hanash, S.M. (1989).. Two-Dimensional Polyacrylamide gel electrophoresis of proteins. In *Protein Structure: A Practical Approach*; Creighton, T.E.;Ed., IRL Press at Oxford University Press: Oxford, England, 65-91.

Szabo, A.G.(2000). Flourescence principles and measurement. In *Spectrophotometry & Spectrofluorimetry*; Gore, M.G.Ed., Oxford University Press: New York, NY, 33-66.

Tanaka, T., Ames, J.B., Harvey, T.S., Stryer,L. & Ikkura, M. (1995). Sequestration of the membrane-targeting myrisoty group of recoverin in the calcium-free state. *Nature* **376**, 444-7

Taniguchi, H. (1999). Protein myristoylation in protein-lipid and protein-protein interactions. *Biophys Chem* **82**,129-37.

Tholey, A., Pipkorn, R., Bossemeyer, D., Kinzel, V. & Reed, J. (2001). Influence of Myrisotylation, Phosophorylation, and Deamidation on the Structural Behavior of the N-terminus of the Catalytic Subunit of CAMP-Dependent Protein Kinase. *Biochem* **40**, 225-31.

Utsumi, T., Sato, M., Nakano, K., Takemura, D., Iwata, H. & Ishisaka, R. (2001). Amino Acid Residue Penultimate to the Amino-terminal Gly Residue Strongly Affects Two Cotranslational Protein Modifications, N-Myristoylation and N-Acetylation. *J Biol Chem* **276**, 10505-13.

Van Holde, K.E., Johnson, W.C. & Ho, P.S. (1998). *Priniciples of Physical Biochemistry;* Prentice Hall: Upper Saddle River, NJ.

Van Valkenburgh, H.A. & Kahn, R.A. (2002). Coexpression of Proteins with Methionine Aminopeptidase and/or N-Myristoyltransferase in *Escherichia coli* to Icrease Acylation and Homogeneity of Protein Preparations. *Met Enzymol* **344**, 186-93.

Weaver, J.C. (1995). Electoporation Theory. *Met Mole Biol*, **47**, 1-26

Wong, H. J. (2002). The Role of Temperature, Osmolytes and Myristoylation on the Stability and Folding of Hisactophilin. Masters, University of Waterloo.

Woody, R.W (1996). Theory of Circular Dichroism of Proteins. In *Circular Dichroism and the Conformational Analysis of Biomolecules;* Fasman, G.D.; ED., Plenum Press, New York, NY, 25-68.

Wuthrich, K. (1986). *NMR of Proteins and Nucleic Acids;* John Wiley & Sons, Inc. Toronto, Ont.

Xu, R. & Xiao, Y. (2005). A common sequence-associated physicochemical feature for proteins of beta-trefoil family. *Comp Biol Chem* **29**, 79-82.

Yonemoto, W., McGlone, M.L. & Taylor, S.S. (1993). N-myristoylation of the Catalytic Subunit of cAMP-dependent Protein Kinase Conveys Structural Stability. *J Biol Chem* **268**, 2348-52.

Zozulya, S. & Stryer, L. (1992). Calcium-myristoyl protein switch. *Proc Natl Acad Sci USA* **89**, 11569-73.

APPENDIX 1 – VERIFICATION OF MYRISTOYLATION BY MASS SPECTROMETRY

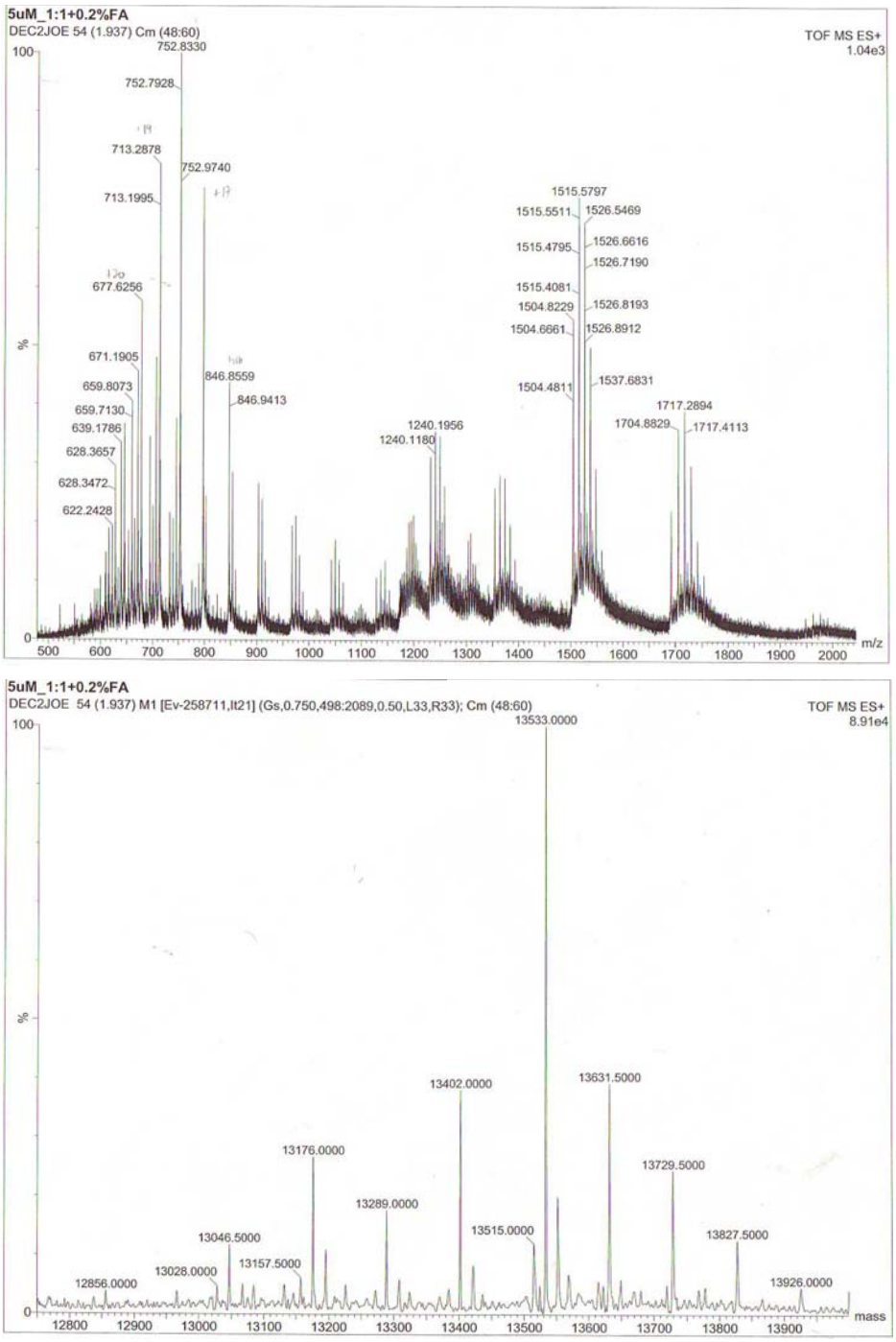

Figure A1.1: Mass spectrometry data used to verify myristoylation of hisactophilin. This determined the mass to be 13533 Da compared to the expected value of 13532 Da. Data was processed using the Micromass software and masses were taken directly from these spectra.

APPENDIX 2 – PULSE PROGRAMS FOR NMR

A2.1 – ^{1}H-^{1}H TOCSY Pulse Program:

```
;dipsi2esgpph
;avance-version (02/02/07)
;homonuclear Hartman-Hahn transfer using
DIPSI2 sequence
; for mixing
;phase sensitive
;water suppression using excitation sculpting
with gradients
;
;A.J. Shaka, C.J. Lee & A. Pines, J. Magn.
Reson. 77, 274 (1988)
;T.-L. Hwang & A.J. Shaka, J. Magn. Reson.,
; Series A 112 275-279 (1995)

prosol relations=<triple>

#include <Avance.incl>
#include <Delay.incl>
#include <Grad.incl>

;;"p2=p1*2"
;;"d11=30m"
;;"d12=20u"
;;"d13=4u"

"FACTOR1=(d9/(p6*115.112))/2+0.5"
"l1=FACTOR1*2"

"d0=in0*0.5-p1*4/3.1416"

1 ze
2 d11
3 d12 pl9:f1
d1 cw:f1 ph29
d13 do:f1
d12 pl1:f1
p1 ph1
d0
p1 ph2

4u
p16:gp1
d16 pl10:f1

;begin DIPSI2
4 p6*3.556 ph23
p6*4.556 ph25
p6*3.222 ph23
p6*3.167 ph25
p6*0.333 ph23
p6*2.722 ph25
p6*4.167 ph23
p6*2.944 ph25
p6*4.111 ph23

p6*3.556 ph25
p6*4.556 ph23
p6*3.222 ph25
p6*3.167 ph23
p6*0.333 ph25
p6*2.722 ph23
p6*4.167 ph25
p6*2.944 ph23
p6*4.111 ph25

p6*3.556 ph25
p6*4.556 ph23
p6*3.222 ph25
p6*3.167 ph23
p6*0.333 ph25
p6*2.722 ph23
p6*4.167 ph25
p6*2.944 ph23
p6*4.111 ph25

p6*3.556 ph23
p6*4.556 ph25
p6*3.222 ph23
p6*3.167 ph25
p6*0.333 ph23
p6*2.722 ph25
p6*4.167 ph23
p6*2.944 ph25
p6*4.111 ph23
lo to 4 times l1
;end DIPSI2

4u
p16:gp2
d16 pl1:f1

p1 ph3

50u UNBLKGRAD
p16:gp3
d16 pl0:f1
(p12:sp1 ph4:r):f1
4u
d12 pl1:f1

p2 ph5
```

```
4u
p16:gp3
d16
54u
p16:gp4
d16 pl0:f1
(p12:sp1 ph6:r):f1
4u
d12 pl1:f1

p2 ph7

4u
p16:gp4
d16
4u BLKGRAD

go=2 ph31
d11 mc #0 to 2 F1PH(ip1 & ip29, id0)
exit

ph1=0 2
ph2=0 0 0 0 2 2 2 2
ph3=0 0 0 0 0 0 0 0 2 2 2 2 2 2 2 2
ph4=0 0 1 1
ph5=2 2 3 3
ph6=0 0 0 0 1 1 1 1
ph7=2 2 2 2 3 3 3 3
ph23=3
ph25=1
ph29=0
ph31=0 2 2 0 0 2 2 0 2 0 0 2 2 0 0 2

;pl0 : 120dB
;pl1 : f1 channel - power level for pulse (default)
;pl9 : f1 channel - power level for presaturation
;pl10: f1 channel - power level for TOCSY-
spinlock
;sp1 : f1 channel - shaped pulse 180 degree
;p1 : f1 channel - 90 degree high power pulse
;p2 : f1 channel - 180 degree high power pulse
;p6 : f1 channel - 90 degree low power pulse
;p12: f1 channel - 180 degree shaped pulse
(Squa100.1000) [2 msec]
;p16: homospoil/gradient pulse
;d0 : incremented delay (2D)
;d1 : relaxation delay; 1-5 * T1
;d9 : TOCSY mixing time
;d11: delay for disk I/O [30 msec]
;d12: delay for power switching [20 usec]
;d13: short delay [4 usec]
;d16: delay for homospoil/gradient recovery
;l1: loop for DIPSI cycle: ((p6*115.112) * l1) =
mixing time
;in0: 1/(1 * SW) = 2 * DW
;nd0: 1
;NS: 8 * n
;DS: 16
;td1: number of experiments
;FnMODE: States-TPPI, TPPI, States or QSEC

;use gradient ratio: gp 1 : gp 2 : gp 3 : gp 4
; 1 : 3 : 31 : 11

;for z-only gradients:
;gpz1: 1%
;gpz2: 3%
;gpz3: 31%
;gpz4: 11%

;use gradient files:
;gpnam1: SINE.100
;gpnam2: SINE.100
;gpnam3: SINE.100
;gpnam4: SINE.100

;set pl9 to 120dB when presaturation is not
required
; use 75 - 80dB to reduce radiation damping

;Processing

;PHC0(F1): 90
;PHC1(F1): -180
;FCOR(F1): 1

;$Id: dipsi2esgpph,v 1.5 2002/06/12 09:04:31
ber Exp $
```

A2.2 – ^{1}H-^{1}H NOESY Pulse Program:

```
;noesyesgpph
;avance-version (02/02/07)
;2D homonuclear correlation via dipolar
coupling
;dipolar coupling may be due to noe or chemical
exchange.
;phase sensitive
;water suppression using excitation sculpting
with gradients
;
;T.-L. Hwang & A.J. Shaka, J. Magn. Reson.,
; Series A 112 275-279 (1995)

prosol relations=<triple>

#include <Avance.incl>
#include <Grad.incl>

;;"p2=p1*2"
;;"d11=30m"
;;"d12=20u"

"d0=in0/2-p1*4/3.1416"

1 ze
2 d1
3 d12 pl1:f1
p1 ph1
d0
p1 ph2
d8
p1 ph3

50u UNBLKGRAD
p16:gp1
d16 pl0:f1
(p12:sp1 ph4:r):f1
4u
d12 pl1:f1

p2 ph5
4u
p16:gp1
d16
54u
p16:gp2
d16 pl0:f1
(p12:sp1 ph6:r):f1
4u
d12 pl1:f1
p2 ph7

4u

p16:gp2
d16
4u BLKGRAD
go=2 ph31
d1 mc #0 to 2 F1PH(ip1, id0)
exit

ph1= 0 0 2 2
ph2= 0
ph3= 0 0 0 0 2 2 2 2 1 1 1 1 3 3 3 3
ph4= 0 0 0 0 1 1 1 1
ph5= 2 2 2 2 3 3 3 3
ph6= 2 3
ph7= 0 1
ph31=0 2 2 0 0 2 2 0 1 3 3 1 1 3 3 1

;pl0 : 120dB
;pl1 : f1 channel - power level for pulse (default)
;sp1 : f1 channel - shaped pulse 180 degree
;p1 : f1 channel - 90 degree high power pulse
;p2 : f1 channel - 180 degree high power pulse
;p12: f1 channel - 180 degree shaped pulse
(Squa100.1000) [2 msec]
;p16: homospoil/gradient pulse
;d0 : incremented delay (2D)
;d1 : relaxation delay; 1-5 * T1
;d8 : mixing time
;d12: delay for power switching [20 usec]
;d16: delay for homospoil/gradient recovery
;in0: 1/(1 * SW) = 2 * DW
;nd0: 1
;NS: 8 * n
;DS: 16
;td1: number of experiments
;FnMODE: States-TPPI, TPPI, States or QSEC

;use gradient ratio: gp 1 : gp 2
; 31 : 11

;for z-only gradients:
;gpz1: 31%
;gpz2: 11%

;use gradient files:
;gpnam1: SINE.100
;gpnam2: SINE.100

;Processing

;PHC0(F1): 90
;PHC1(F1): -180
;FCOR(F1): 1

;$Id: noesyesgpph,v 1.5 2002/06/12 09:05:07 ber
Exp $
```

A2.3 – ^{1}H-^{15}N HSQC Pulse Program

```
;invifpf3gpsi
;avance-version
;2D H-1/X correlation via double inept transfer
;   using sensitivity improvement
;phase sensitive using Echo/Antiecho-TPPI
gradient selection
;with decoupling during acquisition
;using f3 - channel
;using flip-back pulse
;A.G. Palmer III, J. Cavanagh, P.E. Wright & M.
Rance, J. Magn.
;   Reson. 93, 151-170 (1991)
;L.E. Kay, P. Keifer & T. Saarinen, J. Am.
Chem. Soc. 114,
;   10663-5 (1992)
;J. Schleucher, M. Schwendinger, M. Sattler, P.
Schmidt, O. Schedletzky,
;   S.J. Glaser, O.W. Sorensen & C. Griesinger, J.
Biomol. NMR 4,
;   301-306 (1994)
;S. Grzesiek & A. Bax, J. Am. Chem. Soc. 115,
12593-12594 (1993)

define list<gradient> EA=<EA>

;$Id: Grad1.incl,v 1.7 2002/06/12 09:04:22 ber
Exp $
# 20 "C:/Bruker/XWIN-
NMR/exp/stan/nmr/lists/pp/invifpf3gpsi" 2

# 1 "C:/Bruker/XWIN-
NMR/exp/stan/nmr/lists/pp/Delay.incl" 1
;Delay.incl  -  include file for commonly used
delays
;
;version 00/02/07

;general delays

define delay DELTA
define delay DELTA1
define delay DELTA2
define delay DELTA3
define delay DELTA4
define delay DELTA5
define delay DELTA6
define delay DELTA7
define delay DELTA8

define delay TAU
define delay TAU1
define delay TAU2
define delay TAU3
define delay TAU4
define delay TAU5

;delays for centering pulses

define delay CEN_HN1
define delay CEN_HN2
define delay CEN_HN3
define delay CEN_HC1
define delay CEN_HC2
define delay CEN_HC3
define delay CEN_HC4
define delay CEN_HP1
define delay CEN_HP2
define delay CEN_CN1
define delay CEN_CN2
define delay CEN_CN3
define delay CEN_CN4
define delay CEN_CP1
define delay CEN_CP2

;loop counters

define loopcounter COUNTER
define loopcounter SCALEF
define loopcounter FACTOR1
define loopcounter FACTOR2
define loopcounter FACTOR3

;$Id: Delay.incl,v 1.11 2002/06/12 09:04:22 ber
Exp $
# 21 "C:/Bruker/XWIN-
NMR/exp/stan/nmr/lists/pp/invifpf3gpsi" 2

"p2=p1*2"

"p22=p21*2"

"d0=3u"

"d11=30m"

"d26=1s/(cnst4*4)"

"DELTA=p16+d16+p2+d0*2"
"DELTA1=p16+d16+8u"

"CEN_HN1=(p21-p1)/2"
"CEN_HN2=(p22-p2)/2"

"l3=(td1/2)"

1 ze
  d11 pl16:f3
2 d1 do:f3
  6m
3 d11
  18m
```

```
4 (p1 ph1)
  d26 pl3:f3
  (CEN_HN2 p2 ph2) (p22 ph6):f3
  d26 setnmr2|0 setnmr0|34|32|33
  (p1 ph2)
  4u pl0:f1
  (p11:sp1 ph1:r):f1
  4u
  p16:gp1
  d16 pl1:f1
  (p21 ph3):f3
  d0
  p2 ph7
  d0
  p16:gp2*EA
  d16
  (p22 ph4):f3
  DELTA
  (CEN_HN1 p1 ph1) (p21 ph4):f3
  d24
  (CEN_HN2 p2 ph1) (p22 ph1):f3
  d24
  (CEN_HN1 p1 ph2) (p21 ph5):f3
  d26
  (CEN_HN2 p2 ph1) (p22 ph1):f3
  d26
  (p1 ph1)
  DELTA1
  (p2 ph1)
  4u
  p16:gp3
  d16 pl16:f3
  4u setnmr2^0 setnmr0^34^32^33
  go=2 ph31 cpd3:f3
  d1 do:f3 wr #0 if #0 zd
  3m ip5 igrad EA
  3m ip5
  lo to 3 times 2
  d11 id0
  3m ip3
  3m ip3
  3m ip6
  3m ip6
  3m ip31
  3m ip31
  lo to 4 times l3
exit

ph1=0
ph2=1
ph3=0 2
ph4=0 0 2 2
ph5=1 1 3 3
ph6=0
ph7=0 0 2 2
ph31=2 0 0 2

;pl0 : 120dB
;pl1 : f1 channel - power level for pulse (default)
;pl3 : f3 channel - power level for pulse (default)
;pl16: f3 channel - power level for CPD/BB
decoupling
;sp1: f1 channel - shaped pulse  90 degree
;p1 : f1 channel -  90 degree high power pulse
;p2 : f1 channel - 180 degree high power pulse
;p11: f1 channel -  90 degree shaped pulse
;p16: homospoil/gradient pulse                [1
msec]
;p21: f3 channel -  90 degree high power pulse
;p22: f3 channel - 180 degree high power pulse
;d0 : incremented delay (2D)                  [3
usec]
;d1 : relaxation delay; 1-5 * T1
;d11: delay for disk I/O                      [30
msec]
;d16: delay for homospoil/gradient recovery
;d24: 1/(4J)YH for YH
;     1/(8J)YH for all multiplicities
;d26: 1/(4J(YH))
;cnst4: = J(YH)
;l3: loop for phase sensitive 2D using  E/A
method : l3 = td1/2
;in0: 1/(2 * SW(X)) = DW(X)
;nd0: 2
;NS: 1 * n
;DS: >= 16
;td1: number of experiments
;MC2: echo-antiecho
;cpd3: decoupling according to sequence defined
by cpdprg3
;pcpd3: f3 channel - 90 degree pulse for
decoupling sequence

;use gradient ratio:           gp 1 : gp 2 : gp 3
; 50 :   80 : 20.1       for C-13
; 50 :   80 :  8.1       for N-15

;for z-only gradients:
;gpz1: 50%
;gpz2: 80%
;gpz3: 20.1% for C-13, 8.1% for N-15

;use gradient files:
;gpnam1: SINE.100
;gpnam2: SINE.100
;gpnam3: SINE.100
```

A2.4 – ^{15}N-edited 3D TOCSY Pulse Program

```
;dipsiif3gpsi3d
;avance-version (00/10/05)
;TOCSY-HSQC
;3D sequence with
;   homonuclear Hartman-Hahn transfer using
DIPSI2 sequence
;      for mixing
;   H-1/X correlation via double inept transfer
;      using sensitivity improvement
;phase sensitive (t1)
;phase sensitive using Echo/Antiecho-TPPI
gradient selection (t2)
;using trim pulses in inept transfer
;using f3 - channel
;A.G. Palmer III, J. Cavanagh, P.E. Wright & M.
Rance, J. Magn.
;   Reson. 93, 151-170 (1991)
;L.E. Kay, P. Keifer & T. Saarinen, J. Am.
Chem. Soc. 114,
;   10663-5 (1992)
;J. Schleucher, M. Schwendinger, M. Sattler, P.
Schmidt, O. Schedletzky,
;   S.J. Glaser, O.W. Sorensen & C. Griesinger, J.
Biomol. NMR 4,
;   301-306 (1994)

define list<gradient> EA=<EA>

;version 00/02/07

;general delays

define delay DELTA
define delay DELTA1
define delay DELTA2
define delay DELTA3
define delay DELTA4
define delay DELTA5
define delay DELTA6
define delay DELTA7
define delay DELTA8

define delay TAU
define delay TAU1
define delay TAU2
define delay TAU3
define delay TAU4
define delay TAU5

;delays for centering pulses

define delay CEN_HN1
define delay CEN_HN2
define delay CEN_HN3
define delay CEN_HC1
define delay CEN_HC2
define delay CEN_HC3
define delay CEN_HC4
define delay CEN_HP1
define delay CEN_HP2
define delay CEN_CN1
define delay CEN_CN2
define delay CEN_CN3
define delay CEN_CN4
define delay CEN_CP1
define delay CEN_CP2

;loop counters

define loopcounter COUNTER
define loopcounter SCALEF
define loopcounter FACTOR1
define loopcounter FACTOR2
define loopcounter FACTOR3

;$Id: Delay.incl,v 1.11 2002/06/12 09:04:22 ber
Exp $
# 25 "C:/Bruker/XWIN-
NMR/exp/stan/nmr/lists/pp/dipsiif3gpsi3d" 2

"p2=p1*2"
"p22=p21*2"
"d0=3u"
"d10=3u"
"d11=30m"
"d12=20u"
"d13=4u"
"d26=1s/(cnst4*4)"

"DELTA=p16+d16+p2+d10*2"
"DELTA1=d13+p16+d16+4u"
"DELTA2=p22+d0*2"

"CEN_HN1=(p21-p1)/2"
"CEN_HN2=(p22-p2)/2"

"FACTOR1=(d9/(p6*115.112))/2+0.5"
"l1=FACTOR1*2"

aqseq 321

# 1 "mc_line 61 file C:/Bruker/XWIN-
NMR/exp/stan/nmr/lists/pp/dipsiif3gpsi3d
expanding definition part of mc command before
ze"
; dimension 3 aq-mode (F2) Echo-Antiecho (F1)
States-TPPI  F2->F1
define delay MCWRK
define delay MCREST
define loopcounter ST1CNT
```

```
"ST1CNT = td1 / (2)"
define loopcounter ST2CNT
"ST2CNT = td2 / (2)"
"MCWRK = 0.090909*d11"
"MCREST = d11 - d11"
# 61 "C:/Bruker/XWIN-
NMR/exp/stan/nmr/lists/pp/dipsiif3gpsi3d"
1 ze
# 1 "mc_line 61 file C:/Bruker/XWIN-
NMR/exp/stan/nmr/lists/pp/dipsiif3gpsi3d
expanding definition of mc command after ze"
# 62 "C:/Bruker/XWIN-
NMR/exp/stan/nmr/lists/pp/dipsiif3gpsi3d"
  d11 pl16:f3
# 1 "mc_line 63 file C:/Bruker/XWIN-
NMR/exp/stan/nmr/lists/pp/dipsiif3gpsi3d
expanding start label for mc command"
2 MCWRK  * 2 do:f3
LBLSTS2, MCWRK  * 4
LBLF2, MCWRK  * 4
LBLSTS1, MCWRK
LBLF1, MCREST
# 64 "C:/Bruker/XWIN-
NMR/exp/stan/nmr/lists/pp/dipsiif3gpsi3d"
3 d12 pl9:f1
  d1 cw:f1 ph29
  4u do:f1
  d12 pl1:f1

  (p1 ph8)
   DELTA2 pl3:f3
  (p2 ph9)
  d0
  (p22 ph1):f3
  d0
  (p1 ph10)
  d20 pl10:f1

;begin DIPSI2
7 p6*3.556 ph23
  p6*4.556 ph25
  p6*3.222 ph23
  p6*3.167 ph25
  p6*0.333 ph23
  p6*2.722 ph25
  p6*4.167 ph23
  p6*2.944 ph25
  p6*4.111 ph23

  p6*3.556 ph25
  p6*4.556 ph23
  p6*3.222 ph25
  p6*3.167 ph23
  p6*0.333 ph25
  p6*2.722 ph23
  p6*4.167 ph25
  p6*2.944 ph23
  p6*4.111 ph25

  p6*3.556 ph23
  p6*4.556 ph25
  p6*3.222 ph23
  p6*3.167 ph25
  p6*0.333 ph23
  p6*2.722 ph25
  p6*4.167 ph23
  p6*2.944 ph25
  p6*4.111 ph23
  lo to 7 times l1

        ;end DIPSI2

d21 pl1:f1
(p1 ph11)

d26
(CEN_HN2 p2 ph1) (p22 ph6):f3
d26 setnmr2|0 setnmr0|34|32|33
p28 ph1
d13
(p1 ph2)
3u
p16:gp1
d16
(p21 ph3):f3
d10
p2 ph7
d10
p16:gp2*EA
d16
(p22 ph4):f3
DELTA
(CEN_HN1 p1 ph1) (p21 ph4):f3
d24
(CEN_HN2 p2 ph1) (p22 ph1):f3
d24
(CEN_HN1 p1 ph2) (p21 ph5):f3
d26
(CEN_HN2 p2 ph1) (p22 ph1):f3
d26
(p1 ph1)
DELTA1
```

```
  (p2 ph1)
  d13
  p16:gp3
  d16 pl16:f3
  4u setnmr2^0 setnmr0^34^32^33
  go=2 ph31 cpd3:f3
# 1 "mc_line 159 file C:/Bruker/XWIN-
NMR/exp/stan/nmr/lists/pp/dipsiif3gpsi3d
expanding mc command in line"
  MCWRK  do:f3 wr #0 if #0 zd igrad EA
MCWRK  ip5*2
  lo to LBLSTS2 times 2
  MCWRK id10  MCWRK  ip3*2  MCWRK
ip6*2  MCWRK  ip31*2
  lo to LBLF2 times ST2CNT
  MCWRK rd10  MCWRK  ip8  MCWRK  ip9
MCWRK  ip29
  lo to LBLSTS1 times 2
  MCWRK id0
  lo to LBLF1 times ST1CNT
# 162 "C:/Bruker/XWIN-
NMR/exp/stan/nmr/lists/pp/dipsiif3gpsi3d"
exit

ph1=0
ph2=1
ph3=0 2
ph4=0 0 2 2
ph5=1 1 3 3
ph6=0
ph7=0 0 2 2
ph8=0 0 0 0 2 2 2 2
ph9=1 1 1 1 3 3 3 3
ph10=2 2 2 2 2 2 2 2 2 2 2 2 2 2 2 2
    0 0 0 0 0 0 0 0 0 0 0 0 0 0 0 0
ph11=0 0 0 0 0 0 0 0 2 2 2 2 2 2 2 2
ph23=1
ph25=3
ph29=0
ph31=0 2 2 0 2 0 0 2 2 0 0 2 0 2 2 0
    2 0 0 2 0 2 2 0 0 2 2 0 2 0 0 2
;pl0 : 120dB
;pl1 : f1 channel - power level for pulse (default)
;pl3 : f3 channel - power level for pulse (default)
;pl9 : f1 channel - power level for presaturation
;pl10: f1 channel - power level for TOCSY-
spinlock
;pl16: f3 channel - power level for CPD/BB
decoupling
;p1 : f1 channel -  90 degree high power pulse
;p2 : f1 channel - 180 degree high power pulse
;p6 : f1 channel -  90 degree low power pulse
;p16: homospoil/gradient pulse                [1
msec]
;p21: f3 channel -  90 degree high power pulse
;p22: f3 channel - 180 degree high power pulse
;p28: f1 channel - trim pulse                 [1
msec]
;d0 : incremented delay (F1 in 3D)
[3 usec]
;d1 : relaxation delay; 1-5 * T1
;d9 : TOCSY mixing time
;d10: incremented delay (F2 in 3D)
[3 usec]
;d11: delay for disk I/O                      [30
msec]
;d12: delay for power switching
[20 usec]
;d13: short delay                             [4 usec]
;d16: delay for homospoil/gradient recovery
;d20: first z-filter delay                    [10 usec]
;d21: second z-filter delay                   [10
usec]
;d24: 1/(4J)YH for YH
;     1/(8J)YH for all multiplicities
;d26: 1/(4J(YH))
;cnst4: = J(YH)
;l1: loop for DIPSI cycle: ((p6*115.112) * l1) =
mixing time
;in0: 1/(2 * SW(H)) = DW(H)
;nd0: 2
;in10: 1/(2 * SW(X)) = DW(X)
;nd10: 2
;NS: 8 * n
;DS: >= 16
;td1: number of experiments
;td2: number of experiments in F2
;FnMODE: States-TPPI (or TPPI) in F1
;FnMODE: echo-antiecho in F2
;cpd3: decoupling according to sequence defined
by cpdprg3
;pcpd3: f3 channel - 90 degree pulse for
decoupling sequence
;use gradient ratio:    gp 1 : gp 2 : gp 3
;                       50 :   80 :  8.1        for N-15
;                       50 :   80 : 20.1      for C-13
;for z-only gradients:
;gpz1: 50%
;gpz2: 80%
;gpz3: 8.1% for N-15, 20.1% for C-13

;use gradient files:
;gpnam1: SINE.100
;gpnam2: SINE.100
;gpnam3: SINE.100

;set pl9 to 120dB when presaturation is not
required
;   use 70 - 80dB to reduce radiation damping

;$Id: dipsiif3gpsi3d,v 1.7.2.1 2001/09/11
10:14:36 ber Exp$
```

A2.5 – ^{15}N-edited 3D NOESY Pulse Program

```
# 1 "C:/Bruker/XWIN-
NMR/exp/stan/nmr/lists/pp/noesiifpf3gpsi3d"
;noesiifpf3gpsi3d
;avance-version (00/10/05)
;NOESY-HSQC
;3D sequence with
;   homonuclear correlation via dipolar coupling
;   dipolar coupling may be due to noe or
chemical exchange
;   H-1/X correlation via double inept transfer
;      using sensitivity improvement
;phase sensitive (t1)
;phase sensitive using Echo/Antiecho-TPPI
gradient selection (t2)
;with decoupling during acquisition
;using flip-back pulse
;using f3 - channel
;
;O. Zhang, L.E. Kay, J.P. Olivier & J.D.
Forman-Kay,
;   J. Biomol. NMR 4, 845 - 858 (1994)
;A.G. Palmer III, J. Cavanagh, P.E. Wright & M.
Rance, J. Magn.
;   Reson. 93, 151-170 (1991)
;L.E. Kay, P. Keifer & T. Saarinen, J. Am.
Chem. Soc. 114,
;   10663-5 (1992)
;J. Schleucher, M. Schwendinger, M. Sattler, P.
Schmidt, O. Schedletzky,
;   S.J. Glaser, O.W. Sorensen & C. Griesinger, J.
Biomol. NMR 4,
;   301-306 (1994)

;avance-version (02/05/31)

define list<gradient> EA=<EA>

;$Id: Grad1.incl,v 1.7 2002/06/12 09:04:22 ber
Exp $
# 30 "C:/Bruker/XWIN-
NMR/exp/stan/nmr/lists/pp/noesiifpf3gpsi3d" 2

# 1 "C:/Bruker/XWIN-
NMR/exp/stan/nmr/lists/pp/Delay.incl" 1
;Delay.incl  -  include file for commonly used
delays
;
;version 00/02/07

;general delays

define delay DELTA
define delay DELTA1
define delay DELTA2
define delay DELTA3
define delay DELTA4
define delay DELTA5
define delay DELTA6
define delay DELTA7
define delay DELTA8

define delay TAU
define delay TAU1
define delay TAU2
define delay TAU3
define delay TAU4
define delay TAU5

;delays for centering pulses

define delay CEN_HN1
define delay CEN_HN2
define delay CEN_HN3
define delay CEN_HC1
define delay CEN_HC2
define delay CEN_HC3
define delay CEN_HC4
define delay CEN_HP1
define delay CEN_HP2
define delay CEN_CN1
define delay CEN_CN2
define delay CEN_CN3
define delay CEN_CN4
define delay CEN_CP1
define delay CEN_CP2

;loop counters

define loopcounter COUNTER
define loopcounter SCALEF
define loopcounter FACTOR1
define loopcounter FACTOR2
define loopcounter FACTOR3

;$Id: Delay.incl,v 1.11 2002/06/12 09:04:22 ber
Exp $
# 31 "C:/Bruker/XWIN-
NMR/exp/stan/nmr/lists/pp/noesiifpf3gpsi3d" 2

"p2=p1*2"

"p22=p21*2"

"d0=3u"

"d10=3u"

"d11=30m"

"d12=20u"
```

```
"d13=4u"

"d26=1s/(cnst4*4)"

"DELTA=p16+d16+p2+d10*2"
"DELTA1=d13+p19+d16+4u"
"DELTA2=p22+d0*2"
"DELTA3=d24-p16-4u"
"DELTA4=d26-p16-d16"

"TAU=d8-p16-d16"

"CEN_HN1=(p21-p1)/2"
"CEN_HN2=(p22-p2)/2"

aqseq 321

# 1 "mc_line 67 file C:/Bruker/XWIN-
NMR/exp/stan/nmr/lists/pp/noesiifpf3gpsi3d
expanding definition part of mc command before
ze"
; dimension 3 aq-mode (F2) Echo-Antiecho (F1)
States-TPPI  F2->F1
define delay MCWRK
define delay MCREST
define loopcounter ST1CNT
"ST1CNT = td1 / (2)"
define loopcounter ST2CNT
"ST2CNT = td2 / (2)"
"MCWRK = 0.100000*d11"
"MCREST = d11 - d11"
# 67 "C:/Bruker/XWIN-
NMR/exp/stan/nmr/lists/pp/noesiifpf3gpsi3d"
1 ze
# 1 "mc_line 67 file C:/Bruker/XWIN-
NMR/exp/stan/nmr/lists/pp/noesiifpf3gpsi3d
expanding definition of mc command after ze"
# 68 "C:/Bruker/XWIN-
NMR/exp/stan/nmr/lists/pp/noesiifpf3gpsi3d"
  d11 pl16:f3
# 1 "mc_line 69 file C:/Bruker/XWIN-
NMR/exp/stan/nmr/lists/pp/noesiifpf3gpsi3d
expanding start label for mc command"
2 MCWRK  * 2 do:f3
LBLSTS2, MCWRK  * 4
LBLF2, MCWRK  * 3
LBLSTS1, MCWRK
LBLF1, MCREST
# 70 "C:/Bruker/XWIN-
NMR/exp/stan/nmr/lists/pp/noesiifpf3gpsi3d"
3 d12
  d1
  (p1 ph8)
  DELTA2 pl3:f3
  (p2 ph9)
  d0
  (CEN_CN2 p22 ph1):f3
  d0
  (p1 ph10)
  TAU setnmr2|0 setnmr0|34|32|33
  p16:gp1
  d16
  (p1 ph11)
  d26
  (CEN_HN2 p2 ph1) (p22 ph6):f3
  d26
  (p1 ph2)

  4u pl0:f1
  (p11:sp1 ph12):f1
  4u
  p16:gp2
  d16

  (p21 ph3):f3
  d10
  p2 ph7
  d10
  p16:gp3*EA
  d16
  (p22 ph4):f3
  DELTA
  (CEN_HN1 p1 ph1) (p21 ph4):f3
  4u
  p16:gp4
  DELTA3
  (CEN_HN2 p2 ph1) (p22 ph1):f3
  DELTA4
  p16:gp4
  d16
  (CEN_HN1 p1 ph2) (p21 ph5):f3
  4u
  p16:gp5
  DELTA3
  (CEN_HN2 p2 ph1) (p22 ph1):f3
  DELTA4
  p16:gp5
  d16
  (p1 ph1)
  DELTA1
  (p2 ph1)
  d13
  p19:gp6
  d16 pl16:f3
  4u setnmr2^0 setnmr0^34^32^33
  go=2 ph31 cpd3:f3
# 1 "mc_line 126 file C:/Bruker/XWIN-
NMR/exp/stan/nmr/lists/pp/noesiifpf3gpsi3d
expanding mc command in line"
  MCWRK  do:f3 wr #0 if #0 zd igrad EA
MCWRK  ip5*2
```

```
  lo to LBLSTS2 times 2
  MCWRK id10  MCWRK  ip3*2  MCWRK
ip6*2  MCWRK  ip31*2
  lo to LBLF2 times ST2CNT
  MCWRK rd10  MCWRK  ip8  MCWRK  ip9
  lo to LBLSTS1 times 2
  MCWRK id0
  lo to LBLF1 times ST1CNT
# 129 "C:/Bruker/XWIN-
NMR/exp/stan/nmr/lists/pp/noesiifpf3gpsi3d"
exit

ph1=0
ph2=1
ph3=0 2
ph4=0 0 2 2
ph5=1 1 3 3
ph6=0
ph7=0 0 2 2
ph8=0 0 0 0 2 2 2 2
ph9=1 1 1 1 3 3 3 3
ph10=0 0 0 0 0 0 0 0 0 0 0 0 0 0 0 0
    2 2 2 2 2 2 2 2 2 2 2 2 2 2 2 2
ph11=0 0 0 0 0 0 0 0 2 2 2 2 2 2 2 2
ph12=2 2 2 2 2 2 2 2 0 0 0 0 0 0 0 0
ph31=0 2 2 0 2 0 0 2 2 0 0 2 0 2 2 0
    2 0 0 2 0 2 2 0 0 2 2 0 2 0 0 2

;pl0 : 120dB
;pl1 : f1 channel - power level for pulse (default)
;pl3 : f3 channel - power level for pulse (default)
;pl16: f3 channel - power level for CPD/BB
decoupling
;sp1 : f1 channel - shaped pulse  90 degree
;p1 : f1 channel -  90 degree high power pulse
;p2 : f1 channel - 180 degree high power pulse
;p11: f1 channel -  90 degree shaped pulse
;p16: homospoil/gradient pulse                [1
msec]
;p21: f3 channel -  90 degree high power pulse
;p22: f3 channel - 180 degree high power pulse
;d0 : incremented delay (F1 in 3D)
[3 usec]
;d1 : relaxation delay; 1-5 * T1
;d8 : mixing time
;d10: incremented delay (F2 in 3D)
[3 usec]
;d11: delay for disk I/O                      [30
msec]
;d12: delay for power switching
[20 usec]
;d13: short delay                             [4 usec]
;d16: delay for homospoil/gradient recovery
;p19: homospoil/gradient pulse
[300 usec]
;d24: 1/(4J)YH for YH
;     1/(8J)YH for all multiplicities
;d26: 1/(4J(YH))
;cnst4: = J(YH)
;in0: 1/(2 * SW(H)) = DW(H)
;nd0: 2
;in10: 1/(2 * SW(X)) = DW(X)
;nd10: 2
;NS: 8 * n
;DS: >= 16
;td1: number of experiments in F1
;td2: number of experiments in F2
;FnMODE: States-TPPI (or TPPI) in F1
;FnMODE: echo-antiecho in F2
;cpd3: decoupling according to sequence defined
by cpdprg3
;pcpd3: f3 channel - 90 degree pulse for
decoupling sequence

;use gradient ratio:          gp 1 : gp 2 : gp 3 :  gp
4 : gp 5 : gp 6
;                                30 :  -50 :   80 :    11
:    5 : 8.1*x

;   with x = p16/p19

;for z-only gradients:
;gpz1: 30%
;gpz2: -50%
;gpz3: 80%
;gpz4: 11%
;gpz5: 5%
;gpz6: 27% (8.1% *p16(=1 ms)/p19(=300 us))

;use gradient files:
;gpnam1: SINE.100
;gpnam2: SINE.100
;gpnam3: SINE.100
;gpnam4: SINE.100
;gpnam5: SINE.100
;gpnam6: SINE.50

;$Id: noesiifpf3gpsi3d,v 1.4 2000/10/06 09:09:32
ber Exp $
```

APPENDIX 3 – UREA DENATURATION CURVE SAMPLE PREPARATION

Denaturation samples were prepared according to the following tables for the various pH values.

Table A3.1: Urea Denaturation Sample Composition for pH 5.7

#	**Volume of 10X Protein Solution** (μL)	**Volume 10M Urea** (μL)	**Volume H_2O** (mL)	**[Urea]** (M)
1	30	0	270	0
2	30	12	258	0.4
3	30	18	252	0.6
4	30	24	246	0.8
5	30	30	240	1
6	30	36	234	1.2
7	30	42	228	1.4
8	30	48	222	1.6
9	30	54	216	1.8
10	30	60	210	2
11	30	66	204	2.2
12	30	72	198	2.4
13	30	78	192	2.6
14	30	84	186	2.8
15	30	90	180	3
16	30	102	168	3.4
17	30	114	156	3.8
18	30	126	144	4.2
19	30	138	132	4.6
20	30	150	120	5
21	30	162	108	5.4
22	30	174	96	5.8
23	30	186	84	6.2
24	30	198	72	6.6
25	30	210	60	7
26	30	222	48	7.4
27	30	234	36	7.8
28	30	246	24	8.2
29	30	258	12	8.6
30	30	270	0	9

Table A3.2: Urea Denaturation Sample Composition for pH 6.7

#	Volume of 10X Protein Solution (μL)	Volume 10M Urea (μL)	Volume H_2O (mL)	[Urea] (M)
1	30	0	270	0
2	30	12	258	0.4
3	30	24	246	0.8
4	30	36	234	1.2
5	30	48	222	1.6
6	30	54	216	1.8
7	30	60	210	2
8	30	66	204	2.2
9	30	72	198	2.4
10	30	78	192	2.6
11	30	84	186	2.8
12	30	90	180	3
13	30	96	174	3.2
14	30	102	168	3.4
15	30	108	162	3.6
16	30	114	156	3.8
17	30	120	150	4
18	30	126	144	4.2
19	30	138	132	4.6
20	30	150	120	5
21	30	162	108	5.4
22	30	174	96	5.8
23	30	186	84	6.2
24	30	198	72	6.6
25	30	210	60	7
26	30	222	48	7.4
27	30	234	36	7.8
28	30	246	24	8.2
29	30	258	12	8.6
30	30	270	0	9

Table A3.3: Urea Denaturation Sample Composition for pH 7.7

#	Volume of 10X Protein Solution (μL)	Volume 10M Urea (μL)	Volume H_2O (mL)	[Urea] (M)
1	80	0	720	0
2	80	32	688	0.4
3	80	64	656	0.8
4	80	96	624	1.2
5	80	128	592	1.6
6	80	160	560	2
7	80	192	528	2.4
8	80	224	496	2.8
9	80	256	464	3.2
10	80	288	432	3.6
11	80	304	416	3.8
12	80	320	400	4
13	80	336	384	4.2
14	80	352	368	4.4
15	80	368	352	4.6
16	80	384	336	4.8
17	80	400	320	5
18	80	416	304	5.2
19	80	432	288	5.4
20	80	448	272	5.6
21	80	464	256	5.8
22	80	480	240	6
23	80	496	224	6.2
24	80	528	192	6.6
25	80	560	160	7
26	80	592	128	7.4
27	80	624	96	7.8
28	80	656	64	8.2
29	80	688	32	8.6
30	80	720	0	9

Table A3.4: Urea Denaturation Sample Composition for pH 8.7

#	Volume of 10X Protein Solution (μL)	Volume 10M Urea (μL)	Volume H_2O (mL)	[Urea] (M)
1	30	0	270	0
2	30	12	258	0.4
3	30	24	246	0.8
4	30	36	234	1.2
5	30	48	222	1.6
6	30	60	210	2
7	30	72	198	2.4
8	30	84	186	2.8
9	30	96	174	3.2
10	30	108	162	3.6
11	30	120	150	4
12	30	126	144	4.2
13	30	132	138	4.4
14	30	138	132	4.6
15	30	144	126	4.8
16	30	150	120	5
17	30	156	114	5.2
18	30	162	108	5.4
19	30	168	102	5.6
20	30	174	96	5.8
21	30	180	90	6
22	30	186	84	6.2
23	30	192	78	6.4
24	30	198	72	6.6
25	30	210	60	7
26	30	222	48	7.4
27	30	234	36	7.8
28	30	246	24	8.2
29	30	258	12	8.6
30	30	270	0	9

APPENDIX 4 – RESIDUE ASSIGNMENTS FOR MYRISTOYLATED HISACTOPHILIN

Residue Assignments made using CARA are listed in Table A4.1

Table A4.1: Residue Assignments for Myristoylated Hisactophilin.

Residue		H_N	N	Hα	Hα2	Hβ	Hβ2	Hγ	Hγ2	Hγ12	Hδ1	Hδ2	Hδ12
2	G	7.78	111.21	4.48	3.46								
3	N	8.74	120.21	5.64		2.45	2.81						
4	R	9.52	125.89	5.05		1.39	1.21						
5	A	8.42	121.55	4.92		1.29							
6	F	10.08	117.26	5.65		2.64	2.42						
7	K	8.86	125.84	4.42		1.66	1.21			0.19			
8	S	10.00	126.06	4.26									
10	H	7.11	113.63	4.14			3.18						
11	G	7.50	106.22	3.96									
12	H	7.04	117.89	4.90		3.28	2.76						
13	F	9.34	118.90	5.72		3.31	2.93						
14	L	8.46	122.76	4.40		1.84		1.51					
15	S	8.80	117.33	5.09		3.54	3.18						
16	A	8.27	128.14	5.31		1.41							
17	E	8.43	123.52	4.36									
19	E	8.82	124.75	4.50		2.42	2.24			1.86			
20	A	8.17	124.62	4.74		1.45							
21	V	8.21	119.98	4.74		1.92			0.81				
22	K	9.28	127.77	5.01		2.10		1.31					
23	T	7.68	106.08	5.63									
24	H	9.65	120.24	5.11		3.18	2.92						
33	H	7.42	120.54	5.05		3.42	2.84						
34	F	9.60	124.15	5.11		2.92	2.72						
35	H	9.69	123.17	5.05		3.20	3.02						
36	V	8.85	127.71	4.92		2.18		1.11	0.97				
37	E	9.12	126.72	4.54		2.46	2.34			2.04			
38	N	8.59	120.46	5.10		2.75	2.51						

Residue		H_N	N	Hα	Hα2	Hβ	Hβ2	Hγ	Hγ2	Hγ12	Hδ1	Hδ2	Hδ12
39	H	8.94	125.81	4.62		2.87	2.59						
42	K	7.52	120.29	4.84									
43	V	9.25	112.48	5.73		2.10			1.03				
44	A	8.83	122.64	5.25		1.51							
45	L	10.69	125.84	4.78		1.45							
46	K	8.93	126.69	4.90		2.08				0.47			
47	T	9.41	117.92	4.22									
48	H	9.22	123.13										
50	G	7.79	111.85	4.00	3.28								
51	K	7.71	119.75	4.54		1.47	1.33	0.91					
52	Y	9.04	115.19	5.31			3.12						
53	L	8.94	130.76	4.04		1.92	1.21						
54	S	8.68	121.44	5.45		3.02	2.18						
55	I	8.37	121.50	4.80									
56	G	8.57	108.29	3.22									
59	K	7.77	112.15	3.19									
60	Q	9.18	122.48	4.62		1.92	1.82	2.13					
61	V	8.68	124.20	4.96		1.97				0.91			
62	Y	9.27	127.12	4.94		3.18	2.90						
63	L	8.42	117.89	4.40		2.68	2.32						
64	S	8.37	117.73	4.78		3.82	3.64						
66	H	7.70	114.58	4.94									
67	L	8.64	125.49	4.68		3.02	1.37						
68	H	7.65	132.87	4.12		3.18	2.40						
69	G	8.34	114.42	3.60	3.38								
70	D	8.76	117.19	4.84		2.24	2.44						
71	H	8.88	116.18	4.53			2.60						
72	S	8.60	112.73	5.05			4.14						
73	L	6.16	115.71	5.19		1.51	1.03	1.23					
74	F	9.23	119.02	4.84		2.68	2.50						
75	H	9.46	120.57	4.84		3.18	3.02						

Residue		H_N	N	Hα	Hα2	Hβ	Hβ2	Hγ	Hγ2	Hγ12	Hδ1	Hδ2	Hδ12
76	L	8.72	126.50	4.78		1.72	1.21						
77	E	8.88	124.95	4.58		2.18				1.88			
78	H	8.45	120.49	5.05		3.16	2.92						
79	K	8.43	122.07	4.52		1.82	1.57						
82	V	7.82	120.36	5.03		2.20	1.94	1.47					
83	S	9.53	115.01	5.53									
84	I	8.63	115.64	5.15			4.38						
85	K	9.42	116.42	5.27		2.00							
86	G	8.57	123.50	4.46		2.96	2.58			0.31	0.95		
87	H	9.27	116.86	4.64	3.66								
89	H	7.81	116.21	3.86		3.02	2.86						
90	H	8.52	113.70	3.92			3.44						
91	H	7.00	116.49	4.72		3.06	2.88						
92	Y	9.19	119.90	5.55		3.16	2.70						
93	I	6.94	118.46	4.36									
94	S	8.72	122.48	5.06		3.32							
95	A	8.60	125.70	5.29		1.41							
96	D	7.84	119.16	4.74		3.24	2.74						
98	H	7.48	117.92	4.44		2.84	2.70						
99	G	8.20	108.23	3.92									
100	H	8.34	121.23	4.78									
101	V	8.85	128.42	5.09									
102	S	8.89	123.83	4.70		3.96	3.80						
103	T	8.40	108.25	5.83									
104	K	8.61	116.66	4.70									
105	E	8.76	120.99	4.00									
106	H	7.23	115.53	4.86									
108	D	8.96	126.73	4.88									
109	H	9.39	117.06	4.34									
110	D	7.81	118.39	4.64		2.84	2.66						
111	T	7.45	108.23	5.17									

Residue		H_N	N	Hα	Hα2	Hβ	Hβ2	Hγ	Hγ2	Hγ12	Hδ1	Hδ2	Hδ12
112	T	7.47	119.02	4.66		4.04			1.05				
113	F	9.45	123.31	5.11									
114	E	9.42	120.38	4.90		2.34	2.07	1.88	2.15				
115	E	8.95	126.22	4.42						1.98			
116	I	8.81	128.91	4.32		1.66				1.43			
117	I	8.42	128.09	3.80		1.78		0.87					
118	I	6.72	129.57	4.00		1.43		0.67	0.35				

*Unassigned residues are: 9, 18, 19, 25, 26, 27, 28, 29, 30, 31, 32, 38, 40, 41, 49, 57, 58, 65, 78, 80, 81, 97 and 107